CHALMERS

Frequency Stability and Control in Island Operation Using Wind Power

Master of Science Thesis in Electric Power Engineering

MARKUS ERIKSSON

Department of Electrical Engineering
CHALMERS UNIVERSITY OF TECHNOLOGY
Gothenburg, Sweden 2024

Master Thesis EENX30

Frequency Stability and Control in Island Operation Using Wind Power

Markus Eriksson

CHALMERS

Department of Electrical Engineering
Division of Electric Power Engineering
Chalmers University of Technology
Gothenburg, Sweden 2024

Frequency Stability and Control in Island Operation Using Wind Power

Markus Eriksson

Department of Electrical Engineering
Division of Electric Power Engineering
Chalmers University of Technology
SE - 412 96 Gothenburg
Telephone +46 31-772 10 00

Thesis supervisor
Mattias Persson
RISE Research Institutes of Sweden AB
mattias.persson@ri.se

Thesis examiner
Peiyuan Chen
Department of Electrical Engineering
Division of Electric Power Engineering
Chalmers University of Technology, Gothenburg, Sweden
peiyuan.chen@chalmers.se

Typeset in LaTeX
Gothenburg, Sweden 2024

Abstract

An Increased frequency of extreme weather events and concerns of attacks has caused a growing interest in island operation for parts of a power system to increase its resilience. Island operation constitutes designing part of the power system as an island system, able to disconnect from the larger grid and independently sustain its loads. Wind power is also becoming increasingly important for the power system as decarbonizing efforts are made. Wind power does however have an intermittent power production and a detrimental effect on power system inertia. These challenges with wind power raise uncertainties regarding what role it can serve within island systems and still maintain the island stability. Simulations have therefore been conducted in MATLAB/Simulink and in PSS/E to address these uncertainties. The simulations are conducted to evaluate how the stability of a wind and hydro based island system changes when the wind power within the island provides frequency control. The stability was analyzed during transition from grid connected to island operation and during the continued operation thereafter.

The MATLAB/Simulink simulations were conducted to design the wind turbine control and the strategies used for the wind power frequency control. Two wind power frequency control strategies were implemented. The first is inertia emulation, where the synchronous inertial power response to a frequency change is emulated for the wind turbine. The second strategy implemented is droop control while de-rating the turbine, where the wind turbine's power is purposely reduced to create a power reserve that is utilized for controlling the frequency. The design wind turbine control was then converted to PSS/E using user defined models and applied to a simple test network for island operation.

The simulations of the island test network showed that using wind power inertia emulation caused frequency stability improvements for the frequency for all cases analyzed. This frequency stability improvement could be further improved by also including wind power droop control. However, using droop control up-regulation of the frequency comes at the cost of reduced wind power production, as it is necessary to create a power reserve for this method. The frequency improvements from the wind power frequency control for the transition from grid connected to island operation were especially significant. The wind power frequency control also showed an improvement for the voltage stability in the test network. The stability improvements indicate that wind power frequency control can reduce the requirements on the wind power penetration and on the possible power transfer between the island system and the grid when grid connected.

Keywords: *Island operation, Frequency control, Wind power control, Inertia emulation, Wind power de-rating*

Sammanfattning

En ökad frekvens av extrema väderhändelser och oro för attacker har orsakat ett växande intresse för ödrift för delar av ett kraftsystem för att öka dess resilience. Ödrift innebär att utforma en del av kraftsystemet som ett ö-system, vilket kan kopplas bort från det större nätet och självständigt upprätthålla dess belastningar. Vindkraften blir också allt viktigare för kraftsystemet på grund av ansträngningar för att minska koldioxidutsläpen. Vindkraft har dock en intermittent kraftproduktion och har en negativ påverkan på kraftsystemets svängmassa. Dessa utmaningar med vindkraft väcker osäkerhet gälande vilken roll den kan fylla inom ö-system och ändå upprätthålla öns stabilitet. Simuleringar har därför genomförts i MATLAB/Simulink och i PSS/E för att komma till rätta med dessa osäkerheter. Simuleringarna genomförs för att utvärdera hur stabiliteten i ett vind- och vattenkraft baserat ö-system förändras när vindkraften inom ön ger frekvenskontroll. Stabiliteten analyserades vid övergång från nätanslutet till ödrift och under den fortsatta driften därefter.

MATLAB/Simulink-simuleringarna genomfördes för att designa vindkraftsstyrningen och de strategier som används för vindkraftsfrekvensstyrningen. Två vindkraftsfrekvensstyrningsstrategier implementerades. Den första är svängmassaemulering, där det synkrona effektsvaret från svängmassans på en frekvensändring emuleras för vindturbinen. Den andra strategin som implementeras är droop-kontroll samtidigt som turbinen spiler vind, där vindturbinens effekt avsiktligt reduceras för att skapa en effektreserv som används för styra frekvensen. Den designade vindkraftsstyrningen konverterades sedan till PSS/E med hjälp av användardefinierade modeller och applicerades på ett enkelt testnätverk för ödrift.

Simuleringarna av ö-testnätverket visade att användning av svängmassaemulering för vindkraft skulle för alla analyserade fall orsaka till en stabilitetsförbättring för frekvensen. Denna förbättring av frekvensstabiliteten skulle kunna förbättras ytterligare genom att även inkludera droop kontroll av vindkraften. Att använda droo-kontroll för uppreglering av frekvensen kommer dock på bekostnad av minskad vindkraftsproduktion, eftersom det är nödvändigt att skapa en effektreserv för denna metod. Särskilt betydande var frekvensförbättringarna för övergången från nätanslutet till ödrift. Vindkraftens frekvensstyrning visade också en förbättring för spänningsstabiliteten i testnätet. Stabilitetsförbättringarna indikerar att vindkraftens frekvensstyrning kan minska kraven på vindkraftens genomslag och den möjliga kraftöverföringen mellan ön och elnätet medan det är inkopplat.

Keywords: *Island operation, Frequency control, Wind power control, Inertia emulation, Wind power de-rating*

Acknowledgements

I would like to thank my supervisor Mattias Persson for giving me the opportunity to conduct my thesis work at RISE and for all of his guidance and support throughout my work.
I am also thankful to Mahantha Ampavatina Kambagiri for taking time and engaging in my work. His guidance of user defined modeling in PSS/E has been especially useful.
Furthermore, I am grateful to everybody in the power system unit at RISE for welcoming me and providing an enjoyable environment for me to work in.
I would also like to thank my examiner Peiyuan Chen, for his feedback during my work.
Lastly, I would like to thank my family who have supported and believed in me throughout my studies.

Markus Eriksson
Gothenburg, June 2024

List of Acronyms

RISE	Research Institutes of Sweden
FFR	Fast Frequency Reserve
FCR	Frequency Containment Reserve
FRR	Frequency Recovery Reserve
RoCoF	Rate of Change of Frequency
IEEE	Institute of Electrical and Electronics Engineers
RMS	Root Mean Square
FSWT	Fixed Speed Wind Turbine
VSWT	Variable Speed Wind Turbine
PSS/E	Power System Simulator for Engineering
UDM	User Defined Model

Table of Contents

List of Figures

List of Tables

1 Introduction

1.1 Background and motivation

The power system is changing in response to the changing climate and increasing levels of greenhouse gas emissions. As a result, intermittent converter-based renewable energy production is rapidly growing, as efforts are made to decarbonize energy systems. Converter-based renewable production units are often connected to the distribution system as distributed generation units, causing the distribution system to play a more active role in power production [1]. Simultaneously, the power system is put under increasing pressure as climate change causes extreme weather events to become more common and the concerns related to malicious attacks on the power system are growing [2]. Extreme weather is particularly demanding on the distribution power system and outages in these scenarios will bring significant economic damage as well as risk human lives, highlighting the necessity for solutions improving the power system resilience [3].

A solution for increasing the resilience is for areas of the power system to disconnect from the larger grid and continue to operate as islands, using distributed generation resources within the disconnected areas to supply their loads. By disconnecting as an island and locally maintaining power, disruptions to the continued service can be combated preventing large scale blackouts [4]. Rural areas radially connected to the power system are particularly vulnerable as any fault on the radial connection will cause a blackout if not power can be locally maintained as an island [3]. Island operation is therefore a strategy through which critical loads can be maintained, increasing the power systems resilience in the possible event of a crisis.

In Sweden has wind power become a rapidly growing distributed generation resource [5]. However, adding wind power can cause increased frequency instability due to wind power's lack of natural inertial response and its intermittent production. These stability concerns become especially important in the case of island operation as, due to their low inertia, previously minor disturbances now become significant [6]. Questions therefore appear concerning how wind power contributes to the operation stability of islands. However, the island's small size and isolated operation also make them a good testing ground for how frequency control strategies that utilize wind power can mitigate the frequency instability.

1.2 Aim and Scope

The aim of this work is to evaluate the stabilety with focus on frequency of an island system consisting of wind and hydro based generation. The stability is to be studied during the transitioning and operation of the island, while considering different wind power frequency management strategies.

During the duration of will the work the following list of questions be investigated:

- How does the island frequency react during unplanned transition to island operation and during continued island operation thereafter?
- In what way will frequency control strategies utilizing wind power affect the stability of the island in the above cases?
- How will the wind power penetration level impact the frequency stability and what power imbalances caused by the transition can the island handle?

- How does the interaction between the wind and hydro frequency control strategies contribute to the island stability?
- What are the current regulations and recommendations regarding island operation and what concerns exist leading to anti-islanding regulation?
- What are the requirements for the island system for transition to island operation, continued operation considering both planned and unplanned island with respect to the previous answers?

1.3 Limitations

The focus of the work will be on technical aspects related to the control and power quality in an island system. In particular the focus will be on management of the system frequency quality for both the transitions to and from island operation as well as during the continuous operation in an island state. As frequency stability is the primary focus of the work, the work will be limited to studying phenomena on the time scale between 10^{-1} seconds to minutes as this is the time scale of interest for frequency studies. Considering that voltage phenomena also act on the considered time scale will this quantity also be studied during the work. The voltage stibillet will however only be given limited attention where it should stay within its requirements for the cases studied. Rotor angle stability also acts on this time scale and some mentions with regard to this will be included. However it will not be analyzed as it would require a somewhat more sophisticated test network then what was used. Faster phenomena acting on time scales below this, namely resonance stability and converter-driven stability, will not be included in the work.

The islands considered in this work will be limited to systems on the distribution grid with AC and connection to the main grid and can thus operate as both an island and as a part of a larger grid. Furthermore, issues related to monitoring and communication of electrical quantities within the island and to the larger grid will be considered outside the scope of this work. Due to this limitation, it is assumed during this work that an accurate state of the power system will be available for real time study and control. Another limitation of the work is that experimental measurements will not be used with the study focusing solely on a simulated model.

Social, economic and environment aspects will also not be prioritized in this work, however a brief discussion of these subjects will be included. The inclusion of these subjects is because they are driving factors in establishing the possibility for island operation, as island operation often is coupled with mitigating the economical and human harm that are associated with power system faults and outages. Furthermore, the drive for integrating wind power into the islands is directly tied with environmental issues.

1.4 Social, ethical and sustainable considerations

As the work will include the subjects of island operation and wind power, it is important to also consider how these subjects impact society and the environment as well as consider their ethical implications. When regarding island operations is the aspect of resilience important as island operation can increase community resilience. thereby can island operation be beneficial for energy reliability, while also reducing reliance on external assistance, contributing to sustainable development. Furthermore, can island operation

influence local economies as many businesses are reliant on an uninterrupted power supply and thereby can island operation benefit the economic stability.

While island operation offers opportunities for enhancing resilience and empowering the local community, it also poses ethical concerns related to equity. When islanding the energy supply to certain areas may be prioritized and in these scenarios is it important to ensure a fair distribution of the power. Critical infrastructure and vulnerable populations, for example those with medical needs, should be prioritized and care should be taken to not exacerbate existing inequalities through the power prioritizing.

When considering wind power, the environmental impacts become particularly relevant as wind power is an alternative to fossil fuel power generation. As such, wind power development helps in mitigating climate change and the magnitude of detrimental environmental effects associated with it. Care should however be taken with the development in order to minimize its direct environmental impact, such as disruptions for the local wildlife.

Wind power also carries with it certain ethical implications. For one are climate change, which wind power development help mitigate, also unethical along with being environmentally damaging. Climate change is unethical because its effect causes harm and endangers peoples well-being globally and these harms are furthermore not equally distributed. However, wind power development does require land use and therefore for an ethical development is it necessary to consider and respect indigenous land rights as well as the interests of local communities. Consultation and consent as well as participation from local communities are paramount in order to avoid unequal development and to work with the local communities is of particular importance for island operation applications of wind power considering that it constitutes a development on a local level.

1.5 Outline of the thesis

The work carried out is presented in this report and structured into several sections.

Section 2 presents key concepts about power systems and in particular their stability as well as also presenting an introduction to islanded systems, what their purpose as well as challenges are. Furthermore, does the section present the characteristics for controlling a hydro plant as well as the operational principles of wind turbines and their frequency control.

Section 3 describes the modeling of a variable speed wind turbine providing frequency control in MATLAB/Simulink. Models of the wind turbine's different subsystems are presented in this section along with a basic one bus power system model and hydro power model.

Section 4 describes the PSS/E modeling, where a more detailed model of the wind-hydro island system is presented using used defined models derived from the MATLAB/Simulink models to model the wind power. This section also presents the different cases tested on the model to determine to analyze the island system stability.

Section 5 presents the results of the MATLAB/Simulink model showing how the wind power frequency control functions, as well as the MATLAB/Simulink model ability to regulate the frequency for small load variations and large disturbances.

Section 6 presents the results from the PSS/E island simulations.

Section 7 presents the conclusions from the work and recommendations of future work.

2 Theory

2.1 Power system stability

In [7] is power system stability defined as: "Power system stability is the ability of an electric power system, for a given initial operating condition, to regain a state of operating equilibrium after being subjected to a physical disturbance, with most system variables bounded so that practically the entire system remains intact". The purpose of the definition presented in [7] was to provide an easily understood, physically based definition encompassing all practical instability scenarios. The definition refers to a power system as a whole and therefore allows for individual generators and/or load to become disconnected as long as it does not cause a cascading effect, instabilizing the main system. Furthermore, power system stability is categorized in [7] into three main categories, namely: frequency stability, voltage stability and rotor angle stability.

Since the work in [7] was carried out, the power system has undergone significant changes due to the increase of converter interfaced technologies, where wind power is one example. Although there have been changes in the power system, the original definition still applies. The classification has however been expanded to also include faster dynamics, as the converter interfaced technologies extend the interesting timescale for power system stability to include shorter time periods [8]. The expanded classification from [8] is shown in Figure 1 also includes resonance stability and converter-driven stability as categories under power system stability, along with the original categories. This work will however focus on frequency stability and its associated time scale and therefore are only the original stability categories are reviewed in the following sections (Section 2.1.1 - 2.1.4).

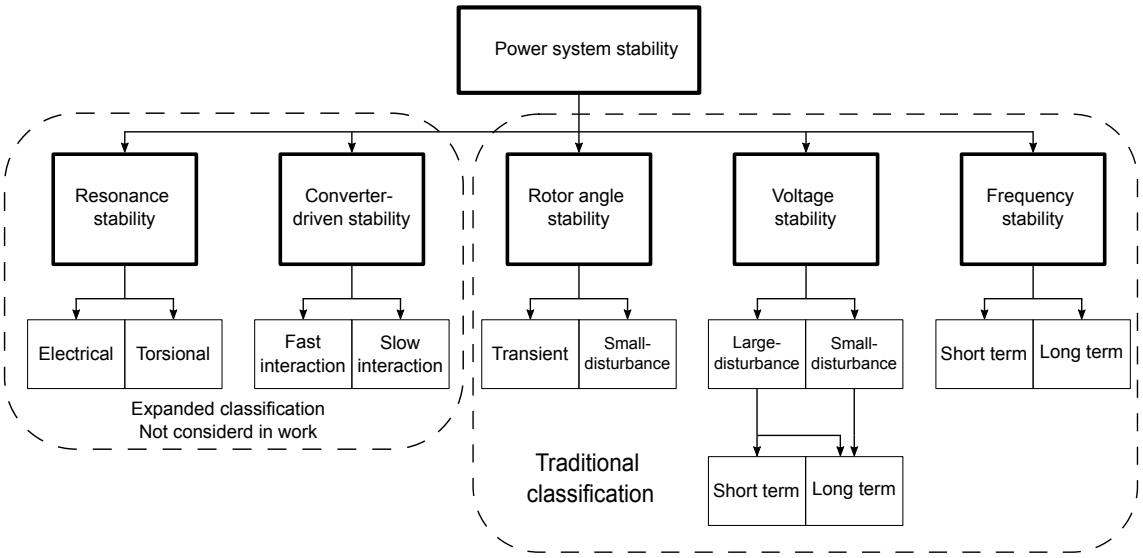

Figure 1: Power system stability classification [8].

2.1.1 Frequency stability

Frequency stability is the ability of a power system to maintain its frequency within an acceptable range and recover the frequency after a disturbance. The power generation in the power system has traditionally consisted largely of synchronous generators which

have large masses rotating in synchronisation. The speed of the generator's synchronous rotation is what dictates the frequency of the system. Because of the energy inherent in the rotating masses, they are resistant to any change in the rotational speed, therefore providing inertia to the system frequency. Additionally, the inertia of individual machines is cumulative due to the generators operating synchronously to one another [9]. When one generator experiences a speed deviation it no longer rotates in step to the other generators, resulting in the other generators using energy stored in their rotation to mitigate the speed deviation until synchronisation is achieved between all generators.

For a rotating mechanical system, the response to rotational speed, ω, due to an acceleration torque, T_a, applied to the system can be expressed as

$$J\frac{d\omega}{dt} = T_a \tag{2.1}$$

where, J is the moment of inertia of the system as a result of its rotating mass. When considering a synchronous machine, the acceleration torque is a result of a power imbalance between the mechanical power, P_m, applied to the rotor shaft and the electrical power, P_e. Hence, for a synchronous machine, (2.1) can be written as

$$J_i\omega_{r,i}\frac{d\omega_{r,i}}{dt} = P_{m,i} - P_{e,i} \tag{2.2}$$

where, $\omega_{r,i}$ is the rotational speed of the machine rotor. The subscript i denotes the individual machine considered. Additionally the moment of inertia is related to the kinetic energy from the rotors rotation and when the machine rotate at the nominal speed, ω_n, J_i can be expressed as

$$J_i = \frac{2E_{k,n,i}}{\omega_n^2} \tag{2.3}$$

in which $E_{k,n}$ is the kinetic energy in the machine rotor when rotating at ω_n. As a result of the relationship in (2.3) it is useful to categorize the inertia of a synchronous machine by introducing an inertia constant, H_i, instead of using J_i. The inertia constant for a specific synchronous machine is defined as

$$H_i = \frac{E_{k,n,i}}{S_{n,i}} \tag{2.4}$$

where $S_{n,i}$ is the machine rated apparent power [10]. The unit of H_i is Ws/VA however, it is usually expressed in seconds. The reason why seconds are used as unit in H_i is due to the value H_i describes the time it takes for a machine to go from operating at ω_n to a stand still while continually supplying the rated capacity by only utilizing the machine's kinetic energy.

By combining (2.2), (2.3) and (2.4) the response of the rotational speed due to a power imbalance is derived as

$$\frac{2H_iS_{n,i}}{\omega_n^2}\omega_{r,i}\frac{d\omega_{r,i}}{dt} = P_{m,i} - P_{e,i}. \tag{2.5}$$

Assuming that the difference between $\omega_{r,i}$ and ω_n is small, it is possible to simplify (2.5) as

$$2H_iS_{n,i}\frac{d(\omega_{r,i}/\omega_n)}{dt} = P_{m,i} - P_{e,i}. \tag{2.6}$$

To represent a larger power system instead of a single synchronous machine, the total inertia constant can be considered the average inertia constant of the individual generators

[11]. Hence, the inertia constant of a system consisting of N synchronous machines can be calculated as

$$H_{sys} = \frac{\sum_{i=1}^{N}(S_{n,i}H_i)}{\sum_{i=1}^{N} S_{n,i}} = \frac{\sum_{i=1}^{N}(S_{n,i}H_i)}{S_b}. \tag{2.7}$$

Where, S_b denotes the system base power and is the sum of the apparent power ratings for all synchronous machines connected to the considered system. Additionally for the system of N machines, the total power imbalance can be represented as

$$P_m - P_e = \sum_{i=1}^{N} P_{m,i} - \sum_{i=1}^{N} P_{e,i}. \tag{2.8}$$

Therefore, when considering a system consisting of multiple synchronous machines and applying (2.7) and (2.8) to (2.6), the synchronous rotational speed of the system is derived as

$$2H_{sys}S_b\frac{d(\omega_r/\omega_n)}{dt} = P_m - P_e. \tag{2.9}$$

In per unit format, the system's rotational speed and power imbalance is normalized by their respective bases, ω_n and S_b. Additionally, as rotational speed and frequency are proportional, ω_r becomes equal to the system frequency, f when in per unit. Therefore, by converting (2.9) to per unit, it becomes

$$2H_{sys}\frac{d\omega_r}{dt} = 2H_{sys}\frac{df}{dt} = P_m - P_e. \tag{2.10}$$

Furthermore, when considering a power imbalance causing a deviation from the nominal operating point, (2.10) can be expressed as

$$2H_{sys}\frac{d\Delta f + f_n}{dt} = P_{m,n} + \Delta P_m - (P_{e,n} + \Delta P_e) \tag{2.11}$$

where the parameters f_n, $P_{m,n}$ and $P_{e,n}$ are the nominal system frequency, mechanical power and electrical power respectively [12]. As the system is in steady state at nominal operating point, $P_{m,n}$ is equal to $P_{e,n}$ and f_n is a constant, resulting in it being possible to reduce (2.11) down to

$$2H_{sys}\frac{d\Delta f}{dt} = \Delta P_m - \Delta P_e. \tag{2.12}$$

Another factor to consider when studying the speed response of the power system due to a power imbalance, is the effect caused by the load. The power demand of the system loads are not constant with respect to both the frequency and the voltage, where the responses are different depending on the load. The overall load demand change due to the frequency is in the same direction as the frequency, and is described using a load frequency dependency constant, D, typical in the range of 1 to 2, meaning that if the frequency goes down by 1% the power demand also reduces by 1% to 2% [9]. The load voltage dependency can be modeled using the second order polynomial ZIP model. The power consumption in the ZIP model vary based on the percentage of the load that can be as a constant impedance, Z_P, the percentage that can be considered as a constant current, I_P, and the percentage that can be considered as a constant power, P_P [13]. The load demand can be represented, considering both frequency dependence and voltage dependence, by expanding ΔP_e to

$$\Delta P_e = \Delta P_L + P_{L0}[Z_P(\frac{V}{V_0})^2 + I_P(\frac{V}{V_0}) + P_P - 1] + D\Delta f \tag{2.13}$$

$$Z_P + I_P + P_P = 1 \tag{2.14}$$

where ΔP_L is a disturbance in the load demand due to external factors, for example a fault, P_{L0} is the nominal load demand, V is the current voltage and V_0 is the nominal voltage.

As the load demand of (2.13) is included in (2.12), the systems frequency dynamics as a result of a disturbance in the power balance is derived as

$$2H_{sys}\frac{df}{dt} + P_{L0}[Z_P(\frac{V}{V_0})^2 + I_P(\frac{V}{V_0}) + P_P - 1] + D\Delta f = \Delta P_m - \Delta P_L. \tag{2.15}$$

Hence lacking any additional control and voltage change, the resulting steady state frequency, f_{ss}, to a power disturbance is decided by the load frequency dependency as steady state is achieved when $D\Delta f_{ss}$ is equal to the power imbalance. Furthermore, (2.15) states that the initial rate of change of frequency (RoCoF) is decided by the system inertia constant [14].

Many processes in a power system depend on the frequency, and it is therefore important to maintain it close to an agreed-upon value (50 Hz in Europe and large parts of the rest of the world). An example of an issue that are caused by the frequency deviating from its agreed upon value is that high stresses are applied to the blades of grid connected steam turbines [14]. As steam turbines operate outside the normal frequency, the rotational speed comes closer to a resonance frequency for the turbine blades which causes increased stress due to vibration by several magnitudes. [14]. Another issue occurring at low frequencies is overheating of the equipment. Because the magnetic flux is proportional to the ratio of voltage over frequency, low frequencies cause excessive flux density in electromagnetic equipment, such as generators and transformers. The excessive flux density results in high magnetizing currents and therefore overheating [14]. This issue is further compounded by a reduced capability of cooling systems, as cooling is often operated by induction machines whose performance is reduced when the frequency drops [14].

Resulting from these issues, the power system equipment is equipped with automatic protection agents frequency deviation. The activation of this protection disconnects the equipment from the system. However, activation at low frequencies leads to a further power imbalance that eventually leads to a blackout. In an effort to avoid having to disconnect generating units, a load shedding strategy is first utilized, where the power demand is reduced by disconnecting loads to try to stabilize the frequency [14].

There is also a trend in power systems in which the inertia constant is reduced, increasing the difficulty of maintaining the frequency [15]. The reason for this trend in power systems is that converter-interfaced wind and photovoltaic generation is becoming particularly prominent due to decarbonization efforts. Because of the power converters of these resources, their power generation does not respond naturally to changes in frequency, which contrasts with the frequency response of directly connected synchronous generators. Therefore, the converter-interfaced power generation is described as being decoupled from the grid and has an inertia constant equal to zero. By considering (2.7), if the added power generation does not provide an inertia constant, the overall system inertia is reduced. It is estimated that the inertia constant in Sweden was reduced by 20 percent between 1996 and 2016 due to the influence of converter-interfaced power generation [15]. Consequently, the frequency response to a disturbance has a higher RoCoF, making it more difficult to handle the disturbance.

An additional trend in the power system that causes frequency disturbances to be more difficult to handle is the connection of motors through converters [9]. This increases the motors efficiency by allowing for speed control. However, as a result the motors lose their dependency on the frequency causing the overall system load frequency dependency to decrees.

2.1.2 Frequency control

In order to improve on the power system frequency, generators perform control actions by increasing or decreasing their active power production to compensate for power imbalances. To perform the control actions a power reserve is required for the control to use. In the Nordic power system, the power reserves used in the control of the generators are divided into three main categories. Each category acts on a different time scale and serves a different purpose for improving the frequency response to a disturbance. These different categories are the Fast Frequency Reserve (FFR), the Frequency Containment Reserve (FCR) and the Frequency Restoration Reserve (FRR). The aim with these reserves is to keep the frequency within +/- 0.1 Hz of 50 Hz during normal operation and within +/- 0.5 Hz during disturbed operation. Transient frequency deviations of maximum +/- 1 Hz are however allowed [16].

The FFR were introduced as a response to the reducing inertia in the power system [17]. FFR acts during a short duration, but is activated rapidly. It aims to complement the slower acting FCR by limiting the initial RoCoF, increasing the time it takes for the frequency to reach its maximum deviation. After the FFR activation the FCR should have taken over the burden of managing the frequency response.

The objective of the FCR is to contain the frequency disturbance by limiting the frequency nadir [18]. It limits the frequency nadir by equipping generators with automatic droop controllers that work independently to counteract changes in the frequency [19]. The droop control is categorized by increasing $\Delta P_{m,i}$ of a generator in proportion to the frequency deviation and is visualized in Figure 2. The droop setting R of the controller decides the change in power and can be expressed as

$$R = \frac{\Delta f}{\Delta P_{m,i}}. \tag{2.16}$$

With using a droop setting of 5% (0.05), the power of the unit, $P_{m,i}$, is changed by 100% due to a 5% change in f. [19] The draw back of droop control used in the FCR are that it is an proportional control and as a result can not fully restore the frequency after a disturbance, leaving a steady state error [20].

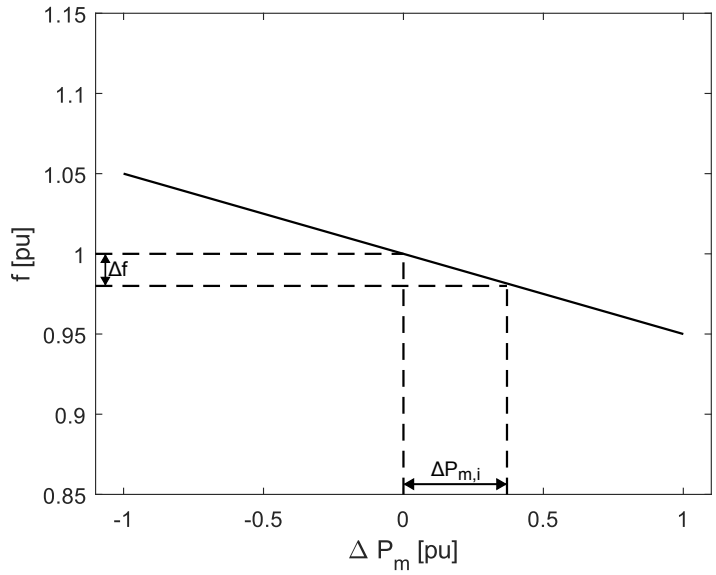

Figure 2: Frequency to power characteristic of a droop controller with a droop setting of 5%, including example of a frequency droop to 49 Hz resulting in a power increase on $P_{m,i}$ of 0.4 [pu].

The FCR is divided into three reserves, Frequency Containment Reserves for Normal operation (FCR-N), for Disturbances Up-regulation (FCR-D up) and for Disturbances Down-regulation (FCR-D down) [21]. FCR-N is utilized to maintain the frequency during the small disturbances and power variations that occur during normal operation [22]. It is a symmetrical reserve, meaning that the reserve acts to contain both over and under frequencies and is fully activated for a frequency deviation of +/- 0.1 Hz. The FCR-D reserves are instead utilized during large disturbances and are separated into individual reserves for up and down regulation. These reserves have a deadband on the frequency of +/- 0.1 Hz resulting in that the FCR-N is used before FCR-D [21]. The size of the FCR-D reserves are made to cover the power system dimensioning fault according to the N-1 criteria. Additionally, FCR-D may use a different droop setting compared to FCR-N [22].

The final reserve used in the Nordic power system to support the frequency is the FRR. Its objective is to eliminate the frequency's steady state error caused by the droop control of the FCR. It also acts to replenish the FCR to prepare the system for another disturbance. This is commonly accomplished by being activated based on the integral of the frequency deviation [16]. FRR is separated into two reserves where the Automatic Frequency Restoration Reserves (aFRR) main objective is to restore the steady state frequency [18]. This reserve utilization is controlled centrally and activated automatically, but acts slower compared to the FCR. The Manual Frequency Restoration Reserve (mFRR) makes up the second part of FRR and is activated manually by the system operator. The objective of mFRR is to restore the FCR and aFRR reserves and is also utilized to manage congestion in the system [18].

2.1.3 Voltage stability

Voltage stability is maintained if all the buses in a system maintain a voltage level within given limits. The voltage is a local quantity in contrast with the frequency which is considered for a power system as a whole. Voltage instability is caused due to the transfer of power to all loads connected to the system contrasted with the inherent voltage drop in transferring power, both active and reactive, across power lines [8]. The voltage drop limits the power transfer capabilities of lines which is further limited by excitation limits of generators. As power transfer to the loads give rise to voltage instability issues, the instability is usually driven by the load characteristic of the system [7]. As there is a disturbance to the voltage causing a voltage drop, the power consumption of the loads usually follows. However it is common for actions of automatic processes, for example slip adjustment of inductive machines and tap changing of transformers, to restore the load power [7]. This will however increase the power over the power lines, causing a further voltage drop. The increased power transfer may therefore be pushed to the limit of the system causing activation of protection, tripping lines or other equipment leading to a cascading outage [8].

2.1.4 Rotor angle stability

Rotor stability is maintained if the synchronous machines connected to the network keep their synchronization during normal operation and regain synchronism after a machine is subject to a disturbance [8]. Rotor angle stability is, similar to frequency stability, governed by motion of a rotating system due to an imbalance in torque. However, unlike the frequency, the rotor angle is observed locally for a generator and (2.2) may therefore be used to describe it. During normal operation there is equilibrium. However a disturbance to the system may cause the acceleration of a machine. This causes the angle between the accelerated machine and the other machines connected to the system to grow. As the power transfer between machines depends on the angle difference, the accelerating machine transfers more power and supplies a greater portion of the system load [7]. By supplying more of the load the machine is again accelerated and an equilibrium will be achieved. The relationship between angle difference and power transfer is however not linear and beyond a point the transfer of power reduces [7]. The system becomes unstable if the angular difference is sufficiently large causing the power transfer from the accelerated machine to be lower compared to the system's equilibrium point.

What effect converter interfaced technologies has on rotor angle stability is not completely understood and they may have a positive or negative effect depending on the system composition and their control [8]. However, the reduction of inertia in the system due to the influence of converter interfaced technologies can result in faster changes of the rotor angle having a detrimental effect on the rotor angle stability [8].

2.2 Island operations

An island system of distributed resources is, according to [23] described as a part of the power system consisting of loads and distributed resources intentionally designed to have the ability to disconnect from the main system. These island systems can also be referred to as microgrids considering that a microgrid is described in [24] as a group of distributed energy resources and loads which operates locally and can operate in either grid connected mode or islanded mode. Grid connected microgrids are further described in [23] to have the ability for seamless transition to island mode. These systems can be of a wide variety of size and complexity, having the possibility of being of hundreds of kW up to tens of MW and usually operating at either low or medium voltages.

When an island system/microgrid operates while disconnected from the grid, the island can no longer rely on the grid to help with its management. The island system therefore requires control systems to locally manage the operation of the connected distributed resources. The control required within the island is to manage voltage and frequency levels, ensure a balance in the power, manage transition from and to island mode of operation and also ensure an economic dispatch of resources [23]. The control of the island can be divided into hierarchies where the fastest controls are involved to manage the island stability and it include frequency and voltage control as well as island detection.

2.2.1 Why and when to island

The main benefit for islading, or having the possibility of islanding, a power system are the increase in resilience it offers [3]. The transition to island operation may either be a planned occurrence where the time is planned out ahead and the transition is performed seamlessly or it may be unplanned and the result of an unexpected event. Reasons for planned transition are forecasted severe weather conditions and stressed system operating point [24]. In both these cases the islanding is a preventive measure to ensure operation of the islanded system even in case of system faults due to the extreme operating conditions. Further can islanding offer flexibility for isolating part of the grid in order to perform maintenance [3]. The Unplanned islanding may instead happen due to faults in the power systems triggering protection to isolate the island system from the fault, ensuring continued operability. The triggering of the protection resulting in the transition could also be to isolate from Cyber-attacks [3].

2.2.2 Island stability aspects

An island system has significant differences when compared to a main grid. For one are island systems of a smaller size and have their power supplied from inverter interfaced production and small synchronous machines resulting in low system inertia [23]. Their small size and the intermittent nature of the inverter interfaced production does additionally results in further difficulties with power balance as there is a greater uncertainty of the power generation in the system which may result in higher discrepancies between generation and consumption [23]. Another difference is that an islanded system has shorter lines resulting in low voltage drops. Furthermore, the lines have a high resistance to reactance ratio compared to in a conventional grid caused by operating at low or medium voltage. The high resistance to reactance ratio results in the assumption of separating active power from the voltage to become invalid [23].

Due to these differences, maintaining frequency stability becomes especially difficult in

islanded systems compared to in the main grid. For example, outages of generation units or loads for an island system represent significant outages, majorly impacting system stability [23]. An unplanned island transition also poses a challenge for the frequency stability as it can result in a large power disturbance. Planned transitions are however less challenging due to being able to change the operating point of the distributed generation to reflect the operating condition of the subsequent island prior to the islanding event [23]. Changing operating points of the generators may therefore cause the system demand to change depending on the load voltage sensitivity which could cause complications for frequency control.

The voltage stability is not as large of an issue in islands compared to frequency stability [23]. In conventional systems, voltage issues often occur due to the voltage drop of long transmission lines. Considering that the power lines in the islands do not have as large of a voltage drop, the islands do not experience the same issues with voltage as in conventional systems. However, as a consequence of the low voltage drops, faults on the system may result in very low voltages across the island system. The low voltages can cause induction motors connected to the system to stall, absorbing large amounts of reactive power and if not disconnected can potentially lead to insufficient reactive power supply and therefore voltage instability [23]. Due to the coupling between active power and voltage in an islanded system may also a power disturbances cause low voltages in the system leading to voltage instability [23].

Instability of the rotor angle of synchronous machines is rarely observed in island systems [23]. One reason for not observing this is that, due to having a high resistance to reactant ratio, the rotor angel does not experience the same acceleration in relation to the other connected synchronous machines due to a fault as in a conventional system. A second reason is that island systems often have a sufficient synchronizing and damping torque to not experience undamped oscillations of the synchronous machines rotor angle.

2.2.3 Risks and Regulations

In [23] it is described that a microgrid (island system) can be considered stable if it has appropriate values at a steady state and that after a disturbance the state variables recover to give a satisfactory operational condition without involuntary load shedding. This description is not unlike the power system stability definition given in [7]. Regarding what constitutes an appropriate state variable, IEEE 1547.4-2011[24] states that the power quality has to be satisfactory for everyone operating within the island system.

In [3] and [25] is the European standard EN-50 160 used to determine whether the island systems have an appropriate power quality. This standard discusses various different characteristics of the voltage quality and the costumer side. The standards include requirements on the line voltage symmetry, the waveform, the magnitude and the frequency. In this work the focus is on the frequency and magnitude limits specified by the standard for island operation. The standard focus is to ensure that the loads are functioning as expected by the customers [3]. Table 1 summarizes the operational limits specified by EN-50 160 for frequency and voltage for an island system while operating in both grid connected and operating as an island [3].

Table 1: Voltage frequency and magnitude requirements for island system as described in [3]

	Grid connected	Island operation
Frequency, continuous	49.5 Hz - 50.5 Hz	49 Hz - 51 Hz
Frequency, momentary	47 Hz - 52 Hz	42.5 Hz - 57.5 Hz
Voltage magnitude	0.9 pu - 1.1 pu	0.85 pu - 1.1 pu

These limits presented in Table 1 must be adhered to at every point in the island system. The continuous limit must be adhered to for 99.5 % of a year while in grid-connected mode or for 95 % of a week while in island mode and the momentary limits must be adhered to 100% of the time regardless of operating mode. Regarding the magnitude, the limits are specified for an average of their RMS value over a 10 minute period. The voltage may therefore temporarily cross these limits [25] however, it may never be less than 0.5 pu [3]. From Table 1 it is noticeable that the constraints put on the system while operating as an island are less strict due to the island operation inertia typically being lower compared to when grid connected. However, the requirements for generators specified in [26] state further requirements on the frequency for which generators need to be connected to a network. The requirements in the Nordic power system are summarized in Table 2. In [26] is it also specified, for at least type C generators operating in the 10 to 30 MW range, that these frequency requirements also apply during island operation.

Table 2: Time period generators are required to stay connected for different frequency ranges as described in [26]

Time period for operation	Frequency range
30 minutes	47,5 Hz - 48,5 Hz
To be specified by the transmission system operator, but not less than 30 minutes	48,5 Hz - 49,0 Hz
Unlimited	49,0 Hz - 51,0 Hz
30 minutes	51,0 Hz - 51,5 Hz

There are also regulations concerning anti islanding protection. The anti islanding applies for unintentional islanding of a system, where an island is created without being designed for it, and any distributed generation unit connected to the island should be disconnected within 2 s [3]. This is due to the energizing of such a system can lead to undesired and potentially dangerous consequences. For example:

- If the disconnected system is not recognised as operating as an island can it appear to be de-energized while still being energized by connected distributed generators, potentially causing harm to maintenance and restoration personnel [27]
- If the island remains undetected the voltage and frequency quality may rapidly deteriorate, damaging equipment connected to the formed island [27].
- If island is formed due to a fault on a downstream line connecting the island to the main grid, can also automatic re-closing of relays be damaging to equipment due

to the island may lose synchronization with the grid during the fault, causing large transients in the resynchronization event [27].

2.2.4 Island detection

The anti islanding concerns highlight the necessity of reliable island detection methods in order to take appropriate response actions. The importance of island detection applies both for unintentional islanding but also for unplanned islanding of a system having the ability to operate as an island considering that there are substantial differences in operation between grid-connected mode and island model [28]. There are a wide variety of different solutions for detecting island operation. Some of the more common detection methods include the traditional passive and active island detection methods [29] . The passive island detection method utilizes measurements of voltage and frequency at the terminals of distributed generators to detect islanding if these parameters pass set thresholds. An island may be detected using this method based on under/ over frequency and voltage as well as based on frequency RoCoF. This method is however not reliable, failing to detect island operation in many cases and also detecting many false islands. Active island detection purposely introduces a disturbance whose response is monitored and if the response is sufficiently large island operation is detected. This method is more reliable compared to the passive method, however it causes a reduced power quality. More modern island detection methods are an evolution of the passive detection method where signal processing tools, for example the Wavelet transform, are applied in order to extract additional information from the measured parameters, significantly improving the detection reliability [29].

2.3 Hydro power characteristic and frequency control

There is a wide variation in turbines used in hydro power plants, however common amongst the turbines is that the power produced is proportional to the water's potential energy and kinetic energy, represented by the water pressure and flow respectively [14]. The power production can therefore be controlled by controlling the water flow by changing the position of a gate. A commonly used representation of the power production of a hydro turbine in per unit is the transfer function

$$\frac{\Delta P_m}{\Delta G} = \frac{1 - T_w s}{1 + \frac{1}{2} T_w s} \tag{2.17}$$

expressing the change in power production as a result of a change in the gate position, ΔG. A derivation of this transfer function can be found in [14] [1] and [30]. The parameter T_w is called the starting time constant and results from the water inertia. It is representative of the time for the water flow to increase after the gate position is opened. The transfer function is a simplified hydro turbine representation as the water is assumed to be incompressible and the pen-stock pipe is assumed inelastic. Further are also the hydraulic resistance and any dampening effects resulting from the turbine speed, for example due to friction, neglected. However the representation is still sufficient for power stability studies [14].

Figure 3 shows the power response of eq (2.17) for a unit step increase of the gate position. When the gate position is changed to allow for an increased flow the power output immediately drops, having a reaction opposite to the desired reaction. This special characteristic of hydro turbines is due to the inertia of the water as when the gate is opened the water flow will not change instantly [14]. However, due to the reluctance of the flow to change, the water pressure will immediately decrease when the gate is opened. As water flow accelerates according to T_w, the pressure will also increase resulting in the power increase seen in Figure 3, until a new steady state is achieved.

[1] page 379 - 383

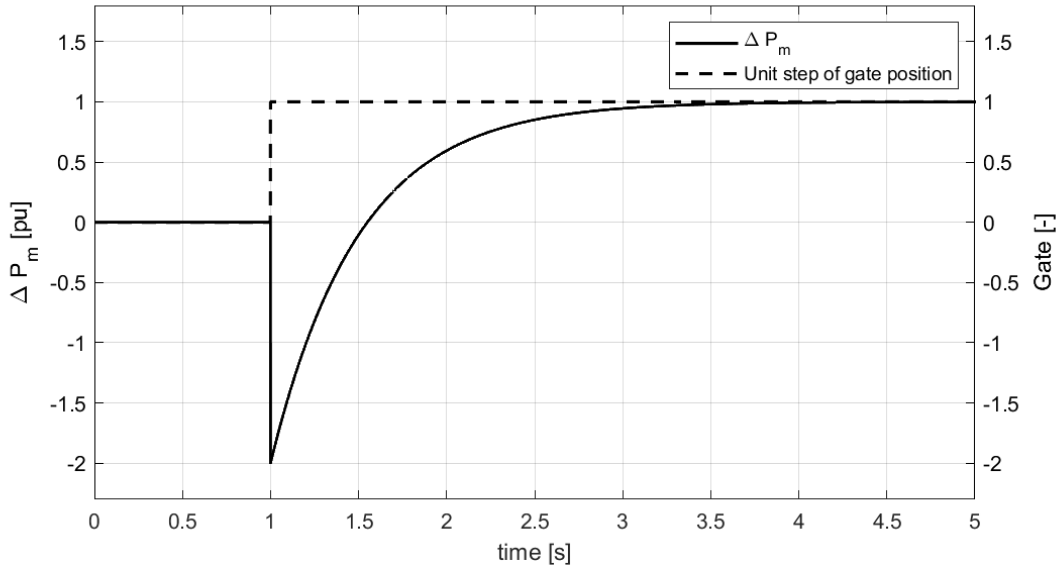

Figure 3: Hydro turbine power step response from unit step of gate position according to (2.17) ($T_w = 1\,s$).

2.3.1 Hydro droop control

An effect of the initial reverse response to a change in the gate position is that it becomes infeasible to use a fixed droop for the hydro-governor. Due to the initial power drop, the droop controller initially amplifies the frequency error potentially, leading to an unstable control action if the droop is low. However, using a high droop reduces the strength of the control action. One solution is to use a combination of a high transient droop and low permanent droop by filtering the permanent droop through a lead-lag filter [14]. The lead-lag filter can be expressed as

$$G(s) = \frac{T_r s + 1}{T_r \frac{R_t}{R_p} s + 1} \tag{2.18}$$

where, R_t, is the transient droop, R_p, is the permanent droop and T_r is a reset time constant. The unit step response of the filter is shown in in Figure 4 where it is shown that the filter initially has a low gain, corresponding to the high transient droop, with transition in to a higher gain corresponding to the low permanent droop. This transition from transient to permanent droop causes a smoother change of the gate position, giving the flow of water time to respond and not causing as severe drops in water pressure. The speed of the droop transition is decided by the reset-time constant.

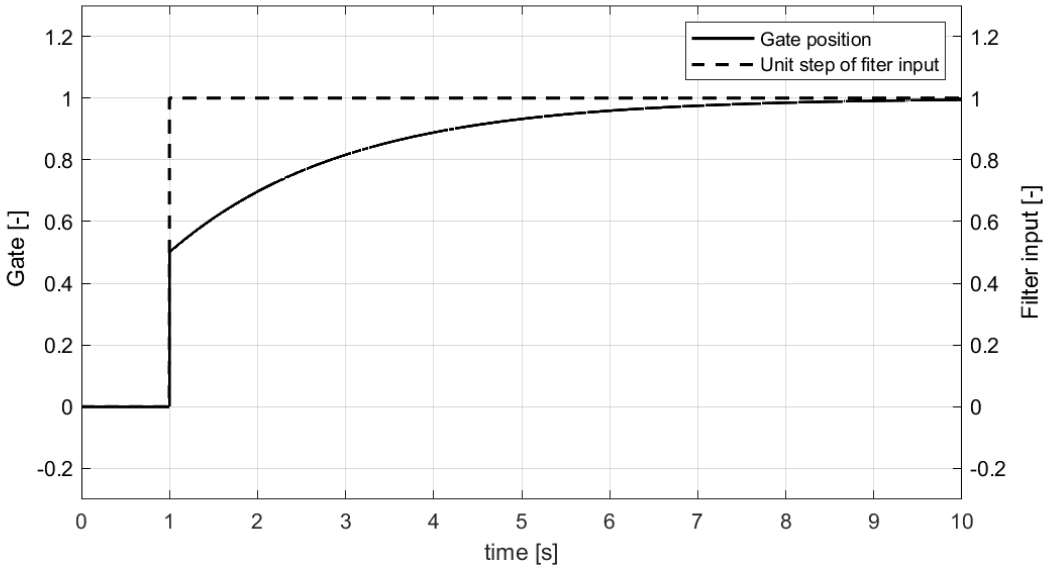

Figure 4: Unit step response of hydro droop controller as presented in (2.18) ($R_t = 2, R_p = 1$ and $T_r = 1\,s$).

2.4 Wind power theory

2.4.1 Power extraction

The main principle of a wind turbine is to convert kinetic power from the wind into electrical power. The total kinetic power in wind can be calculated by

$$P_k = \frac{1}{2}\frac{m}{t}v_w^2 \tag{2.19}$$

where, m is the mass of the air considered, v_w is the wind speed and t is time [31]. When considering a wind turbine the mass of the air is equal to the product of air volume, V passing affecting the turbine and air density, ρ . The air volume can be further expressed as $V = Av_wt$, where A is the swept area of the turbine, therefore making it possible to modify (2.19) to

$$P_k = \frac{1}{2}\rho A v_w^3. \tag{2.20}$$

To note is that the wind kinetic power increases by the cube of the wind speed causing even a small changes wind speed to have a large impact on the wind power

Wind turbines can however not convert the total P_k to mechanical power, driving the wind turbine, $P_{m,wt}$, and the ratio between these powers are called the power coefficient, C_p. By including C_p in to (2.20) the driving power of the wind turbine can be expressed as

$$P_{m,wt} = \rho A\frac{v_w^3}{2}C_p. \tag{2.21}$$

It is also useful to describe a wind turbine in per unit format and converting (2.21) to per unit by normalizing it with the wind turbines rated value, P_0, results in

$$P_{m,wt} = \rho A\frac{v_w^3}{2P_0}C_p. \tag{2.22}$$

The value of C_p is based on the aerodynamics of the turbine blades and their efficiency in gathering the energy of the wind. Consequently, C_p for a given turbine depends on the turbine blade design and blade angel, β. Additionally C_p also depends on the the tip speed ratio, λ, which has the relationship

$$\lambda = \omega_0\frac{R\omega_{wt}}{v_w} \tag{2.23}$$

in which ω_{wt} is the rotational speed of the turbine in per unit and ω_0 is the wind turbine rated rotational speed in rad/s. For an ideal rotor the value of C_p would be 16/27 or approximately 0.593 according to Betz law. However, as the blades are not ideal and due to losses in the drive train and electrical losses which are often included in to C_p, turbines usually have a maximum C_p of no more than 0.5 [32]. The C_p profile for a turbine is determined by measurements, however a fourth order polynomial can be used to fit an analytical expression of C_p to the measurements. The analytical fourth order polynomial for C_p can be written as

$$C_p(\beta,\lambda) = \sum_{i=1}^{4}\sum_{j=1}^{4} a_{i,j}\beta^i\lambda^j \tag{2.24}$$

where, $\alpha_{i,j}$ are fitting constants used to match the function to measured data [33]. A representation of C_p versus λ and β is shown in Figure 5

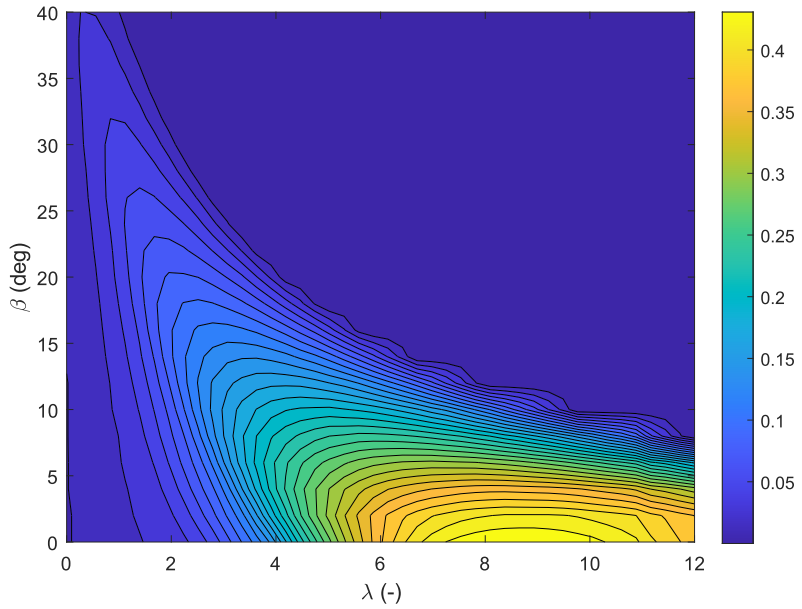

Figure 5: A contour plot of C_p depending on λ and β based on data from Chalmers wind turbine on Björkö.

2.4.2 One mass drive train

The drive train of a wind turbine consists of the turbine blades, gearbox and generator along with other masses part of the wind turbine's rotation [34]. In order to accurately model the dynamic response of ω_t due to a change in the torque, every part of the drivetrain can be individually represented in the model. However the drive train model can be simplified to an aggregated one mass model similar to the power system model of (2.15) and expressed as

$$2H_{wt}\frac{d\omega_{wt}}{dt} + b = \frac{1}{\omega_{wt}}(P_{m,wt} - P_{e,wt}). \tag{2.25}$$

Where, H_{wt} represent the inertia constant of all the drive trains parts, the parameter b represent a dampening factor which consists of the friction and air resistance present in the drive train and $P_{e,wt}$ is the electrical output power of the wind turbine [33] [34]. The inertia constant of a wind turbine in determined through

$$H_{wt} = \frac{J_{wt}\omega_0^2}{2P_0} \tag{2.26}$$

where J_{wt} is the combined inertia moment of the wind turbine drive train in $kg\,m^2$.

2.4.3 Wind turbine characteristics and types

Wind power turbines can be categorized into either Fixed-Speed Wind Turbines (FSWT) or Variable-Speed Wind Turbines (VSWT). For FSWT, power is generated by an induction machine that is directly connected to the grid, resulting in very little variation in the rotor speed. A consequence of the fixed speed is that the power extraction from the wind becomes inefficient, as λ cannot be controlled to achieve the maximum C_p for optimal power extraction in accordance with (2.21) and (2.24). An additional drawback of this

category of wind turbines is that the induction generator draws reactive power, often resulting in the need for external reactive power support [35]. Because of these factors, FSWTs are seldom used today. However, because FSWT are directly connected to the grid, the speed is linked to the system frequency. Therefore, if the frequency decreases, the speed of the turbine decreases, and the energy inherent within the speed change is pushed to the grid, resulting in FSWT providing a natural inertial response [36].

Instead, the VSWT are designed to optimize their efficiency by controlling the rotor speed for an optimal tip speed ratio λ_{opt} to maximize C_p. This speed control is achieved primarily using one of the two technologies. The first technology is the doubly fed induction generator (DFIG) turbine. The DFIG utilizes an AC to DC to AC converter connected to the rotor winding to control the excitation frequency, thereby allowing for rapid speed control [34]. As the converter is only connected to the rotor circuit, it is not required to be rated at the full output of the turbine, and only a rating of 30 percent is usually sufficient. Furthermore, this arrangement allows for control over the reactive power, resulting in the fact that external reactive power support is not required, in contrast to FSWT [35].

The second technology that is utilized for the speed control of a VSWT is the full converter interfaced generator, in which the generator is completely decoupled from the grid as the only connection is through an AC to DC to AC converter [35]. This grants the turbine a fully independent speed, active power and reactive power control, thereby making it possible to operate at optimal efficiency with respect to wind speed. However, this type of turbine has an increased cost compared to the DFIG, considering that the converter is required to be rated for the full output of the wind turbine.

One inherent characteristic of VSWT is that there is no natural inertia response to frequency variations in the power system [36]. The reason for this lack of inertia response is the speed control. As the control endeavors to maintain the speed for λ_{opt} it will be unaffected by changes in the system frequency, in contrast to FSWT. Consequently, no kinetic energy is extracted from a change in speed, resulting in the VSWT reducing the overall system inertia.

2.4.4 Control system

The control of a VSWT can be divided into different operations depending on either rotational speed of the turbine or the wind speed condition[34], [37], [38]. In this work, the VSWT operation has been divided into 4 different operational regions based on rotational speed visualized in Figure 6

For region 1 the ω_{wt} of the turbine is sufficiently low that the correlating wind speed does not produce sufficient power according to (2.21) to justify the wear on equipment [34]. Therefore when operating in this region, the VSWT does not produce any power. Additionally this region is used to quickly accelerate the VSWT during start up, when the wind speed has increased beyond the cut in limit [38]. This quick acceleration is useful due to the wind turbine having a low C_p at low values of λ, which can be seen from Figure 5, causing a limited mechanical output until the VSWT has picked up speed.

Region 2 for the VSWT is characterized by ω_{wt} being greater than the limit for region 1 while also being below its rating. For this region, the goal of the control is to optimize the power extraction from the wind by operating at $C_{p,max}$ [34],[37], [38]. By studying how C_p depends on λ and β as represented in Figure 5, it is possible to determine the optimal angle of β, β_{opt}, and the optimal value of λ, λ_{opt} that represents $C_{p,max}$, causing

the optimal wind power extraction. As β do not have an external influence, this parameter can simply be set to β_{opt}, which is also its minimal value, when operating in region 2. The control focus of region 2 is therefore on achieving λ_{opt} by controlling the output power to change ω_{wt} proportionally to the current wind speed.

The third region for the VSWT shown in figure 6 may appear as the VSWT ω_{wt} rating is reached before the power rating of the VSWT while operating in region 2. Therefore in operating region 3, the VSWT deviated from tracking the optimal power point due to the limit imposed by the speed rating. Instead the output power is adjusted in order to keep operating at the rated speed [37].

When the wind speed increases, causing the output power of the VSWT to also hit its limit, it is no longer possible to increase the output power for limiting ω_{wt}. Instead is it therefore necessary to reduce the mechanical power to not have ω_{wt} increase uncontrollably[34], [37]. Therefore, in region 4, the turbine C_p is controlled in order to control the effectiveness of the wind turbine aerodynamics. The control strategy of this region is to change the angle of β to effectively control C_p in order to keep ω_{wt} constant.

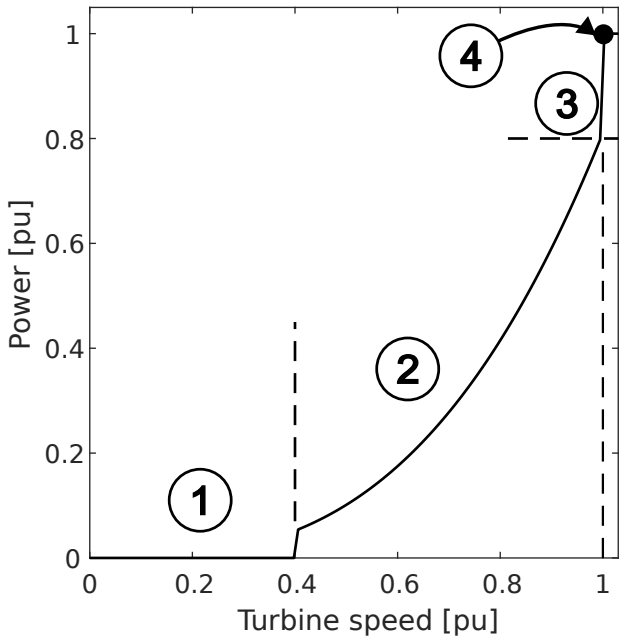

Figure 6: VSWT operating regions based on turbine speed.

2.4.5 Inertia emulation

As mentioned in Section 2.4.3, VSWT does not naturally provide inertia to the power system frequency. The mass and rotational speed of the combined drivetrain of a VSWT does have an inertia constant comparable to traditional generation units. However, this inertia is normally not accessible to the power system due to the control of the VSWT for optimal power [15]. Therefore, by modifying the control for the VSWT to emulate the synchronous generator response to a frequency deviation, the power system can access the inertia constant of the VSWT. This inertia emulation control will mitigate the reduction of the power system inertia constant caused by the increase of converter interfaced generation. It is however important to keep in mind that unlike a directly connected synchronous

generator which always operates close to the synchronous speed, the speed of a VSWT can vary depending on the wind condition. Therefore the available inertia of a VSWT to support the system frequency is not constant, but varies with regards to ω_{wt} [33]. Hence the emulated inertia from a VSWT is reduced for low wind speeds. Additionally, if the VSWT already operates close to its rated power, could the inertia emulation cause the VSWT to shortly exceed its rated power. It is therefore also important to ensure that this exceed operation does not damage the equipment in the VSWT before inertia emulation is applied when at rated operation [33].

A additional important factor to consider when it relates to the ability of VSWT to provide inertial response is that, unlike a synchronous generators which response to the frequency is unchangeable and entirely decided by the mass of the machine and its electromagnetic coupling to the grid, the inertial response of a VSWT can be controlled. As a result, there is a freedom in creating an inertia response of VSWT that is optimized for the power system frequency control needs. For example can the VSWT inertia response be used to compensate for the initial opposite response a hydro power governor has to a frequency disturbance, as discussed in Section 2.3.1.

2.4.6 De-rated operation with droop control

A VSWT can also provide the power system with frequency control if the turbine is controlled to not operate at its optimal point and if the rated power of the turbine is limited. This control action creates a de-rated operation of the VSWT and establishes a power reserve which is used for frequency containment. The de-rating of the VSWT is achieved by either changing the pitch angle of the turbine blades or increasing the rotational speed of the turbine. [39] The first method causes the turbine to operate at a suboptimal β while the second causes the turbine to operate at a sub optimal λ. Both methods can therefore be used to reduce $C_p(\beta, \lambda)$ to a desired value. De-rating speed control has a more rapid rapid response to desired change in the de-rating of the turbine when compared to the pitch control for de-rating. The speed control however risks significantly overspeeding the turbine when creating only a small power reserve and using the pitch may therefore be necessary if a larger power reserve is desired [39]. It is also possible to reduce the speed in order to change λ. However, power is required for accelerating the turbine in order to extract the power from the created power reserve. This acceleration will therefore mitigate any frequency control using this de-rating method for the first seconds after a disturbance [15].

Using droop control, the power reserve can be deployed by reducing the de-rating level for up-regulation of the frequency or more power can be shedded for regulating down the frequency. As a wind turbine does not have the initial opposite reaction to a change in power as a hydro generator, there is no need for a high transient droop and the same droop constant can be used for the complete control action. As a result, the wind power frequency droop control is quicker compared to the hydro control. The main drawback for the VSWT droop control is the requirement of a de-rated operating point, reducing the output power [8]. Therefore the de-rating is preferably kept low to limit the loss in power, but at the cost of increased frequency stability. As the reserve for up regulation usually is smaller than the power that can be shedded, different droops can be used for up and down regulation [40]. Using different droops has the benefit of not limiting the strength of the down regulation due to a limited up regulation reserve. Figure 7 shows the power response as a function of the frequency when using different droops.

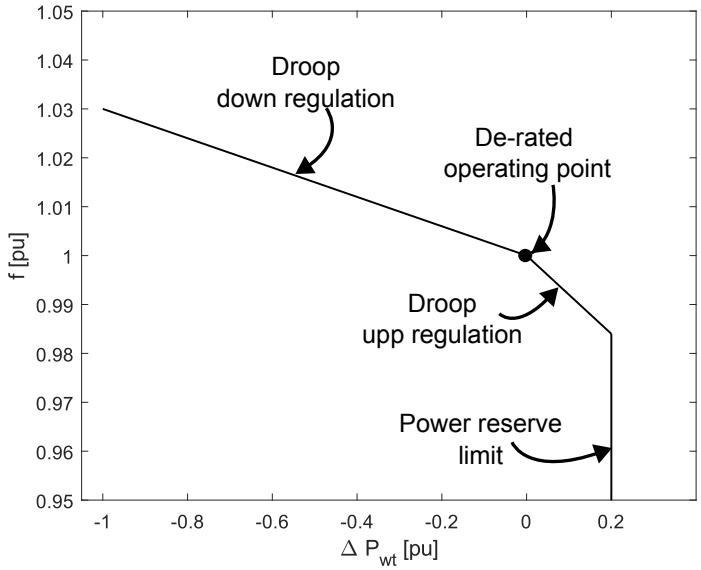

Figure 7: Example of frequency to power relationship with using a different droop for up and down frequency regulation [40].

3 One bus modeling of a wind-hydro system for frequency stability studies

Frequency stability simulations of a wind-hydro system was first conducted using the MATLAB/Simulink environment. In the Simulink environment a model of a VSWT providing frequency support was created to represent an aggregated wind farm. This VSWT model is then added to a one bus model of a power system which is using a hydro governor for frequency control. In the following sections, the MATLAB/Simulink models used for the frequency stability studies are described and values for the parameters in the models can be found in Appendix A. The MATLAB/Simulink model does not include voltages or electrical distances in the form of power lines. These will however instead be included in the PSS/E simulations described in Section 4.

3.1 One bus system model

Figure 8 depicts the model for the single bus power system used in the MATLAB/Simulink simulations. The model is constructed by transforming (2.15), describing the power system frequency change due to a power imbalance, to the frequency domain by replacing the derivative with the Laplace operator. Additionally due to not modeling voltage in the MATLAB/Simulink simulations, the voltage dependency of the load is neglected. In frequency domain, (2.15) can be therefor expressed as

$$\Delta f = \frac{1}{2H_{sys}s + D}(\Delta P_m - \Delta P_L). \tag{3.1}$$

When considering that the power system model consist of a combination of wind and hydro power, the change of the mechanical power, ΔP_m, experienced by the system can be divided in to a wind power part, $\Delta P_{e,wt}$ and a hydro power, ΔP_h part. Additionally, when increasing the wind power penetration, WPP, the inertia constant, H_{sys}, of the system will change according to 2.7, describing that the aggregate system H_{sys} is the mean of the H_i of all individual generators connected to the system. Considering that VSWTs do not inherently providing inertia to the power system, the system inertia for the simplified system consisting of an aggregated hydro and VSWT unit can therefore be calculated using

$$H_{sys} = H_h \cdot (WPP - 1) \tag{3.2}$$

where H_h is the hydro inertia constant. The H_h used for the system model is 4.9 s and based on the system model in [11] of a hydro dominated system. Furthermore, the control strength of the hydro power decrees relative to the size of the system when WPP increases. Therefore, to represent this control strength decrease when changing ΔP_h from being represented on the machine base to being represented on the system base, it is multiplied with $1 - WPP$. $\Delta P_{e,wt}$ is instead multiplied with WPP when going from machine base to system base as the strength of the wind power control increases with the penetration of the wind power.

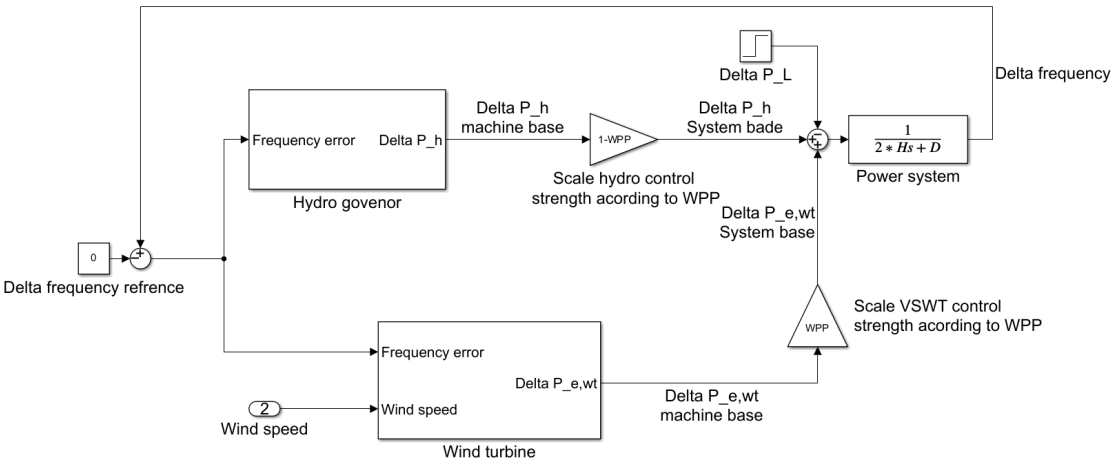

Figure 8: Single bus power system model showing the incorporation of the hydro governor and VSWT

3.2 Hydro unit with governor

The model used to represent the hydro governor power response from a deviation of the system frequency is shown in Figure 9. The governor model is created to give an equivalent frequency control response as the model presented in [11] which, in turn, was made to emulate the aggregated response of a hydro dominated system example. From the model presented in Figure 9 are the turbine transfer function recognizable from (2.17) and the lead-lag filter is presented in (2.18). Additionally, the model has two first order low pass filters where one is meant to represent the actuator dynamics which physically changes the gate position and the other represents a filter on the input frequency error.

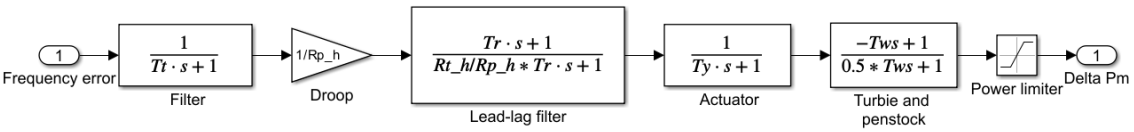

Figure 9: Hydro model based on [11] and [14] tuned to give an equivalent response as the model in [11].

3.3 Wind turbine model

To represent wind power into the power system, a model of a VSWT is used and Figure 10 shows an overview of the VSWT model. The parameters used for the VSWT model are based on the Chalmers wind turbine located on Björkö and available in Appendix A. The output of the turbine model is treated as the aggregated output of a wind farm. The inputs of the model are the frequency deviation from its nominal value,Δf, and the wind speed. The model is able to use both a constant wind speed and a variable wind speed where for the variable wind speed, a time series of the wind speed is imported. To implement the control structure used in this model, no changes to the wind turbine hardware are required and can therefore be implemented though software changes.

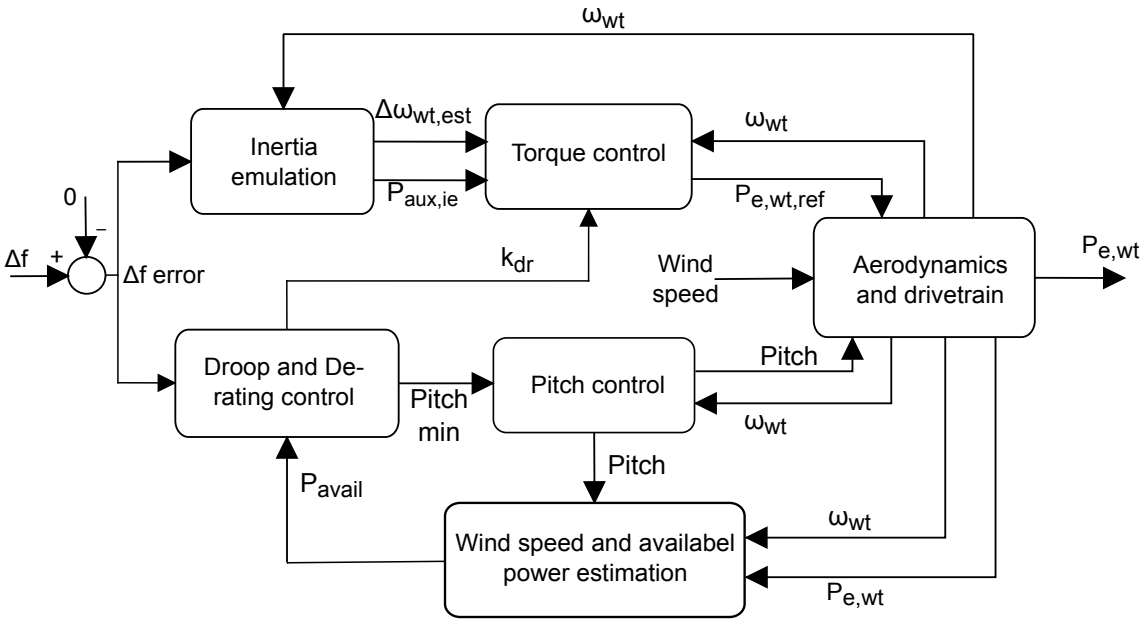

Figure 10: Wind turbine overall control structure including inertia emulation and de-rated control with droop support form an available power estimate.

3.3.1 Aerodynamic and drivetrain model

The part of the VSWT model representing the physical turbine is presented in Figure 11. The model takes the wind speed, the current pitch as well as the set point for the VSWT electrical power, $P_{e,wt,ref}$, as inputs and outputs ω_{wt}. The model can be divided in to a aerodynamic part and a drivetrain part, where in the aerodynamic part, the VSWT's power extraction from the wind's kinetic energy is implemented according to (2.21) to get the $P_{m,wt}$ driving the turbine rotation. Necessary for (2.21) is $C_p(\beta, \lambda)$ which is determined through the use of a look-up table. The value of the VSWT C_p is measured for different β and λ to create the look-up table. Based on the supplied λ and β to the table a linearly interpolate estimation is made from the measured data points to determine C_p, where λ is calculated from the wind speed and ω_{wt} using (2.23). A limit is also placed on the look-up table output to not have a C_p less than 0, as the interpolation sometimes can produce negative values.

For the drive train section of the model is $P_{m,wt}$ compared to $P_{e,wt}$ where the difference, once divided with ω_{wt}, constitutes the accelerating torque applied to the VSWT drive train. To note is that the electrical efficiency of the turbine generator has been neglected to simplify the designing of the models. One simple method for including the efficiency is to multiply $P_{m,wt}$ by an efficiency factor. Including the generator efficiency in this way would however only result in a small power reduction and not impact the dynamic performance of the wind turbine. By also considering that the generator efficiency is usually high, has therefore the generator efficiency been neglected. The drivetrain is implemented in the VSWT model by converting (2.25) to the frequency domain by the use of the Laplace operator. The VSWT drivetrain is model is therefore implemented as

$$\omega_{wt} = \frac{1}{2H_{wt}s + b}\frac{1}{\omega_{wt}}(P_{m,wt} - P_{e,wt}). \tag{3.3}$$

Within the MATLAB/Simulink modeling is the electric power set point, $P_{e,wt,ref}$, the same as the electric power $P_{e,wt}$ due to neglecting the influence of the converter. Neglecting the

converter influence is motivated by the fact that the speed of the converter is typically much faster than the speed of the mechanical system while also assuming that any current limitations on the converter are not exceeded.

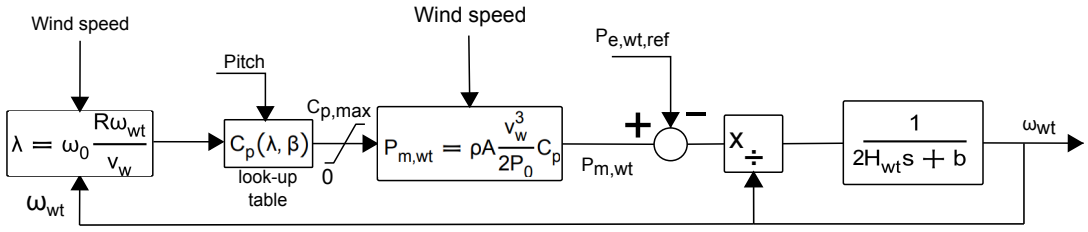

Figure 11: Wind turbine aerodynamic and drivetrain model.

3.3.2 Torque control model

The torque control of a wind turbine is utilized for controlling ω_{wt} when operating in region 2 and 3 referring to Figure 6. The block diagram of the torque controller used in the VSWT model which is based on [41] is shown in Figure 12. The controller has as inputs the VSWT rotational speed, ω_{wt}, a estimation of the speed change due to inertia emulation, $\Delta\omega_{wt,est}$, a de-rating factor, k_{dr}, and the inertia emulation auxiliary power, $P_{aux,ie}$. The inputs of $P_{aux,ie}$, $\Delta\omega_{wt,est}$ and k_{dr} will be further explained in Section 3.3.5 and 3.3.6 describing VSWT control for supporting the frequency. The output of the torque controller is the VSWT electrical power set point, $P_{e,wt,ref}$. The Torque controller is constructed around a PI controller which uses a speed error to adjust the load torque reference. The load torque reference is limited to be within $T_{max} = P_{max}/\omega_{wt}$ and $T_{min} = P_{min}/\omega_{wt}$ where P_{max} and P_{min} are decided by the converter ratings. If the $b\omega_{wt}$ compensation shown in Figure 12 is disregarded for the moment is the load torque reference then multiplied with ω_{wt} to get the electrical power set point excluding any frequency control, $P'_{e,wt,ref}$. The $P'_{e,wt,ref}$ are then modified for de-rated operation to provide droop based frequency control and/or modified to emulate the VSWT inertia by multiplying $P'_{e,wt,ref}$ with k_{dr} and adding $P_{aux,ie}$. The resulting $P_{e,wt,ref}$ is then supplied to the drivetrain to get the $P_{e,wt}$ and ω_{wt} for the VSWT model as described in Section 3.3.1. The resulted ω_{wt} is fed back to the torque controller where its difference compared to the sum of the speed reference, $\omega_{wt,ref}$, and $\Delta\omega_{wt,est}$ creates the speed error for the PI controller.

$\omega_{wt,ref}$ for the torque controller in Figure 12 is calculated from a pre-defined relationship between $P'_{e,wt,ref}$ and ω_{wt}, derived to control the speed for operating the turbine at $C_{p,max}$. The relationship for calculating the $\omega_{wt,ref}$ is derived by combining (2.22) and (2.23) resulting in

$$P_{m,wt} = \frac{\rho A C_p}{2P_0}\left(\frac{R\omega_{wt}\omega_0}{\lambda}\right)^3. \tag{3.4}$$

By then stating that the turbine operates at optimal power with λ_{opt}, $C_{p,max}$ and that $P'_{e,wt,ref}$ is equal to $P_{m,wt}$ by considering that the wind turbine generator electrical efficiency has been neglected, (3.4) can be rearranged to determine a preliminary $\omega'_{wt,ref}$ as

$$\omega'_{wt,ref} = \frac{\lambda_{opt}}{R\omega_0}\left(\frac{2P_0 P'_{e,wt,ref}}{\rho A C_{p,max}}\right)^{1/3}. \tag{3.5}$$

$\omega'_{wt,ref}$ is then limited and sent through a first order transfer function to get the $\omega_{wt,ref}$ which is used for calculation the speed error. The limit is to avoid operating at turbine speeds higher than what it is rated for and $\omega'_{wt,ref}$ is therefore limited by a max reference

speed parameter, *RefSpd*, set to 0.97 pu. The limit of $\omega'_{wt,ref}$ would ideally be set to its rated speed at 1 pu. However for this VSWT model, when both the speed and pitch controllers control the speed to the rated speed, it results in interference between the controllers and to early pitching. By including a 0.03 pu cushion between the max speed used for the torque control and the rated speed used for the pitch, the torque control has time to fully activate before the pitching starts. Therefore by increasing the speed of the torque control could this cushion be reduced. The $\omega'_{wt,ref}$ is also limited by a cut in speed, *CutSpd*. The cut in speed results in the VSWT quickly accelerating during start up but has limited effect on the VSWT during operation as the power at the cut in speed is low. If the wind speed is low enough to cause ω_{wt} to drop down to the cut in speed the operation VSWT should fall within region 1 referring to Figure 6 and hence stop producing power. The filter is also included in the calculation of $\omega_{wt,ref}$ to allow for some variation of ω_{wt} around the optimal power point and therefore reduce transients in the torque control [41].

Also to note is that once the power rating of the converter is reached, the torque controller is no longer able to control the speed. Instead the pitch controller is used to maintain the rated speed. However, there may still be a speed error supplied to the PI controller which, due to the converter power limit, it is unable to act upon, causing a build up of the error in the PI controllers integrator. This error build up causes the controller to not respond to changes in the speed once the speed goes down until the error is removed. Therefore, to avoid the integrator error build up, an anti wind-up loop is added to the controller (not included in figure 12 but symbolized by the PI saturation). The anti wind-up loop adds a term proportional to the difference between the power limited by the converter and the unlimited power to the PI integrator input, creating a zero input to the integrator after the power reaches the converter rating.

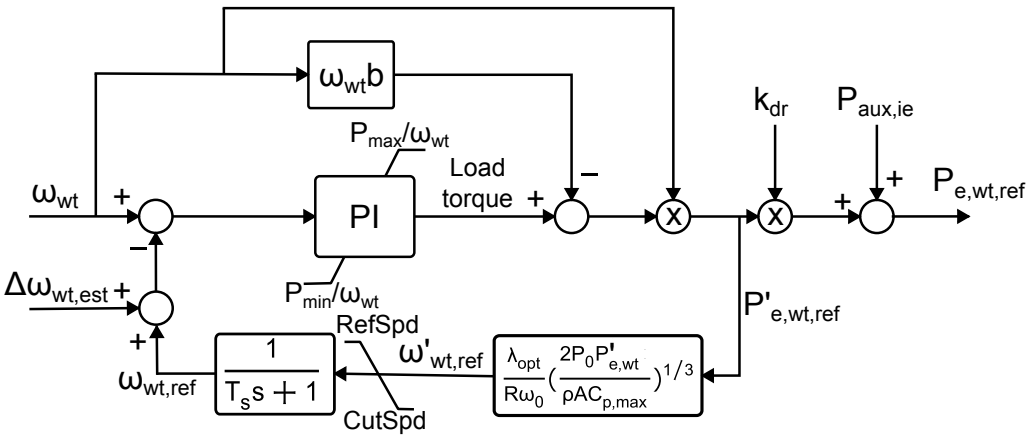

Figure 12: Torque control model including modification to allow for inertia emulation and de-rated control.

It is important to note that, due to assuming optimal power operation when using (3.5) to calculate $\omega_{wt,ref}$ the result will differ from the optimal speed of the turbine if the VSWT

is not operating at its optimal point. However, the VSWT mechanical power is affected by the a change in ω_{wt} through C_p while the electrical power is proportional to the cube of ω_{wt} and considering that the blades are designed to have a high C_p for a large variation of ω_{wt}, the electrical power will be affected by the speed error to a greater extent compared to the mechanical power. As a result, if the calculated reference speed is lower than the optimal speed, the electrical power will be lower than the mechanical power causing the speed to increase until equilibrium is found. The same reasoning applies when $\omega_{wt,ref}$ is higher than the optimal speed. This phenomena is visualized in Figure 13 showing how $P_{m,wt}$ and $P_{e,wt}$ changes depending on ω_{wt} while the wind speed is constant. The $P_{m,wt}$ is decided by the VSWT aerodynamics and the wind speed when the $P_{e,wt}$ is decided by the torque controller. Figure 13 shows that ω_{wt} will accelerate or decelerate if ω_{wt} deviates from the intersection point causing it to operate close to this point. This method will however still create a small error between ω_{wt} and the optimal speed at steady state. This error is a result of the damping, b, in the drivetrain creating a difference between $P_{m,wt}$ and $P_{e,wt}$ at steady state. This error can be compensated for by subtracting the term $b\omega_{wt}$ from the load torque reference calculated by the PI controller as shown in Figure 12.

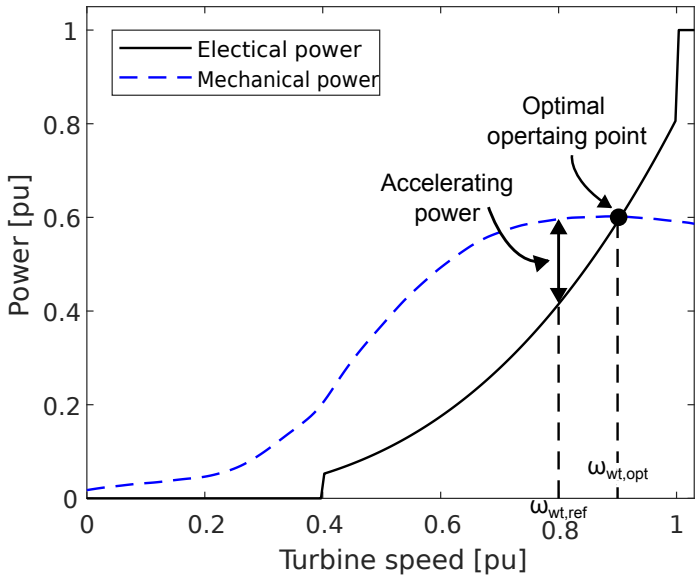

Figure 13: Operating principle for finding the optimal speed, $\omega_{wt,opt}$, of the wind turbine by visualising how the $P_{m,wt}$ and $P_{e,wt}$ depends on ω_{wt} for a constant wind speed

3.3.3 Pitch control model

To avoid an uncontrolled runaway of ω_{wt} at high wind speeds, as a result of the torque control retching the VSWT power rating, $P_{m,wt}$ is limited by pitching the blades of the VSWT. The control used for the blade pitching in the VSWT model is presented in Figure 14. The pitch is controlled using a PI controller on the speed difference between ω_{wt} and $\omega_{0,pu}$, where $\omega_{0,pu}$ is the VSWT rated speed in pu. The pitch is then saturated to keep it within its allowed range as well as its allowed rate of change. The minimum pitch for the saturation is determined in the de-rating and droop control model of Section 3.3.5 where it is set to 0 during normal operation and increased as the VSWT is de-rated. It is

also important to keep the integrator in the PI controller from winding up as the VSWT often will operate with a saturated pitch when at the same time there is a large speed error going in to the controller, i.e. when the VSWT operate below rated ω_{wt}. Therefore, the pitch controller is supplied with an anti windup loop which removes the input to the integrator when the controller hits saturation.

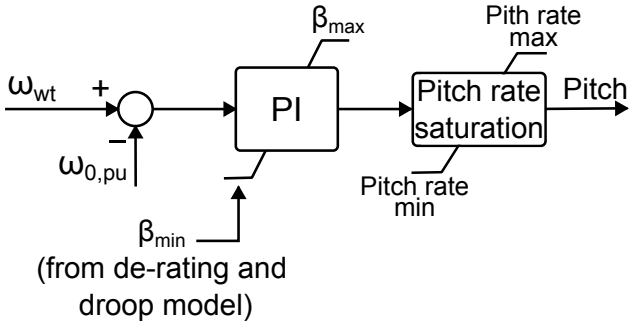

Figure 14: Pitch controller and actuator model.

3.3.4 Available power estimation

For a VSWT to be able to contribute to frequency regulation by controlling its de-rated operation to provide droop support, it is required to be able to reliably estimate the power available to the VSWT. The available power estimate is used as a reference signal for the de-rated control to know by how much the VSWT should be de-rated. The method used to estimate the available power is based on the method described in [42]. This method of estimation of the available power can be divided into two stages where initially the wind speed seen by the wind turbine is estimated using parameters from the wind turbine. This estimated wind speed is then used to calculate the available power.

The wind speed is estimation is shown in Figure 15 and is based on

$$v_{w,est} = (\frac{2P_{e,wt}P_0}{\rho A C_p})^{(1/3)} \tag{3.6}$$

which is a rewrite of (2.22) where ρ and A is known for the VSWT. $P_{m,wt}$ form (2.22) is however replaced by $P_{e,wt}$ as the $P_{m,wt}$ applied to the VSWT is difficult to measure and $P_{e,wt}$ should equal $P_{m,wt}$ considering that the VSWT generator electrical efficiency has been neglected. That $P_{e,wt}$ and $P_{m,wt}$ is equal does however not hold when inertia emulation is applied and the case of inertia emulation on the wind speed estimation is further discussed in Section 3.3.7. The VSWT C_p is required for (3.6) and is determined through a look-up table of $C_p(\beta, \lambda)$ measurement in a similar manner as in Section 3.3.1. λ is however calculated in this case through (2.23) by feeding the estimated wind speed back instead of using the applied wind speed. By feeding back estimated wind speed does the wind speed estimation become an iterative method, performing a new iteration every simulation time step. This iterative method of estimating the wind speed could cause issues if the initial wind speed used is far from the applied wind speed. However, unless the initial wind speed is 0 causing problems in the division in (2.23), where there is no problem in finding an estimated wind speed. Using an initial wind speed of 3 m/s worked for all cases tested in this work. As the estimated wind speed is based on the VSWT current C_p and power output, it will be able to correctly estimate the wind speed even when the VSWT is de-rated. Using this method to estimate the wind speed causes

the moment of inertia of the VSWT to become included in the estimation and there is therefore no need for compensating for the inertia when calculating the available power.

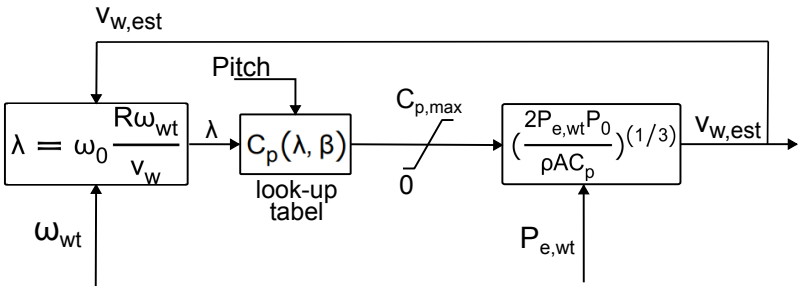

Figure 15: Flow diagram of wind speed estimation based on (3.6) where Cp is determined from a lookup table.

Figure 16 shows the block diagram of how the available power is calculated based on the estimated wind speed. For the available power calculation is (2.21) utilized. However the C_p used is the optimal C_p possible with regards to the estimated wind speed. The optimal C_p is determined by firstly calculating the VSWT optimal rotational speed for the estimated wind speed according to

$$\omega_{wt,opt} = \frac{\lambda_{opt} \cdot v_{w,est}}{R\omega_0} \tag{3.7}$$

where λ_{opt} is the value of λ corresponding to $C_{p,max}$. The calculated $\omega_{wt,opt}$ is added with $\Delta\omega_{wt,est}$ to avoid controller interference, see Section 3.3.7, then limited to keep it within the speed ratings of the VSWT, i.e. within 0 to 1 pu. This limited $\omega_{wt,opt}$ is then through (3.7) converted to a λ representing the optimal λ possible for the estimated wind speed while considering the limitations of the VSWT rotational speed. A look-up table $C_p(\lambda)|_{\beta=0}$ is then used which gives the value of C_p based on the λ supplied to the table while the pitch is 0. By supplying the most optimal possible λ to the look-up table, the optimal C_p is gathered for use in (2.21) to determine the available power. However, up to this point in the available power calculation, the power limit of the VSWT has not been taken into account. Hence a saturation is necessary at the end to limit the available power to the rating of the VSWT. In the limitation there is also a inclusion of the auxiliary inertia emulation power, $P_{aux,ie}$, from the inertia emulation model. $P_{aux,ie}$ is included to avoid controller interference and further discussed in Section 3.3.7.

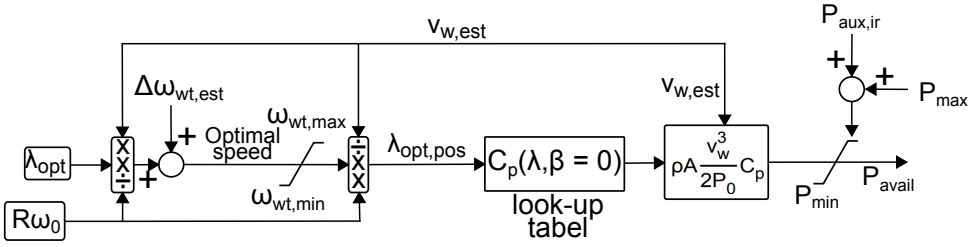

Figure 16: Flow diagram of available power estimation based on 2.21 using Cp determined from $\beta = 0$ and the optimal possible λ.

3.3.5 Control model for de-rated operation

The control structure used for providing droop frequency support by creating a power reserve through de-rated operation from the VSWT as discussed in Section 2.4.6 is shown in Figure 17. The de-rating control calculates the factor, k_{dr}, which states at what percentage of available power the VSWT should operate in order achieve the desired output. k_{dr} is calculated through the equation

$$k_{dr} = \frac{P_{avail} - P_{reserve} + P_{aux,dr}}{P_{avail}} \tag{3.8}$$

where P_{avail} is the available power, $P_{reserve}$ is the specified power reserve and $P_{aux,dr}$ is the droop based frequency power support for the frequency control. The reason for placing the filter on P_{avail} is to break up a loop in the VSWT model, making it easier for the solver to find a solution. The filter will also help by removing any high frequency noise on the signal. To not have the filter significantly influence the VSWT operation should the time constant for the filter, T_a, be low, where 0.01 s is what has been used in the work. The filter output does also have a small lower limit in order to not have a division by 0 to occur. A limit is also set on k_{dr} to keep it within 0.2 to 1. The upper limit is there for the control to not try to operate the VSWT beyond its optimal point while the lower limit is there because the wind speed estimation needs some power production to function correctly. Additionally, the lower limit is in place to avoid issues when reducing the power too much. When the power reduces, C_p in (3.6) follows as the pitch is changed. However when C_p is low are any inaccuracies in the wind speed estimation amplified and the wind speed estimation sensitivity to changes in the pith is increased. As a result, the wind speed estimation can produce large errors when the VSWT is de-rated by too much. The $P_{aux,dr}$ is decided by using a proportional gain on the frequency error to decide the desired wind power frequency support. Considering that the ability for a VSWT to down regulate the frequency is greater, different droops are used for up and down regulation where a lower droop (higher gain) is used for down regulation as shown in Figure 7. A deadband on the droop control is also implemented causing frequency deviations within the deadband to not be acted upon by the controller. Furthermore can the droop and de-rating control be turned off by setting the parameter *DeRatedON* to 0.

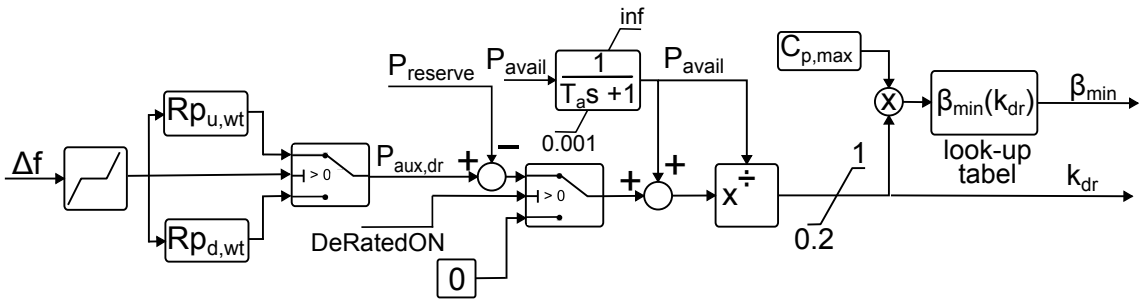

Figure 17: Model of droop frequency control and de-rated operation showing the calculation of k_{dr} from (3.8) and the β_{min} for the pitch control.

The operational principle of the de-rating controller is shown in Figure 18. The solid lines show how $P_{m,wt}$ and $P_{e,wt}$ change depending on ω_{wt} for a constant wind speed during normal operation while the dotted lines show the same for de-rated operation. Figure 18 shows that in order to operate de-rated at the same ω_{wt} as normal operation, both the

driving and the load power for ω_{wt} needs to be reduced by the same amount. The load power is modified by taking the product of $P'_{e,wt,ref}$ in Figure 12) and the de-rating factor, k_{dr}, as the new VSWT power reference. This product causes the power-to-speed curve of the VSWT to be reduced by the factor, k_{dr}. The reduction of $P_{m,wt}$ is achieved by pitching the turbine blades and therefore reducing the VSWT's C_p. Pitching for de-rating the VSWT were chosen over increasing the speed as pitching gives more freedom over the size of the created power reserve. As noted in Section 2.4.6 , using the speed for de-rating the VSWT will limit the possible power reserve due to limitations of the possible speed of the turbine. The determination of the required pitching is shown in Figure 17 and is achieved by calculating a desired C_p though the product of k_{dr} and $C_{p,max}$. Then, using a look-up table, the pitch associated with the desired value of C_p is determined. This pitch becomes the minimum pitch for the pitch controller, see Figure 14, where normal pitching still applies when the VSWT reaches its specified de-rated power limit.

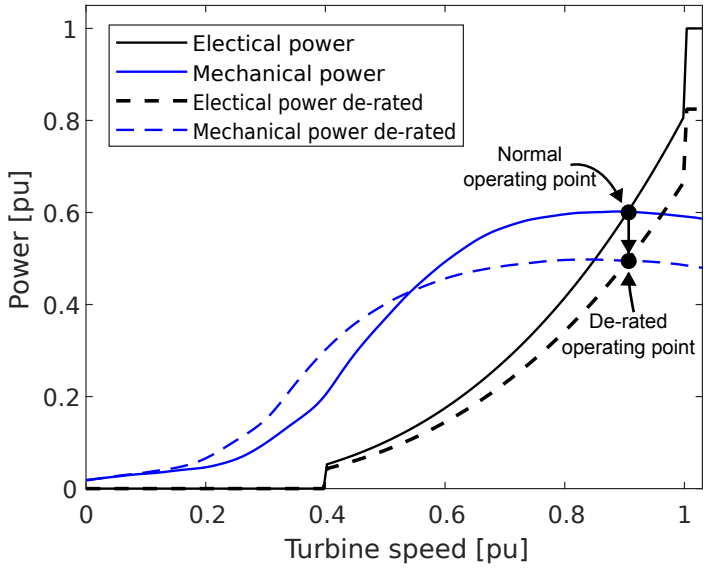

Figure 18: $P_{e,wt}$ and $P_{m,wt}$ dependency of ω_{wt} for a constant wind speed during VSWT normal operation and de-rated operation, showing how the VSWT operation point moves when de-rated

Figure 19 shows how the de-rating factor and the minimum pitch changes for the model based on Chalmers wind turbine when creating a 0.1 pu power reserve for different wind speeds. Up until approximately 3.5 m/s is the wind speed not large enough to to be able to de-rate the turbine by the desired amount. Instead the lower limit on k_{dr} is reached. This showed that there is a lower limit for the wind speed in order to have the de-rated control function as desired. As the wind speed increases, the wind turbine is de-rated less percentage wise to achieve the 0.1 pu power reserve, causing the pitch to decrease and move closer to optimal operation. At approximately 7.5 m/s, the wind turbine's new de-rated rated operating point is reached. Further increase of the wind speed has therefore no impact on the de-rated control. From Figure 19 it can be noted that the de-rated control and droop support prefers a high wind speed. When at a high wind speed there is greater range of possible power production for the wind turbine, resulting in an increased flexibility in the amount of power which can be de-rated. The increased flexibility allows

for the possibility of greater power reserves, both for up and down-regulation.

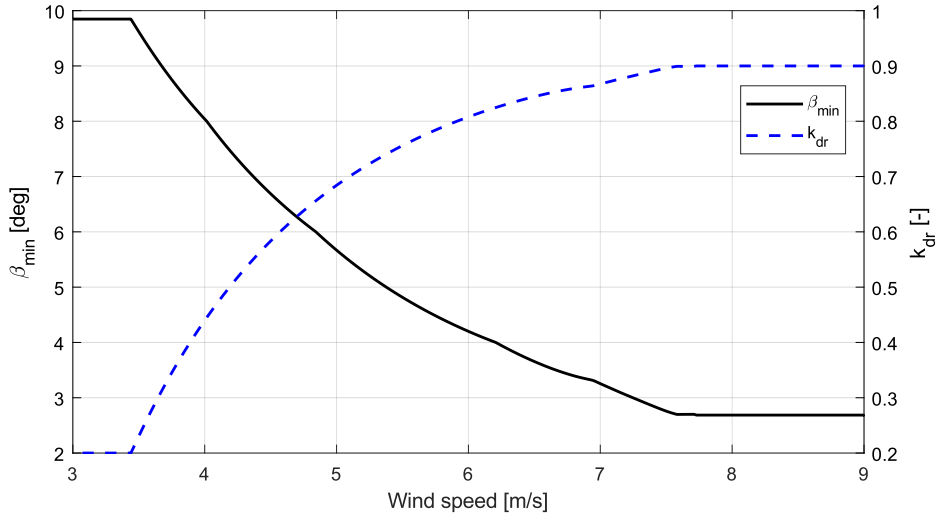

Figure 19: How k_{dr} and β_{min} relate to the wind speed when creating a power reserve of 0.1 pu.

The use of $C_{p,max}$ to calculate the desired C_p is an approximation as the VSWT C_p is not equal to $C_{p,max}$ during the VSWT operating regions 3 and 4. This approximation is not relevant for region 4 as the minimum pitch is not used in this region. The $P_{e,wt}$ curve from the torque control is moved down when de-rated. This effectively causes the rated operating point of the VSWT to be less than 1 pu. The VSWT will therefore reach region 4 at a lower power output and use pitching over the minimal pitch to control the speed. This approximation however causes inaccuracies when in region 3. The result of the approximation of using $C_{p,max}$ is that the de-rated control creates a too small power reserve compared to what is desired. The reduced power reserve is due to the approximation giving a slightly too large target C_p for the look-up table, causing a too small minimum pitch angle. The approximation is however justified by it being difficult to measure the current value of C_p for the VSWT and by considering that the C_p curve is usually quite flat along the λ-axis around $C_{p,max}$ causing the current C_p to not stray far. It is potentially possible to use the estimated C_p from the wind speed estimation of Section 3.3.4. However this was not done as the use of $C_{p,max}$ where considered to be sufficiently accurate.

3.3.6 Control model for inertia emulation

Section 2.4.5 describes how the VSWT can be utilized for providing a power response to the power system which emulates inertia response from an synchronous generator. Figure 20 shows the controller used for supplying an emulated inertia response of the VSWT drivetrain to the power system. The auxiliary power, $P_{aux,ie}$, of the emulated inertia response is calculated by the controller as

$$P_{aux,ie} = 2H_{wt}k_i\frac{d\Delta f}{dt}f \tag{3.9}$$

and is based on the synchronous machine response to a frequency deviation as is described in eq 2.12 [43]. k_i is a gain used to change the impact of inertial response of the VSWT

by controlling what inertia constant the inertial response of the VSWT should emulate. An additional difference is the inclusion of the frequency, f, in (3.9) compared to (2.12). This difference is due to the assumption of a rotational speed close to the nominal speed in (2.12) is not used in (3.9).

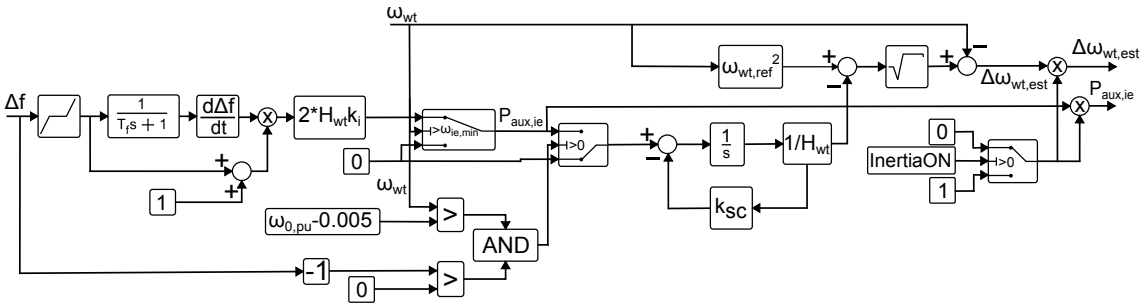

Figure 20: Inertia emulation control model showing the calculation of $P_{aux,ie}$ according to (3.9) and $\Delta\omega_{wt,est}$ according to (3.15)

Figure 20 also includes a filter on the frequency derivative to avoid large spikes in $P_{aux,ie}$ due to sharp transients on the frequency signal. This filter will however reduce the responsiveness of the inertia emulation, causing a difference compared to the response of a synchronous generator. The size of the response difference is decided by the filter time constant. An additional difference to the synchronous response is the possible inclusion of deadbands in the inertia emulation. There is also a block in the inertia emulation which turns it off when the VSWT is operating at a speed lower than the value specified in the parameter $\omega_{ie,min}$. The kinetic energy in the rotation is low when speed is below this limit. Therefore may the inertia emulation reduce the wind turbine rotational speed too much if applied at the low speed, causing the turbine to stall. The output $P_{aux,ie}$ of the controller is added to the VSWT power reference as shown in Figure 10 to facilitate the inertia emulation.

Of note is that the current implementation has no upper limit on the inertia emulation power support being implemented. Consequently, could the VSWT power shortly increase over the VSWT rating if the inertia emulation tries to regulate a frequency drop while close to rated power. Whether this overloading condition is possible is decided by the converter. The mechanical system has enough thermal mass that operating it shortly over the rating will not cause any damages. However the converter may quickly overheat causing significant aging. Therefore must the converter be able to handle the operating overrated caused by the inertia emulation for this implementation to be possible. To prevent overloading a maximum power limit P_{max} can be added on the output of Figure 12 if the converter cannot operate beyond its rated power.

The inertia emulation control of Figure 20 also consists of a second part where the estimated turbine speed change $\Delta\omega_{wt,est}$ due to the added $P_{aux,ie}$ is determined. This estimation is necessary to have the torque controller not try to compensate for the inertia emulation causing speed change and therefore cause the inertia emulation to be weaker than calculated. Hence the speed reference of the torque control is modified by adding $\Delta\omega_{wt,est}$ as shown in Figure 10. The estimation of $\Delta\omega_{wt,est}$ is derived by using the equation calculating the change in the turbine's kinetic energy caused by the extraction of $P_{aux,ie}$ and can be set up as

$$E_{k,ie} = E_k - E_{ie} \tag{3.10}$$

$E_{k,ie}$ is the kinetic energy of the VSWT after the inertia emulation and E_{ie} is the energy extracted by the inertia emulation. By taking the integral of E_{ie} and using (2.3) to rewrite $E_{k,ie}$ and E_k, (3.10) becomes

$$\frac{J\omega_{wt,ie}^2}{2} = \frac{J\omega_{wt}^2}{2} - \int P_{aux,ie}dt. \tag{3.11}$$

Important to note is that the speed and power is in rad/s and W respectively. Rearranging (3.11) to single out $\omega_{wt,ie}$ and removing ω_{wt} from both sides the following relationship is derived:

$$\omega_{wt,ie} - \omega_{wt} = \sqrt{\omega_{wt}^2 - \frac{2}{J}\int P_{aux,ie}dt} - \omega_{wt}. \tag{3.12}$$

Through combining (2.3) and (2.4) as well as letting P_0 be the base power J can be expressed as

$$J = \frac{2H_{wt}}{\omega_0^2}P_0. \tag{3.13}$$

Combining (3.12) and (3.13) results in

$$\omega_{wt,ie} - \omega_{wt} = \sqrt{\omega_{wt}^2 - \frac{\omega_0^2}{H_{wt}P_0}\int P_{aux,ie}dt} - \omega_{wt}. \tag{3.14}$$

Converting (3.14) to pu by normalizing the speeds with ω_0 and $P_{aux,ie}$ with P_0 and also defying $\Delta\omega_{wt,est}$ as $\omega_{wt,ie} - \omega_{wt}$, $\Delta\omega_{wt,est}$ is derived as

$$\Delta\omega_{wt,est} = \sqrt{\omega_{wt}^2 - \frac{1}{H_{wt}}\int P_{aux,ie}dt} - \omega_{wt}. \tag{3.15}$$

When adding $\Delta\omega_{wt,est}$ to $\omega_{wt,ref}$, the VSWT behaves similarly to a synchronous machine and as such the VSWT will have a small deviation from its optimal speed when the frequency deviates from 50 Hz. Another solution creating a similar effect is to use the Δf multiplied with a gain in place of $\Delta\omega_{wt,est}$. This solution however lacks the integral of (3.15) and is therefore less flexible to modify in order to accommodate special needs.

For example can (3.15) be modified to cause the ω_{wt} to return after an emulated inertia response. This can be done by removing the integration output scaled by a gain, k_{sc}, from the integrator input as seen in Figure 20. The value of k_{sc} decides the time for ω_{wt} to return to its optimal value and should be chosen quite low in order for it to not majorly impact the estimation of $\Delta\omega_{wt,est}$ during the inertia response. However if chosen too low and the return time to ω_{wt} becomes long. A value of 0.02 k_{sc} where found in this case to be appropriate. The Parameter *InertiaON* in Figure 20 is used to turn off the inertia emulation control by setting this parameter to 0.

Figure 21 shows a comparison of the inertia emulation from the VSWT when the $\Delta\omega_{wt,est}$ estimation is used compared to when it is not used. The solid line shows the $P_{aux,ie}$ signal that result from a power disturbance of 0.04 pu on the system causing a under-frequency, while the blue dashed and the red dashed and dotted lines show the achieved inertia response when the $\Delta\omega_{wt,est}$ is used and when it is not respectively. From 21 is it clear that by using the $\Delta\omega_{wt,est}$ estimation, the VSWT inertia estimation can be made significantly more accurate. Some errors compared to the reference still exist and can be resonated due to the factor k_{sc} needing to reduce the output power to bring ω_{wt} back to its optimal point.

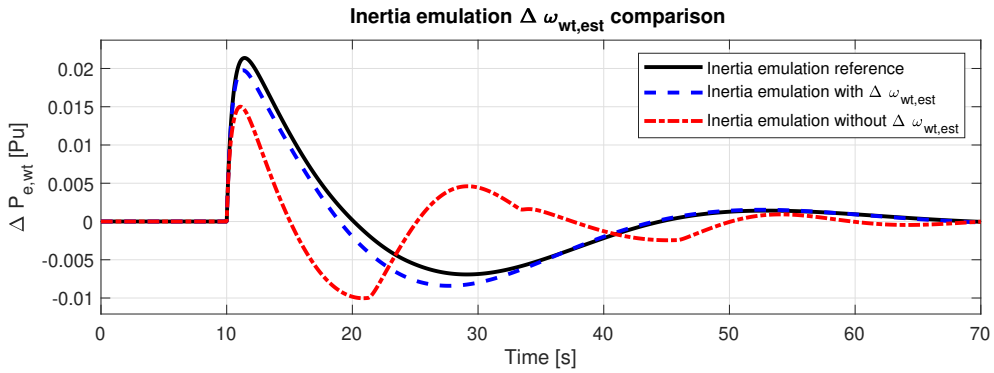

Figure 21: Comparison of VSWT inertia emulation against references when $\Delta\omega_{wt,est}$ estimation is used and when $\Delta\omega_{wt,est}$ estimation is not used for a power disturbance of 0.04 pu causing over-frequency.

Lastly do Figure 20 additionally contain a logic operation with turns of the $\Delta\omega_{wt,est}$ estimation during the specific circumstance of when the frequency is greater than 50 Hz and when ω_{wt} is within a 0.005 pu range of its rated speed or greater. This is due to the $\Delta\omega_{wt,est}$ estimation causing unintended consequences when the inertia emulation down-regulates the frequency and the VSWT is operating at rated speed. At this point the pitch controller is used to regulate the VSWT speed to 1 pu and therefore can the $\Delta\omega_{wt,est}$ not be realized as an over frequency event occurs. Due to the $\Delta\omega_{wt,est}$ not being realized, the speed error for the PI controller in the torque controller changes, reducing the VSWT power production. The requirement of the 0.005 pu range is a result of using a variable wind speed during which the wind speed causes oscillations on the ω_{wt} signal and the value of 0.005 pu where chosen as it was observed that reduced power production occurred when the ω_{wt} where within 0.005 pu of rated speed. The effect of the logic control is visualized in Figure 22 where the red dashed and dotted line representing the VSWT inertia emulation response to a 0.04 pu power disturbances on the system causing a over-frequency while the $\Delta\omega_{wt,est}$ calculation is active and the VSWT operates at rated speed. It is observed that this response is too large compared to the desired response, $P_{aux,ie}$, as shown by the solid black line. The solution to turn of the $\Delta\omega_{wt,est}$ during these circumstance is shown by the blue dashed line in Figure 22 which is overlaid on top of the reference, suggesting that this solution does well in eliminating the unintended increased inertia emulation response.

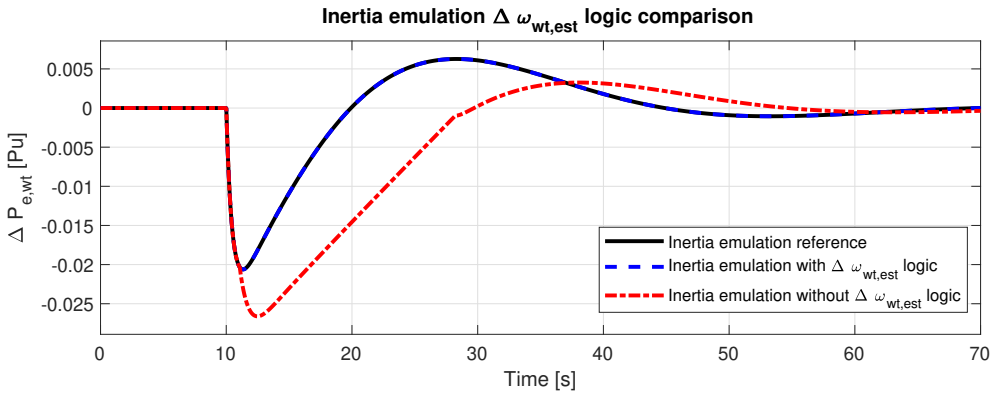

Figure 22: Comparison of VSWT inertia emulation against references when the logic control is used and when the logic control is not used for a power disturbance of 0.04 pu causing over-frequency when the VSWT is operating at rated speed.

A other solution for the down-regulation at rated speed could possibly be to limit the $\Delta\omega_{wt,est} + \omega_{wt,ref}$ to the VSWT rated speed. However, due to having the $\omega_{wt,ref}$ in this case be limited to 0.97 pu as described in Section 3.3.2 would this limit not have any effect. Setting the $\Delta\omega_{wt,est} + \omega_{wt,ref}$ limit to 0.97 pu would resolve the issue when the VSWT operates at the rated speed. However the $\Delta\omega_{wt,est}$ would be lost during the ω_{wt} range of 0.97 to 1 pu during which it should still be active. Furthermore the solution with placing a limit on $\Delta\omega_{wt,est} + \omega_{wt,ref}$ causes windup in the integral for calculating $\Delta\omega_{wt,est}$ creating the need for an anti wind up solution.

3.3.7 Droop and inertia emulation controllers interference compensation

Using both the inertia emulation and the droop control of the VSWT, there is some interference between the two controllers. This interference originates from the available power estimation used as a reference for the de-rated control which is used for establishing the power reserve for the droop control. A power change caused by inertia emulation should also be included in the available power as otherwise would the inertia emulation reduce the power reserve available for the droop control. The droop control would as a result be reduced by the inertia emulation, effectively eliminating the support from the inertia emulation. However, the method used for available power estimation described in Section 3.3.4 causes the inertia emulation to be reflected in the available power due to the use of $P_{e,wt}$ as an analog for $p_{m,wt}$ in the wind speed estimation. As the inertia emulation increases $P_{e,wt}$, the estimated wind speed is also increased, see Figure 15, and the increased wind speed estimation propagates to the available power, causing it to also increase. There are however two issues which cause interference between the inertia emulation and the droop control resulting in the available power increase not properly following the $P_{e,wt}$ increase.

The first is that the inertia emulation, along with increasing $P_{e,wt}$, causes a reduction of ω_{wt} when the VSWT operates below rated power. This ω_{wt} reduction in turn causes C_p in the wind speed estimation to reduce and therefore does the estimated wind speed increase more than if only $P_{e,wt}$ was changed by the inertia emulation. As a result in the available power estimation to high, resulting in calculating the power reserve as more then is actually available. To compensate for the ω_{wt} reduction, the estimated $\Delta\omega_{wt,est}$ is added to the optimal speed calculated in the available power block as shown in Figure

16. The aim by adding $\Delta\omega_{wt,est}$ is to reduce C_p in the available power estimation by the same amount as it is reduced in the wind speed estimation and thereby eliminating the influence of the changing ω_{wt}. The result of including the compensation of $\Delta\omega_{wt,est}$ is shown in figure 23b describing the power reserve that is available to the droop control for a low constant wind speed and a frequency disturbance at 10 s. The de-rating been turned off in order to give a clearer view of the inertia emulation effect on the power reserve. The power reserve would therefore ideally be kept at 0 pu. From figure 23b it is shown that the compensation reduces the interference, but does not eliminate it. This effects are most prominent at low wind speed due to causing the greatest reduction in ω_{wt} while there is no interference at higher wind speeds as the pitch is used to keep ω_{wt} at rated.

The second issue causing interference is the power limit on the available power. If a disturbance occurs when the power is rated, inertia emulation would cause the power to shortly exceed the VSWT rating. Therefore, the available power also needs to exceed the 1 pu limit which is done by adding the $P_{aux,ie}$ to the available power upper limit, as shown in Figure 16. The result of adding the power limit compensation is shown in figure 23a describing a similar case to Figure 23b however using a high wind speed to operate at rated power. Figure 23a shows that by adding the inertia emulation power signal to the available power limit, the interference is completely removed considering that in the presented case a power reserve of 0 pu is ideal. This available power limit compensation should only be performed if the inertia emulation is allowed to cause the VSWT to operate over rated power, it is otherwise not necessary.

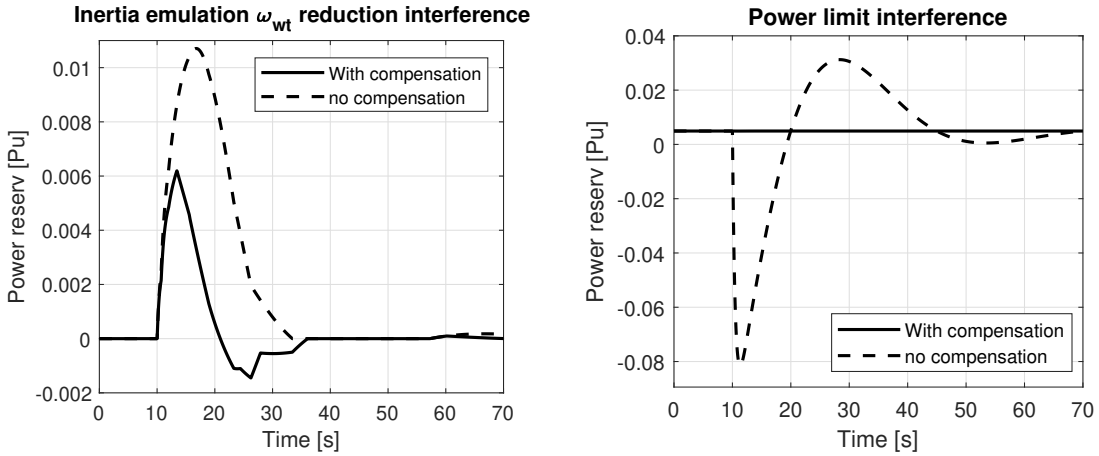

(a) Result of compensation of interference on power reserve due to a reduction on ω_{wt} caused by the inertia emulation at a wind speed of 6 m/s

(b) Result of compensation of interference on power reserve due to a the limit on the available power at a wind speed of 8.5 m/s

Figure 23: Comparison of the interference on the droop power reserve caused by inertia emulation from a power imbalance of 0.05 pu with and without compensation and without using de-rated operation

3.3.8 Initialization of VSWT

In order for the VSWT model to not start from stand still every time the model is simulated, the initial conditions of the integrals and transfer functions in the VSWT model needs to be determined. The blocks in the model that need an initialization are the drive

train in Figure 11, the pitch control integral in Figure 14, the available power filter in Figure 17 and the torque control integral as well as the speed reference filter in Figure 12. Any other integral or transfer function will have an initial condition of 0.

The initialization process is carried out by running the model until steady state while increasing the wind speed and saving ω_{wt} from the drivetrain, $\omega_{wt,ref}$ from the reference speed filter, the pitch integral output, the torque integral output, and also the power output for every wind speed just before steeping to a new speed. The available power filter outputs do not need to be saved, as $P_{avail} = P_{e,wt} + P_{reserv}$ is used as the initial condition. This relationship holds for initialization considering that there is no initial frequency deviation and therefore no initial droop support.

To determine the initial condition for any wind speed which is not specifically included in the wind speeds used for the initialization, a linear interpolation of the saved data points is carried out to artificially increase the sample size. A look-up table is then used to find the wind speed in the extended data set closest to a desired initial wind speed, as well as the initial condition values corresponding to the wind speed found. The same table can be used if instead an initial power output is specified, where then the closest power output in the data set is found along with the corresponding initial conditions.

4 Modeling of island operation of wind-hydro system in PSS/E

The stability analysis of a wind-hydro island will primarily be conducted through simulations using the tool Power System Simulator for Engineering (PSS/E) from Siemens. This tool is used as it is more easily able to analyze a more complex power system consisting of multiple buses and measure additional quantities within the power systems over only the frequency. In PSS/E, the island stability analysis is conducted through dynamic simulations that simulate how the island responds to a disturbance and variations in power over time. To perform the dynamic simulation, dynamic models of the power units subsystems are required in order to simulate how the units behave over time. The dynamic models used for the island simulations are based on the control systems presented in Section 3 and the parameters used for dynamic models as well as for the island network are presented in Appendix B.

4.1 Network model

Figure 24 shows the one line diagram of the island network model used for the island studies and it is based on the network used in [44] on which some modifications are done. The base network is an example of a medium voltage distribution level system from the west coast of Sweden and consists of a hydro unit and a paper and pulp factory as a load connected to a 140/11 kV substation. The load nominally has a power consumption of 18.4 MW and 10.4 MVAr. The modifications that were done to the network were to add a wind power unit connected through a cable to the load bus. Additionally where a power line was added between the load bus and the substation as the original network did not include distances. The parameters for the added line are imported from branch 25 in the IEEE 33 bus distribution system network in [45]. The imported branch has a resistance of 0.203 Ω and a reactance of 0.1034 Ω. These parameters correspond to what can be observed in a practical distribution system [45]. The cable used to connect the wind power unit was based on [46] and made to have a distance of 5.8 km and therefore where a resistance of 0.58 Ω and a reactance of 0.620 Ω used. The island network model is connected to a larger power system from which it is disconnected when operating as an island. Considering that the main grid is not the interest of the studies and that it will also be largely unaffected by what happens at the island due to their difference in size, the main network has been approximated as an infinite grid.

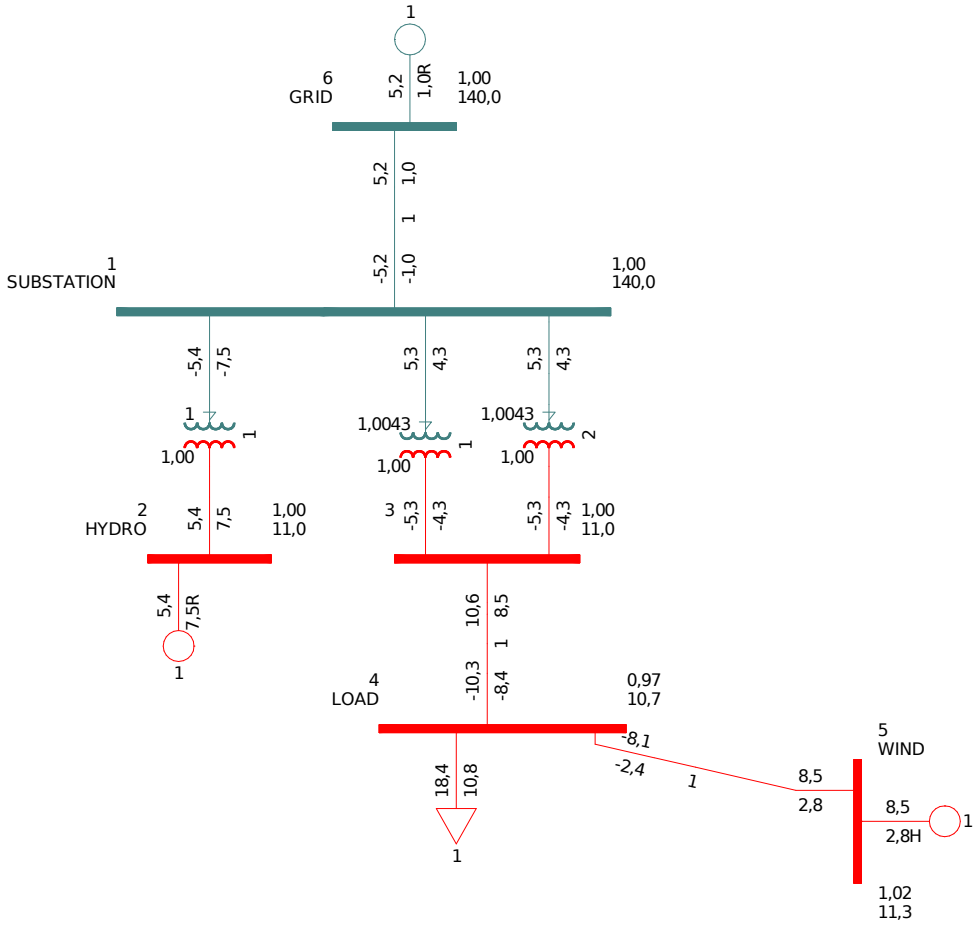

Figure 24: PSS/E one line diagram of island network used for stability analysis including connection to the grid represented by a single machine infinite bus [44]

4.2 Dynamic models for generation and loads

Dynamic models are necessary in PSS/E for performing dynamic simulations to analyze how a system behaves over time when subjected to a change in condition. PSS/E provides users with many built-in dynamic models of subsystems within the network, for example generators, loads and exciters. Information regarding the models and their use is supplied in the model library, which is part of the PSS/E documentation. However, PSS/E do support the use of a user defined model (UDM) if it is necessary to use models not available in the PSS/E model library for performing a desired simulation. An UDM is a model of subsystems within the network built in FORTRAN by the user.

4.2.1 Hydro unit dynamic implementation

The hydro unit shown in the one-line diagram in Figure 24 is modeled for the PSS/E dynamic studies using existing models within PSS/E. To model the hydro units generator's dynamics, the model GENROU where chosen, which is a representation of solid rotor generators down to the subtransient level. The SEXS excitation system model was chosen to represent the voltage control of the hydro unit. SEXS is a general model of an excitation system representing their characteristics and is useful when the details for the excitation system are not known as in this case. Further is the stabilizer model STAB1 included to

represent the hydro unit dynamics. Stabilizing models are useful as excitation systems tend to reduce the dampening of rotor angle oscillations, where the use of an additional stabilizing signal during transient events can mitigate the loss of dampening. The STAB1 model uses the generator speed as input to supply the excitation system with the stabilizing signal.

For representing the hydro units governor dynamics have the governor model HYGOV be chosen and then tuned in order to resemble the Simulink hydro governor model of Section 3.2. An additional turbine load controller model LCFB1 has been included to model frequency restoration from the hydro unit for returning the frequency to its nominal value after a disturbance. This frequency restoration is accomplished by integrating with the HYGOV model and adding an integrator on the generator speed deviation. The reason for including the LCFB1 model for the PSS/E studies was for the ability to run simulations of the length of several minutes, during which changes in wind speed and loading causes multiple power variations. The LCFB1 will restore the wind unit's power reserve after a variation in the power, allowing for the wind unit to be able to continuously support the frequency during the minutes-long simulation.

4.2.2 Wind power dynamic implementation

The wind power unit used in the island network shown in Figure 24 is an agrogated representation of 3.6 MW VSWTs. Why 3.6 MW VSWTs have been used instead of the Chalmers wind turbine as was used in Section 3 are due to the Chalmers turbine being too small, 2.5 kW, compared to the size of the test network. The parameters of the 3.6 MW VSWT are loosely based on the General Electric wind turbine [41]. However the rated speed, ω_0, has been set to 1.8 rad/s to have a similar speed to power curve as the Chalmers turbine and the Chalmers turbine $Cp(\beta, \lambda)$ curve has also been kept. The reactive power from the wind power unit is controlled to keep a constant power factor of 0.95 if not otherwise stated.

The wind power units have been modeled for dynamic studies using a combination of UDM and built-in models. The use of UDMs allows for added control over the wind power units to design their speed and frequency control. The systems within the wind power units that use UDM to model their dynamics are the aerodynamics of the turbine, the turbine drivetrain, the torque controller, the pitch controller and the control systems used for the frequency regulation. The UDMs were developed to be used together and therefore are all UDMs required for the VSWT to function correctly and it is not possible to replace a model for a built in alternative. The input to the wind power models is the wind speed which is imported from a file containing a time series of a variable wind speed. The UDMs are made to be as equivalent as possible to the MATLAB/Simulink models presented in Section 3.3.1 - 3.3.6, where the UDM of the frequency control consists of the available power estimation, the droop along with the de-rated control and the inertia estimation. The source code for the UDMs is included in Appendix D.

Additionally, the PSS/E dynamic studies do also require a generator and electrical model for the wind power unit, which were neglected for the MATLAB/Simulink modeling. There is no requirement on what generator and electrical models are used as the only output from the UDMs are the electrical power setpoint. In this work the built in models REGCA1 and REECA1 from the PSS/E model library were used. Furthermore, as noted in Section 3.3.6 were any overloading limits on the inertia emulation neglected in the MATLAB/Simulink modeling. However in PSS/E were power and current limits included

in the REECA1 model. These limits were chosen as 1.2 pu for the power and 1.3 pu for the current to allow for overloading, causing the PSS/E model to behave similarly to the MATLAB/Simulink implementation with respect to inertia emulation.

There are, however, differences between the UDM and the MATLAB/Simulink models. Firstly, the look-up tables used in the MATLAB/Simulink have been approximated as polynomial functions for the UDMs. This change was made as implementing look-up tables in FORTRAN can be quite challenging. Look-up tables were used in MATLAB/Simulink to determine $C_p(\beta, \lambda)$ in the turbine aerodynamic model and the wind speed estimation. Look-up tables were also used in the available power estimation to determine $C_p(\lambda)\big|_{\beta=0}$ and to determine the $\beta_{min}(k_{dr})$ for the de-rated control. In the UDM is the $C_p(\beta, \lambda)$ approximated using a two-dimensional fourth-order polynomial of 2.24 and $C_p(\lambda)\big|_{\beta=0}$ as well as $\beta_{min}(k_{dr})$ has been approximated as one-dimensional fourth-order polynomials.

$$C_p(\lambda)\big|_{\beta=0} = \sum_{i=1}^{4} b_i \lambda^i \tag{4.1}$$

$$\beta_{min}(k_{dr}) = \sum_{i=1}^{4} c_i (C_{p,max} k_{dr})^i. \tag{4.2}$$

Figure 25a - 25c shows how well these polynomial approximations correspond to the lookup tables. An additional difference between the UDMs and their MATLAB/Simulink counterparts is that the low-pass filter and the derivative in the inertia emulation control in Section 3.3.6 have been combined in the UDM to form a high- pass filter. Furthermore, the filter on the available power signal in the de-rated control system, shown in Section 3.3.5, has been removed for the UDM as it is not necessary for the PSS/E dynamic simulations. Lastly, also a rate of change limit of 0.5 per second has been placed on the calculated k_{dr} in the de-rated and droop control of Section 3.3.5 as this value where observers to start oscillating quickly as the wind power unit approached a low power operating point. The rate of change limit was included to mitigate these oscillations without otherwise impacting its function as the source of the oscillations were not discovered. The oscillations are however believed to be caused by the polynomial approximation of the $C_p(\beta, \lambda)$ and it at some point increases C_p as β is increased.

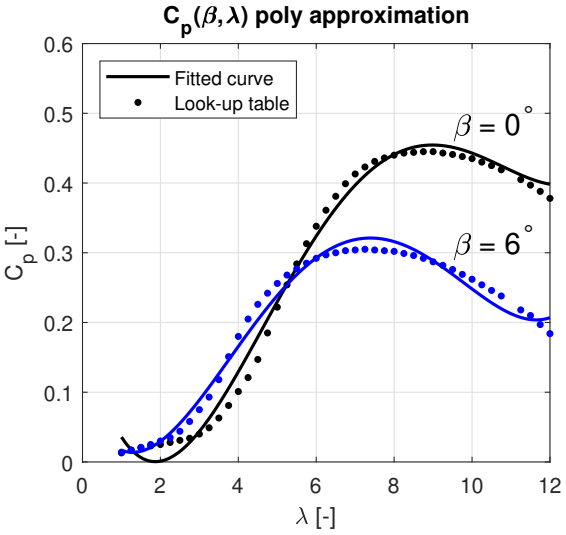

(a) $C_p(\beta, \lambda)$ curve for a β of 0 and 6 degrees of turbine measurement and polynomial fit according to (2.24)

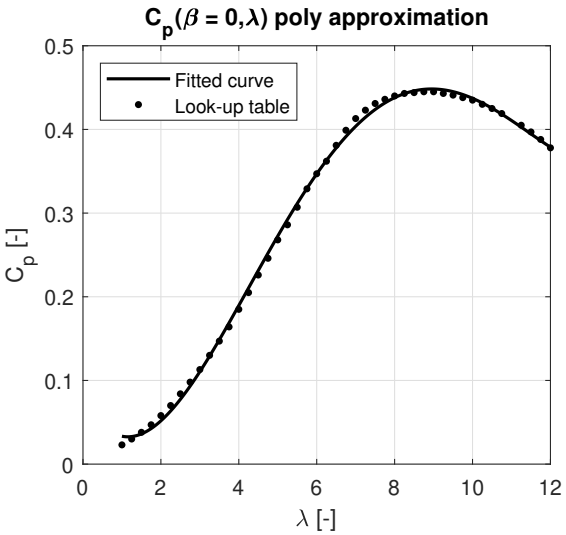

(b) $C_p(\lambda)\big|_{\beta=0}$ of turbine measurement and polynomial fit according to (4.1)

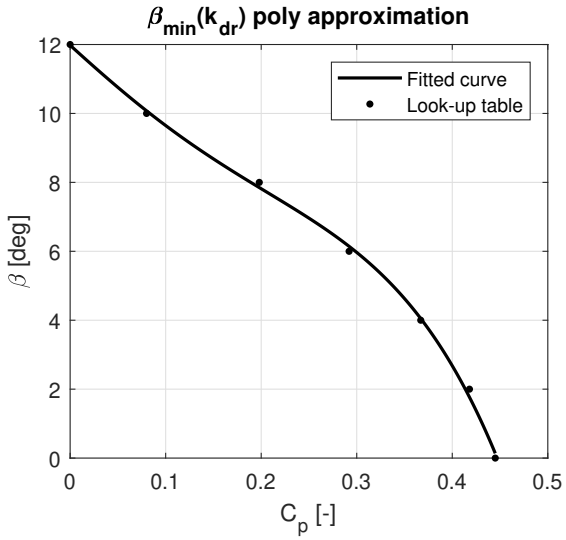

(c) $\beta_{min}(k_{dr})$ of turbine measurement and polynomial fit according to (4.2)

Figure 25: Comparison between measured data form wind turbine used for lookup tables and fourth order polynomial fittings (missing axis labels)

In order for the wind power units to operate in steady state at the start of the dynamic simulation, the UDM has to be initialized. The initialization calculates, similar to the MATLAB/Simulink initialization, the initial condition of the states within the UDM where states refer to any transfer function and integral. The most important states to initialize are the torque integrator in the torque controller, the speed reference feedback filter in the torque controller, the turbine drive train and the pitch integral in the pitch controller. Any other states, namely the states in the inertia emulation, are initialized to zero for steady state. Before running a dynamic simulation, a load flow is performed to calculate the unit's power production in order to satisfy the load demand and losses. Therefore the

wind units power production is the known quantity with the initialization of the UDMs are based on.

The initialization in the torque controller back calculates the speed reference state from (3.5) and the initial torque state from $P_{e,wt}/\omega_{wt}$ where $\omega_{wt} = \omega_{wt,ref}$ as there is steady state. Considering that ω_{wt} is equal to $\omega_{wt,ref}$, the drive train can also be initialized using the calculated $\omega_{wt,ref}$. For steady state of the drive train, the condition $P_{m,wt} = P_{e,wt} + b\omega_{wt}$ also needs to be fulfilled. Therefore requiring the pitch angle to be set to acquire the $P_{m,wt}$ that satisfy the condition based on the wind speed data. However, instead of setting the pitch based on the wind speed in the initialization, the pitch is set to zero and the corresponding wind speed is calculated. The time series containing the wind speed data is then shifted up or down to have it start at the calculated initial wind speed. The initial wind speed is calculated by increasing the wind speed in small increments and using (2.19) to determine the $P_{m,wt}$ that relates to the wind speed until the condition$|P_{m,wt} - P_{e,wt} - b\omega_{wt}| < \epsilon$ is met, where ϵ is an error tolerance.

When initializing the turbine for de-rated operation, some changes are made to the initialization. For properly calculating the speed, speed reference state and the torque integral state in de-rated operation, $P_{e,wt}$ needs to be divided by the de-rating factor k_{dr} beforehand. During initialization k_{dr} cannot be calculated according to (3.8) as P_{avail} is not available. However considering that there is no frequency error at the start and therefore no droop support, P_{avail} is equal to $P_{e,wt} + P_{reserv}$ causing (3.8) to be written as

$$k_{dr} = \frac{P_{e,wt}}{P_{e,wt} + P_{reserve}} \tag{4.3}$$

during initialisation. Another change that is necessary when initializing for de-rated operation is to set the pitch at $\beta_{min}(k_{dr})$ calculated according to (4.2) in the de-rated control instead of setting the pitch at zero.

4.2.3 Load dynamic implementation

To model the dynamics of the load the user-defined load model presented in [47] is used. This model introduces load variations of a specified power factor to a load's power consumption by reading a time series of these variations from a file. The file used consists of load variations created by a random walk which changes the load every time step by a random amount within a set limit. The voltage dependency of the load is introduced according to the ZIP model when converting loads for dynamic studies in PSS/E. To add the frequency dependence of the load the UDM from [47] is used as it also has this functionality resulting that the load ultimately has a dependency with regards to voltage and frequency in accordance with (2.13). Regarding the load voltage dependency, the load has been modeled as a constant current type causing Z_p and P_p in (2.13) to become 0 while I_p become 1.

4.3 Simulation cases for island stability analysis

From the created dynamic model of an island network is the island stability analyzed while considering the transition to island operation and the continuous operation thereafter. These transition and continuous operations have been divided up into two simulation cases where the transition to island and the continuous operation of the island are analyzed individually. Table 3 presents the simulation cases run on the PSS/E island network and

the main analysis of the island for that case. For both cases the stability improvement will be analyzed using only inertia emulation and when using inertia emulation along with droop support while de-rated. Using only droop support while de-rated will be included briefly in Section 6.3. However it is not included as a main test case as inertia emulation as well as droop with inertia emulation where regarded as more significant test cases. Additionally are the voltage levels observed for all cases to ensure that these are reasonable.

Table 3: Overview of dynamic simulations run on the PSS/E island network and the main analysis of each case

Test case	No VSWT frequency support	VSWT inertia emulation	VSWT inertia emulation and droop support while de-rated
Continuous operation	Acceptable wind power penetration	Changed in frequency distribution compared to no support	Changed in frequency distribution compared to no support
Transition to island	Acceptable power transfer from grid	Change in frequency nadir / change in acceptable power transfer compared to no support	Change in frequency nadir / change in acceptable power transfer compared to no support

For the continuous island operation case is a simulation of 15 minutes run during which the island is disconnected from the larger grid throughout the simulation. The continuous operation case can also be considered as an analysis of a planned transition to island operation, as in these cases there is no power flow from the grid causing a disturbance during the transition. While in continuous operation the frequency variations will come from the changing wind speed and from load variations caused by the dynamic load. The changing wind speed is a main contribution to the power variations the island experiences, resulting in changes in the wind power production. Therefore increasing the wind power penetration will reduce the frequency quality in the island. Regarding the load variation, a time series for a variable load used. The time series caused the load to change by approximately +/- 3MW and it was derived using a random walk function. The wind power penetration will therefore be set at a level during which the frequency quality in the island is at the limit of what is acceptable when wind power is not supporting the frequency. The acceptable frequency quality limit has been chosen as 49.5 to 50.5 Hz which is the widest continuous frequency range allowed in the Nordic power system [16]. By keeping to this range, there will also not be any issues through disconnections of generators as they are required to be connected for a wider frequency range as presented in Table 2. The range 0.85 to 1.1 pu has been used for the voltage requirements and corresponds to the voltage magnitude requirement presented in Table 1 for islanding. The solid rectangle in Figure 26 summarizes the continued operating limits. The frequency quality improvement will be recorded when using the frequency support of the wind power unit, namely when utilizing inertia emulation and when utilizing both inertia emulation and droop support while de-rated by 0.1 pu. When de-rated the same wind speed will be

used as in the normal operating case, causing a decrease in the wind power penetration while de-rated.

For the transition case is the island network initially connected to the larger grid with a power flow across the grid connection. The island is then disconnected from the grid where the power flow causes a large disturbance to the island frequency. The initial acceptable power flow to the island is determined in order for the island frequency to not pass the chosen frequency range of 49 to 51 Hz. This frequency range was chosen as the instantaneous frequency needs to be within this range in the Nordic synchronous area [16]. Similarly to the continuous cases, the used range does not surpass what presented in Table 2, requiring the generators to stay connected. The instantaneous voltage limit used is also 0.85 to 1.1 pu, as they were for the continuous island operation. In Figure 26 are the instantaneous limits used summarized by the dashed rectangle. The wind power production set for the initial load flow will be equal to the power production set in the continuous operation case and the same wind speed and load variation will be used in both cases. For the transition to island operation is the frequency nadir improvement evaluated when using wind power inertia emulation and when using both inertia emulation and a droop support while being de-rated by 0.1 pu. Similar to the continuous operation case will the same wind speed be used while de-rated and compared to continuous operation causing a slight decrease in wind power penetration. Additionally will also the possible increase in power transfer from the grid be determined while using wind power frequency support in order to achieve the same frequency nadir as the no frequency support case.

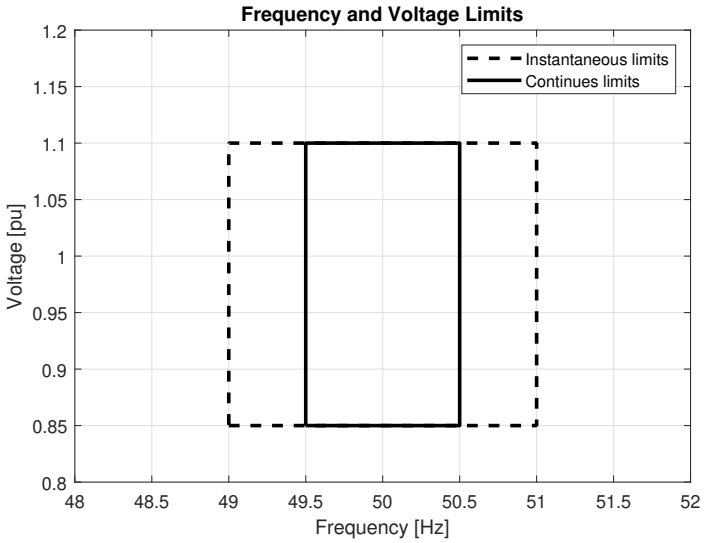

Figure 26: Frequency and voltage limits used.

5 Frequency simulations in MATLAB/Simulink

This section shows the MATLAB/Simulink one-bus frequency simulation results for the VSWT. The focus of this section is to show the behavior of the VSWT frequency support strategies, namely inertia emulation, droop support with de-rated operation as well as the use of both together, and show how they influence the operation of the wind turbine. The section also investigates the impact of using a variable wind speed on the accuracy of the frequency support. The system set up used for the MATLAB/Simulink simulations is shown in Figure 8. It consists of a hydro governor, a VSWT and a load connected to a simple representation of a power system. This power system representation has been derived in (3.1). The wind power penetration used for all MATLAB/Simulink simulations is 30%.

5.1 Wind power frequency support accuracy

For the wind power to be able to help support the frequency, it is important that the control strategies for frequency support produce a response from the VSWT which is accurate to a desired response based on the frequency deviation. The following Sections 5.1.1 - 5.1.3 shows how the VSWT responds to an under-frequency event due to a power disturbance on the system of 0.04 pu while de-rated and providing droop support, while providing inertia emulation and while providing both simultaneously. The influence of using a variable speed on the accuracy of the wind power response is also shown. The system frequency for all the analyzed cases are shown in Appendix C. Further analysis of the VSWT influence on the frequency is also included in Section 5.2 and Section 5.3.

5.1.1 De-rated operation with droop

Figure 27 shows the VSWT behavior and frequency control accuracy while de-rated by 0.1 pu on the machine base and providing droop support. A power disturbance of 0.04 pu applied to the system at 20 s causing an under-frequency event and a constant wind speed of 7 m/s is used. Waiting 20 s before applying the disturbance is to allow the VSWT to find steady state after initialization errors. The VSWT uses a droop setting of 5% for the up-regulation. In Figure 27a the estimate of available power and the output power of the VSWT is shown along with a comparison between the wind speed used and the estimated wind speed. The wind speed graph shows an initial disturbance to the estimated wind speed due to an initialization error and also a continuous deviation of the estimated speed compared to the used wind speed. These estimation errors are however sufficiently small, at maximum 0.03 m/s, that any effects on the VSWT caused by these errors are negligible. Prior to the disturbance, the VSWT keeps a power reserve of 0.1 pu on the machine base when compared to the available power estimation which is in accordance with the de-rating setting. After the disturbance, the VSWT output power increases by 0.1 pu in accordance with the droop setting, using the entire power reserve. The available power and the wind speed estimations does however remain unaffected by the disturbance. This is important as the available power estimate is used to calculate the de-rating of the VSWT to have the desired output power. Therefore, a disturbance in this signal would cause an error in the frequency support accuracy.

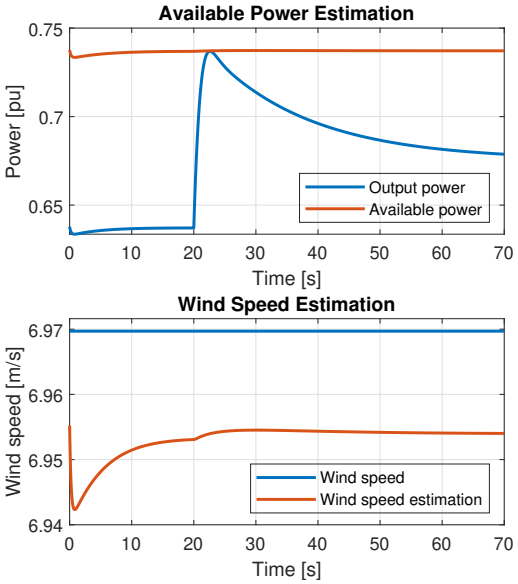

(a) Comparison between available power estimation and output power of VSWT (top) and between wind speed estimation and wind speed input (bottom).

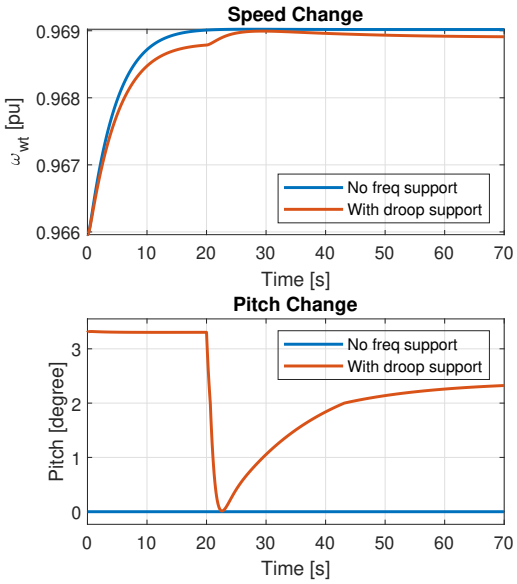

(b) Comparison of VSWT rotational speed (top) and pitch (bottom) between when providing droop frequency support during normal operation.

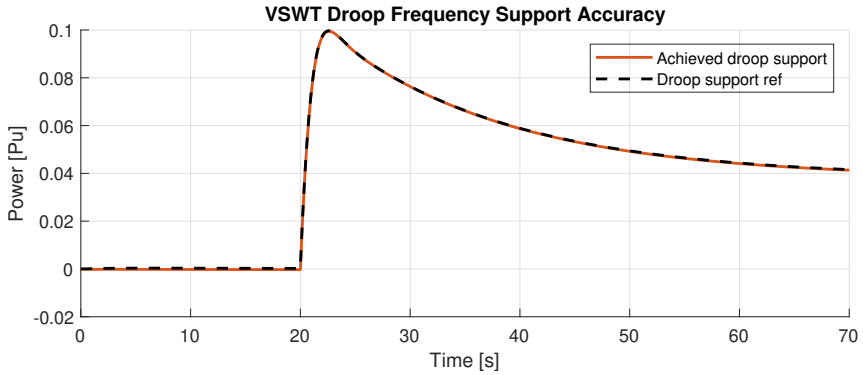

(c) Droop frequency support accuracy while the VSWT de-rated by 0.1 pu.

Figure 27: VSWT behavior and frequency support accuracy while de-rated by 0.1 pu and providing droop frequency support for up-regulation of frequency after a power disturbance of 0.04 pu on the system base at 20 s during a constant wind speed of 7 m/s.

The frequency accuracy of the droop support is shown in Figure 27c in which the increase in power from the VSWT due to the frequency disturbance is compared to a reference. The reference signal is the $P_{aux,dr}$ signal shown in Figure 17 while the increase in output power is derived by running the VSWT with and without frequency support for the same scenario and comparing the difference in output power.

Additionally, Figure 27b shows how the VSWT speed and pitch change when providing droop frequency support while de-rated compared to when the VSWT does not provide frequency support. The de-rating has a negligible effect on the speed, which is the desired

result considering that the de-rating controls were designed to not cause a change in the speed as shown in Figure 18. The initial speed change shown is a result of an initialization error, but is sufficiently small to not cause any issues. The pitch is, on the other hand, what the VSWT uses for controlling the de-rating by limiting the mechanical power. The pitch is therefore higher for the frequency support case to establish the 0.1 pu power reserve and when the frequency disturbance occurs, the pitch decreases down to its minimum value as the entire power reserve is used for supporting the frequency.

Figure 28 shows how the use of a variable wind speed affects the operation and accuracy of the de-rated operation with droop frequency support. Other than the wind speed change, the setup is the same as in Figure 27, except having the disturbance occur at 10 s. The disturbance moved to occur earlier as there is no need to wait on errors in the initialization being corrected. Figure 28a shows a compression between the estimated available power and the VSWT output power, as well as the comparison between the estimated wind speed and the variable wind speed input signal. Similarly to Figure 27a the VSWT attempts to keep a reserve in accordance with the de-rating setting of 0.1 pu and the droop setting. However, in this case this reserve is not always achieved as fast changes in the available power can cause interference on the power reserve. Additionally, the figure shows that there is no disturbance to the estimations when the power disturbance occurs at 10 s, similar to the constant wind speed case, and this is therefore not a source of inaccuracy when using a variable wind speed.

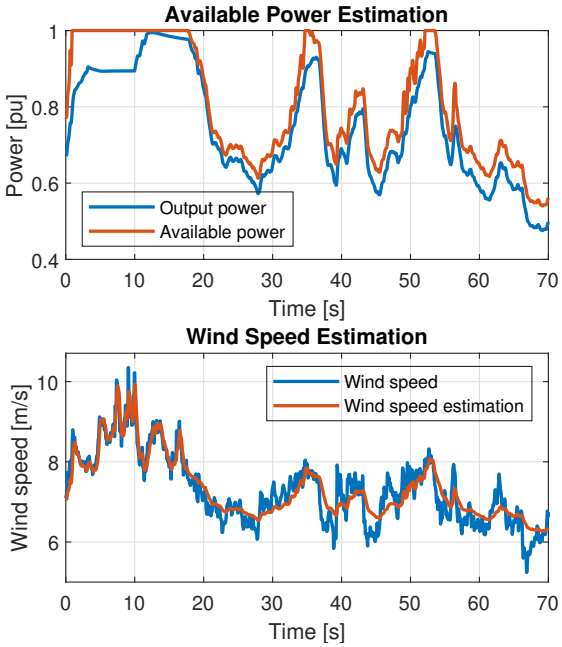

(a) Comparison between available power estimation and output power of VSWT (top) and between wind speed estimation and wind speed input (bottom).

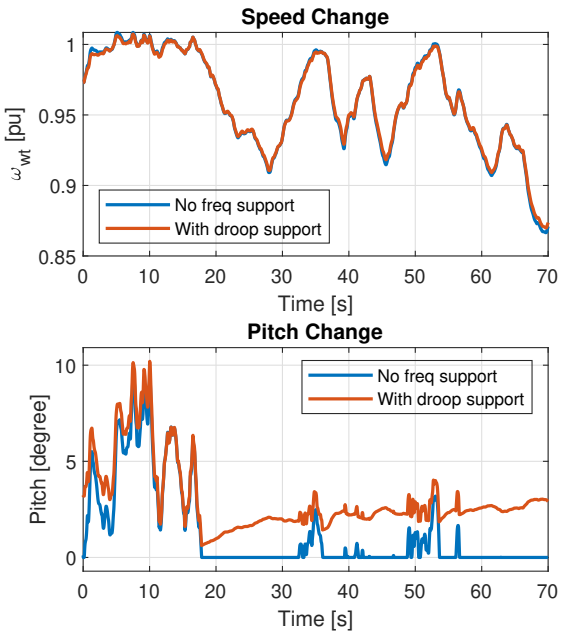

(b) Comparison of VSWT rotational speed (top) and pitch (bottom) between when providing droop frequency support during normal operation.

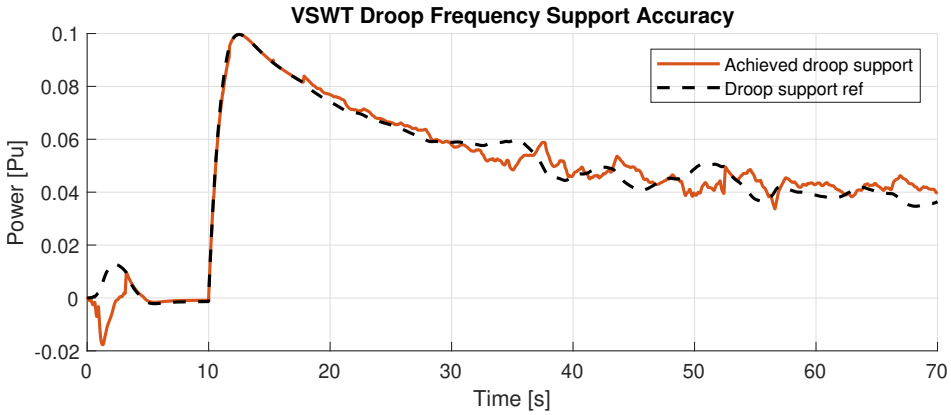

(c) Droop frequency support accuracy while the VSWT de-rated by 0.1 pu.

Figure 28: VSWT behavior and frequency support accuracy while de-rated by 0.1 pu and providing droop frequency support for up-regulation of frequency after a power disturbance of 0.04 pu on the system base at 10 s during a variable wind speed.

The wind speed comparison of Figure 28a shows a wind speed estimation that is very similar to the wind speed input signal when the VSWT operates at maximum power. However there is a low pass filtering effect on the wind speed estimation when the VSWT operates below this power. The filtering is a desired effect and is due to the inertia of the VSWT combined with using the VSWT electrical power as an analog for the mechanical power in the wind speed estimation. When operating at maximum power, there is no change in the rotational speed of the VSWT, causing it to react quickly to changes in wind speed.

However, when operating below the maximum power, the change in VSWT rotational speed becomes a factor and this is a comparatively slow process due to the inertia. As a result the VSWT responds slower to changes in the wind speed when operating below rated rotational speed. Even when the applied wind speed suddenly drops for a short period of time during 38 and 45 s, the estimated wind speed does provide an accurate power reserve. During these times the wind speed is overestimated, however, as stated, it takes time for the VSWT to respond to the change in wind speed. Therefore is this overestimation accurate for a limited time and by then has the wind speed increased again. If fast changes in wind speed were present in the estimated wind speed signal when below rated rotational speed, they would propagate to the available power estimation, causing an inaccuracy in its estimation.

Figure 28c shows the accuracy of the droop frequency support while de-rated when using a variable wind speed as its input signal. The figure shows a very good accuracy during 5 to 17 s, which is the time period during which the VSWT operates at maximum power according to Figure 28a. Outside this time period does however a noise of approximately 0.01 pu appear on the frequency support signal. The source of this noise has partly to do with the power reserve interference due to fast changes in the estimated Wind speed and available power estimation mentioned. An additional source of the noise may have to do with the look-up table for the minimum pitch in the de-rating control. This look-up table assumes that the VSWT operates at λ_{opt}. However, this is not the case when operating in regions 3 and 4 referring to Figure 6. The deviation from λ_{opt} in region 4 is not relevant, as the pitch is greater than minimum in this region. However, minimum pitch is used in region 3. Therefore, the deviation from λ_{opt} in region 3 causes an error in the pitch angle compared to the desired de-rating of the VSWT. One further source of the inaccuracy are the interpolations used in the creation of the look-up table for the minimum pitch. This interpolation can cause the pitch to deviate from the value required for the wanted de-rating. The biggest inaccuracy occurs at the beginning, during the first 5 s when the power is rapidly increasing. The pitch is during this time slightly too high compared to desired. It is not fully known what the cause of this inaccuracy is and the cause can be a combination of the discussed reasons for inaccuracy.

The comparison of the VSWT speed and pitch between de-rated operation and normal operation for a variable wind speed shown in Figure 28b gives similar results as the constant wind speed case of Figure 27b. The rotational speed of the VSWT does not significantly change between the two cases. The pitch is, however, greater in the de-rated case to limit the mechanical power. The difference between the pitch of the two cases is reduced after 10 s and the difference is completely removed when the VSWT uses the entire power reserve to support the frequency.

5.1.2 Inertia emulation

Figure 29 shows the accuracy of the inertia emulation frequency support to a power disturbance of 0.04 pu on the system at 10 s causing an under-frequency event and while using a constant wind speed. Figure 29 does also show how the speed and the pitch behaves when providing inertia emulation. Two different wind speed cases are shown. One case uses a wind speed of 7 m/s causing the VSWT to operate below rated power and use kinetic energy extraction for providing the inertia power. The other case uses a wind speed of 9 m/s causing the VSWT to operate at rated speed and using the pith for providing the inertia power, resulting in an overloading of the VSWT.

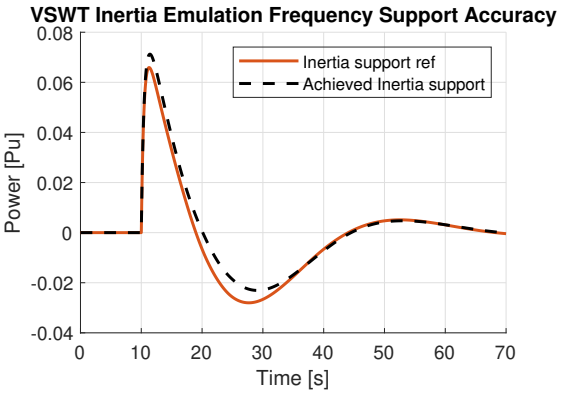

(a) Inertia emulation frequency support accuracy while VSWT operates below rated speed.

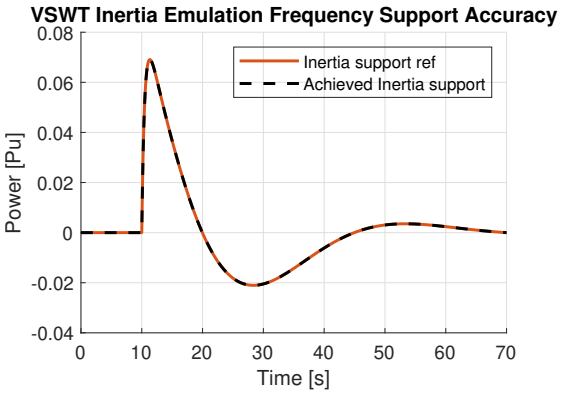

(b) Inertia emulation frequency support accuracy while VSWT operates at rated speed.

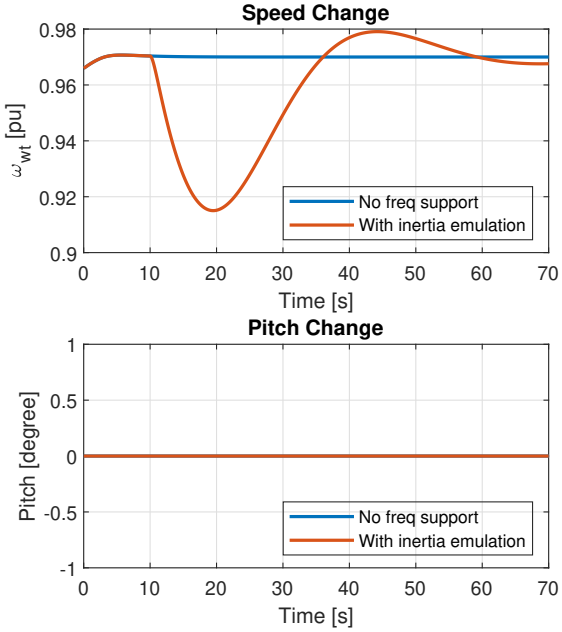

(c) Comparison of speed (top) and pitch (bottom) between normal operation and when providing inertia emulation support through kinetic energy extraction while operating below rated speed.

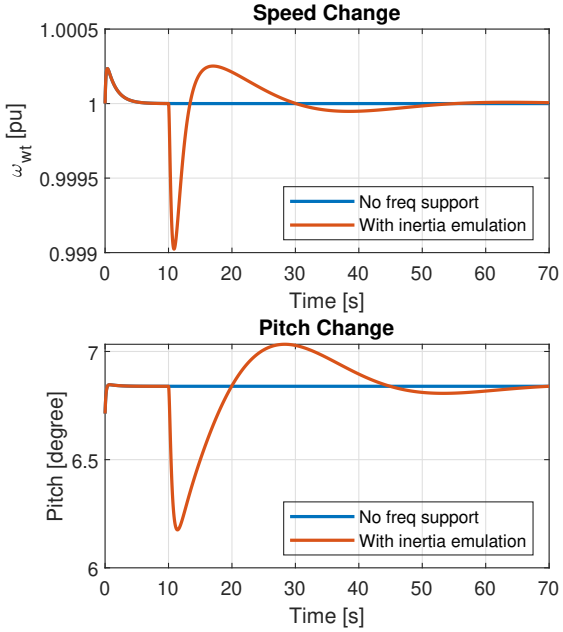

(d) Comparison of speed (top) and pitch (bottom) between normal operation and when providing inertia emulation support through pitch control while operating at rated speed.

Figure 29: VSWT behavior and frequency support accuracy while providing inertia emulation support for up-regulation of frequency after a power disturbance of 0.04 pu on the system base at 10 s during a constant wind speed of 7 m/s (below rated speed) and 9 m/s (above rated speed).

The frequency support accuracy provided by inertia emulation is shown in Figure 29a when operating below rated speed and in Figure 29b when operating at rated speed. For the frequency support reference is the signal $P_{aux,ie}$ shown in Figure 20 with an inertia gain, k_i, equal to 5. The results show that the inertia emulation power response clearly follows its reference. However there are minor differences between them for the case when operating under rated speed. This difference is, as mentioned in Section 3.3.6, due to

the integrator feedback gain, k_s, returning the VSWT speed back to its optimal point, as inertia emulation would otherwise cause a change in the rotational speed of the VSWT in accordance with the frequency change. The reason for being more accurate in the high wind speed case are due to the VSWT being able to reduce the pitch to gain the desired power increase instead of reducing the rotational speed. Therefore, there is no need to use k_s to return the speed to its optimal point, which is the cause of accuracy error in the case of low wind speed.

There are three differences when comparing the inertia emulation power response to the traditional synchronous response. The first is the inclusion of the parameter k_i in the inertia emulation, creating the ability to control the strength of the power response, which is not possible in the traditional synchronous case. The second difference is caused by including a filter on the frequency signal for the inertia emulation. This filter reduces the responsiveness of the inertia emulation, making it act a little bit slower compared to the traditional synchronous power response. The third difference is a result of the parameter k_s, returning the VSWT speed back to optimal speed after the initial power change. The inertia emulation power response is therefore slightly reduced due to k_s, unless pitch controlled inertia emulation is used where the VSWT speed does not change.

Figures 29c and 29d show what effect inertia emulation has on the VSWT speed and pitch compared to normal operation when operating at a rotational speed below rated and at rated respectively. From the Figure 29c when the VSWT operated below rated speed, it is shown how the VSWT speed reduces after the power disturbance as the inertia emulation uses kinetic energy from the rotation to support the frequency. At 20 s, inertia emulation starts to return energy to the rotation to increase the speed back to its optimal point. To increase the speed, the VSWT uses energy from the system, but at this point slower frequency support actions from the hydro have been activated and are able to compensate for the VSWT speed acceleration. The overshot of the speed that is observed stems from a down regulation action as the support of the slower hydro unit governor that is paired with the VSWT causes a slight overshot of the frequency. In Figure 29c it is also shown that inertia emulation has no influence on the pitch when the VSWT operates below the rated speed.

However, when operating at the rated speed as shown in Figure 29d pitching is used to control the inertia emulation power. The pitch is able to be reduced for increasing the VSWT output power. In this case the VSWT rotational speed is kept practically constant, using more energy from the wind instead of using kinetic energy from the VSWT. Important to note is that the converter needs to be able to handle the overloading which the pitch controlled inertia emulation causes for the high wind speed case to be possible. In this work it was assumed that the converter is able to handle being overloaded by up to 0.2 pu, although this may not be the case. It may therefore be necessary to disable pitch controlled inertia emulation or impose limits on the power response size and the length of time it may be active.

The accuracy of inertia emulation and its resulting effect on the pitch and the speed for a variable wind speed is shown in Figure 30. The accuracy of the inertia emulation support is shown in Figure 30a and is, similarly to the droop support case in Figure 28c, very accurate up to approximately 16 s during which the VSWT operates at the power limit. After this point can a fairly large inaccuracy be noticed as the inertia emulation transitions from being controlled by the pith to Boeing controlled by the kinetic energy. The reason for the inaccuracy is due to an error in the calculation of $\omega_{wt,est}$ used to decouple the

torque control from the inertia emulation. During the calculation of $\omega_{wt,est}$ has the pitch controlled inertia emulation not been taken into account. Therefore, during the first couple of s of the inertia emulation are a speed decrease calculated for $\omega_{wt,est}$ which does not occur for the actual ω_{wt}. The torque control therefore has a low speed reference as the inertia emulation transitions from pitch controlled to kinetic energy control. The low speed reference results in the power increase noticed in the achieved inertia emulation response. However, the inertia emulation support still follows the path of the frequency support reference even with this inaccuracy. A similar error is the cause of the error at 33 s, however in this case does the inertia emulation transition from being controlled by the kinetic energy to being pitch controlled.

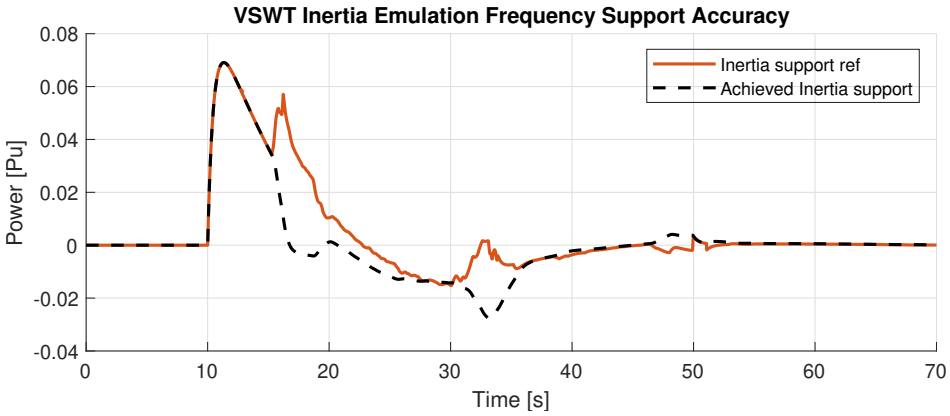

(a) Inertia emulation frequency support accuracy.

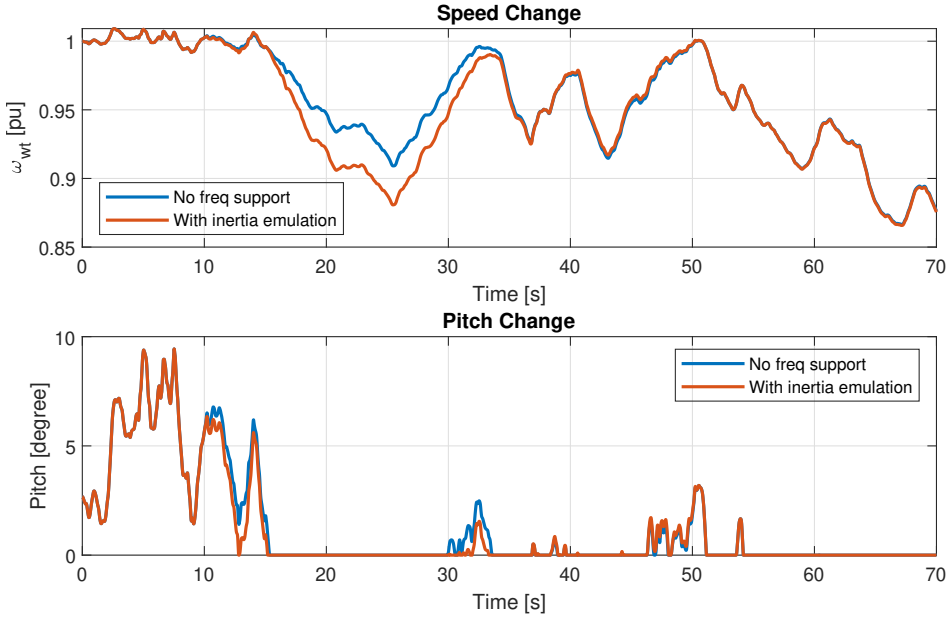

(b) Comparison of speed (top) and pitch (bottom) between normal operation and when providing inertia emulation support.

Figure 30: VSWT behavior and frequency support accuracy while providing inertia emulation support for up-regulation of frequency after a power disturbance of 0.04 pu on the system base at 10 s during a variable wind speed.

The speed and pitch are shown in Figure 30b and shows the expected behavior. When

the frequency disturbance occurs, the VSWT operates at its rated operating point and therefore is the pitch initially used for providing inertia emulation and the rotational speed is left unaffected. However as the wind speed drops, it is no longer possible to use the pitch and kinetic energy from the VSWT rotation is used, causing a decrease in rotational speed.

5.1.3 De-rated operation with droop and inertia emulation combined

Figure 31 shows the VSWT behavior and frequency support accuracy to a 0.04 pu power disturbance applied to the system at 10 s resulting in an under-frequency when the VSWT uses both inertia emulation and droop support while de-rated by 0.1 pu. For the combined inertia and droop support case only the frequency support accuracy and VSWT behavior impact is shown for constant wind speed. The reasons for not showing the variable wind speed case are due to this case not affecting the accuracy in any way that are not observed when using the frequency control strategies individually and the constant wind speed gives a clearer result.

In the available power and wind speed estimates shown in Figure 31a, there is a clear increase in the estimations when the power disturbance is applied. This increase in the estimates is a result of the inertia emulation and is a desired effect. The available power is used as the reference for the droop control. Not including the inertia emulation power in the available power signal would therefore cause a reduction of the power reserve available to the droop. This power reserve reduction would reduce the droop control effectiveness and effectively mitigate any added support from inertia emulation. It is therefore necessary for inertia emulation power to be included in the available power signal, leading to the noticed increase of the estimate. As the available power is a direct result of the wind speed estimation is also the increase due to inertia emulation noticed for the wind speed estimate. This impact of inertia emulation on the droop power reserve has been further discussed in Section 3.3.7.

From figure 31c showing the achieved frequency support accuracy it is observed that the frequency support has a high accuracy. The reference for the frequency support is in this case the sum of $P_{aux,dr}$ and $P_{aux,ie}$. A small deviation is however observed which is a result of the inertia emulations and its work to restore the VSWT speed to its optimal point as discussed in Section 5.1.2. Furthermore, the VSWT power response to the frequency disturbance resembles the case of only using droop support shown in Figure 27c. However, in this case when also including the inertia emulation, the difference is that not the entire power reserve is used, as was the case when only using droop. That there still is a power reserve can be seen from the available power estimation in Figure 31a where, due to the inertia emulation, there is a continuous difference between the output power and the available power. Furthermore can the available reserve also be observed from Figure 31b, where the pitch does not reach its minimum, suggesting that a further decrease is possible to increase the VSWT production further.

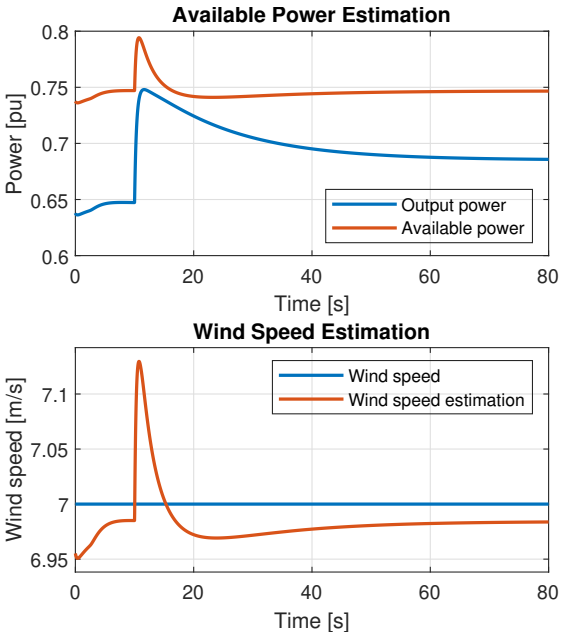

(a) Comparison between available power estimation and output power of VSWT (top) and between wind speed estimation and wind speed input (bottom).

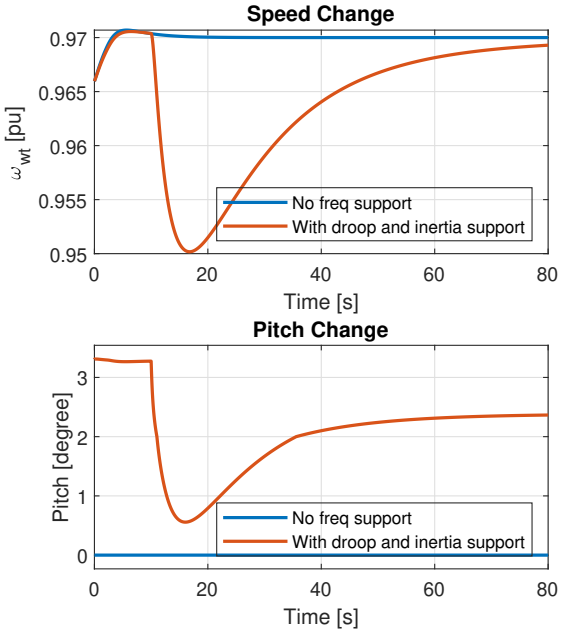

(b) Comparison of VSWT rotational speed (top) and pitch (bottom) between when providing droop and inertia emulation frequency support during normal operation.

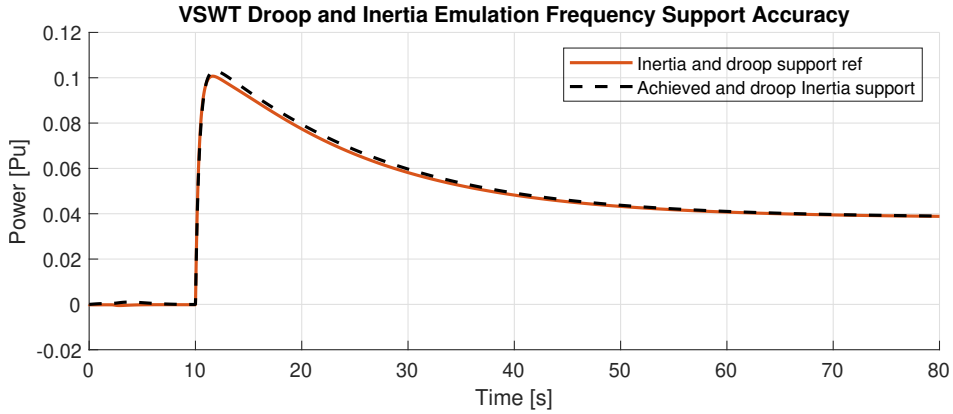

(c) Droop and inertia emulation frequency support accuracy while the VSWT is de-rated by 0.1 pu.

Figure 31: VSWT behavior and frequency support accuracy while de-rated by 0.1 pu and providing droop and inertia emulation frequency support for up-regulation of frequency after a power disturbance of 0.04 pu on the system base at 10 s during a constant wind speed of 7 m/s.

5.2 Frequency response from small load variations

In Figure 32, the frequency of the MATLAB/Simulink system that results from small random load variations is shown together with the combined hydro governor and VSWT frequency control response. In the Figure 32, three cases are analyzed where wind power penetration is set at 30%. The scenarios include when the VSWT is not providing frequency support, when the VSWT is providing inertia emulation, and when the VSWT is de-rated by 0.1 pu while providing both droop support and inertia emulation. For the first case, when the VSWT is not providing frequency support, the effective inertia of the system is 3.43 s. When having the VSWT provide inertia emulation and using a k_i of 5, as in this case, the system inertia would ideally become 8.23 s. However the actual effective system inertia is lower due to having slower wind power inertia response and inaccuracies is wind power inertia.

A variable wind speed has been used for the three cases. However, the frequency variations occurring from the VSWT's power variations are not included for this simulation. The VSWT only affects the system through the power difference between VSWT normal operation and its frequency control operation. Only the changes in load power does therefore cause variations to the frequency. It is therefore assumed that the frequency is kept at 50 Hz if there are no variations of the load. The effects of the frequency variations caused by the VSWT's power variations will be analyzed in Section 6. The load variations for this case have a normal distribution, changes every second and their size were chosen in order to keep the normal operation frequency within approximately 49.9 and 50.1 Hz.

From Figure 32 it is observed that the hydro unit on its own is slow to change its output and often has its peak slightly after the frequency has reached its local maximum or minimum. As a result, it has difficulty containing the frequency. When VSWT inertia emulation is added, the combined control action gains the ability to rapidly change its power output, reducing the frequency range by approximately half. By also including the VSWT droop control while it is being de-rated, the strength of the rapid control action is increased, further limiting the frequency range. These results suggest that proper VSWT frequency control can mitigate frequency variations caused by small and rapid changes in operating conditions. By only including the inertia emulation the frequency is suggested to be significantly improved. However if further improvements are necessary and if the power loss is acceptable, the VSWT can be de-rated to further support the frequency with droop control.

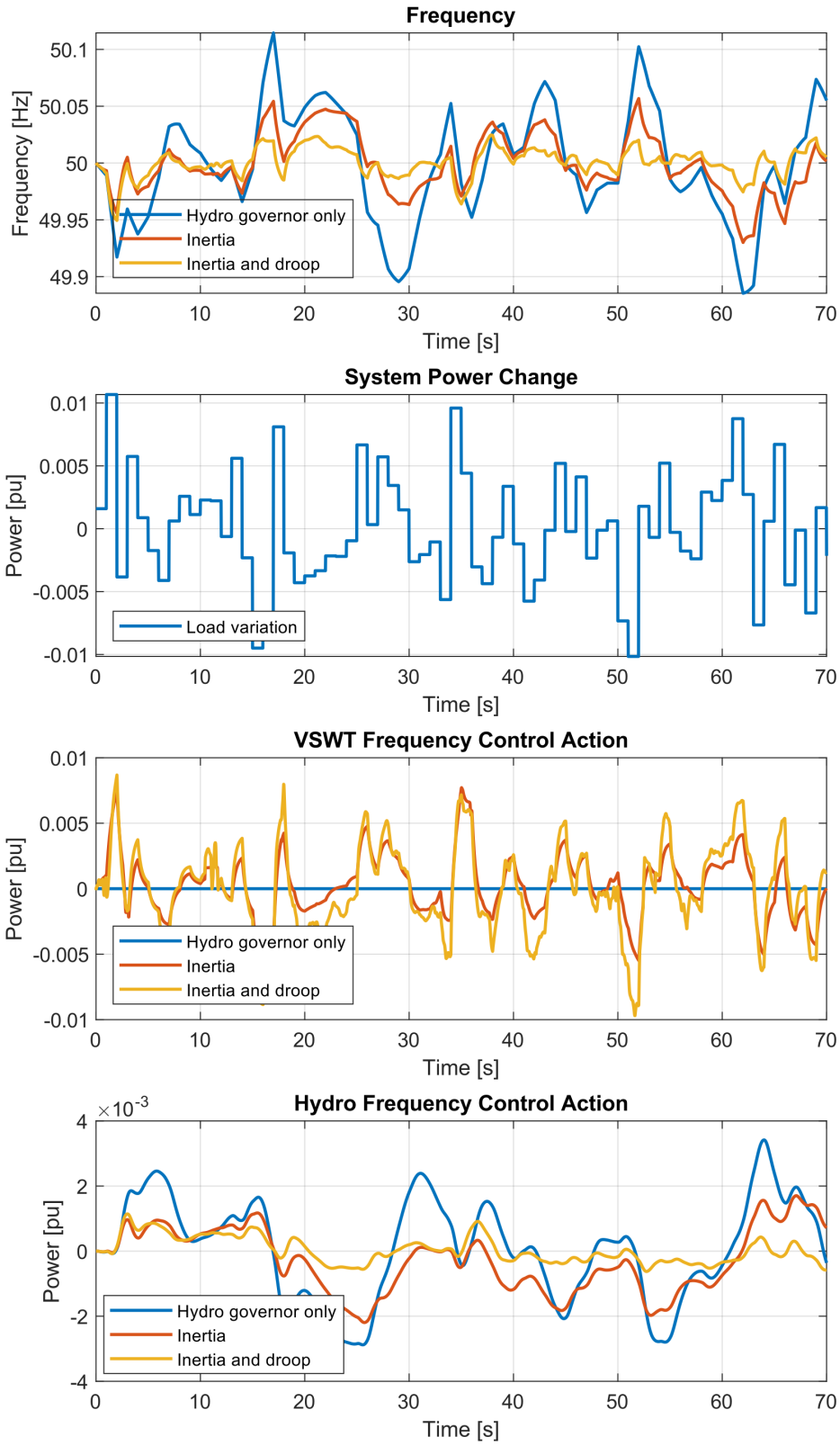

Figure 32: Frequency and frequency control power response from hydro and VSWT to small random variations in the load when the VSWT uses no frequency control, provides inertia emulation and provides inertia emulation along with droop support while de-rated by 0.1 pu.

The power reserve of the VSWT was chosen to be 0.1 pu in Figure 32. However, if the purpose of the droop is to only aid with the continued frequency variations shown in Figure 32, such a large reserve is not necessary. By having a frequency range of +/- 0.1 Hz and a VSWT droop setting of 5% will, according to (2.16), a reserve of 0.04 pu be enough. By also considering that inertia emulation and droop support reduce the frequency range in this case by more than half can the reserve, and therefore also VSWT de-rating, be further reduced to 0.02 pu. Reduction in the VSWT de-rating beyond this should result in reduced droop control strength, but still cause stability benefits. Figure 33, showing the frequency probability distribution when running the case of Figure 32 for 900 s, including cases for 0.02 pu and 0.01 pu power reserves. Table 4 does also show for what percentage of the 900 s simulation time the five analyzed cases are outside specified frequency ranges. Figure 33 and Table 4 suggest that reducing the power reserve, and therefore de-rating, down to even 0.01 pu causes for this case only limited, if any, practical reduction in frequency stability. It is even shown to have less time outside 49.99 - 50.01 Hz compared to the 0.1 pu reserve case. The necessary de-rating will vary depending on the size of the frequency variations for which the droop control is designed to regulate and the necessary stability improvement of the droop control, though these results suggest that significant improvements are possible with only a small reduction in the VSWT average power production.

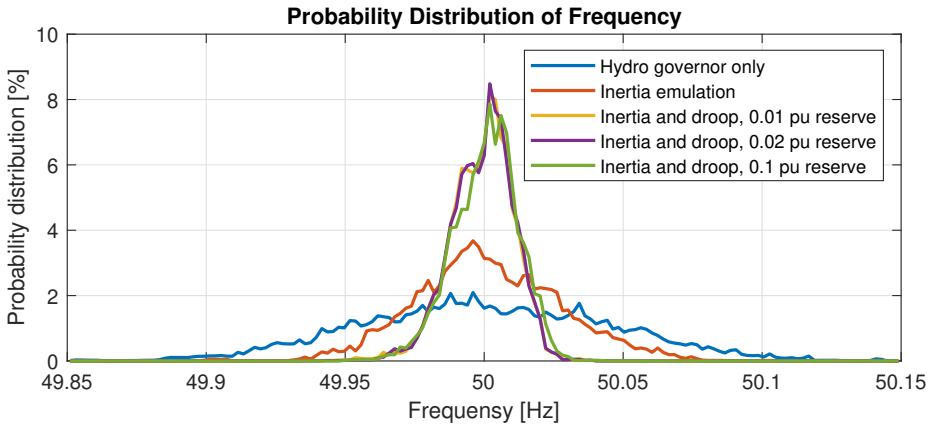

Figure 33: Frequency probability distribution for 900 second simulations of small random load power variations when the VSWT uses no frequency control, provides inertia emulation and provides inertia emulation along with droop support while de-rated 0.1 pu, 0.02 pu and 0.01 pu.

Table 4: Percentage of simulation time in which the analyzed cases are outside certain frequency ranges.

	49.9 - 50.1 Hz	49.95 - 50.05 Hz	49.99 - 50.01 Hz
Hydro governor only	2,61%	27,98%	83,27%
Inertia emulation	0,10%	6,03%	68,70%
Inertia and droop, 0.01 pu reserve	0,00%	0,14%	35,94%
Inertia and droop, 0.02 pu reserve	0,00%	0,05%	35,91%
Inertia and droop, 0.1 pu reserve	0,00%	0,01%	38,30%

Table 5 presents the average VSWT power loss for the analyzed power reserves and the

case of only using inertia emulation and shows that the power loss is similar, but slightly higher compared to the desired power reserve. One factor contributing to the extra power loss is that the strength VSWT droop down-regulation is set higher than for the up-regulation due to the VSWTs having a greater ability in reducing power. There may also be inaccuracies in the control which contributes to the power loss. Furthermore Table 5 shows that any VSWT power losses due to inertia emulation are, on average, small enough to be negligible.

Table 5: Average VSWT power loss when de-rated to give a reserve of 0.1 pu, 0.02 pu and 0.01 pu, using droop as well as inertia emulation to control the frequency. Also shows the power loss of inertia emulation

VSWT frequency control	Power reserve [pu]	VSWT power loss [pu]
Inertia emulation	0	2.10e-5
Inertia emulation and droop	0.01	0.012
	0.02	0.022
	0.1	0.108

5.3 Frequency response from large disturbance

The resulting frequency response of the system from the cases in Section 5.1.2 and Section 5.1.3 for a variable wind speed is shown in Figure 34 along with the frequency response when only the hydro governor is used. The wind power penetration used is 30% for all three cases. The power responses from the VSWT and the hydro governor are also shown in Figure 34, along with the load power change that caused the disturbance. Similar to in Figure 32, only the VSWT affects the system through the power difference between normal operation and frequency control operation, removing the power variations to the system caused by the VSWT changing operational point. Figure 32 shows significant frequency improvements when including the VSWT inertia emulation and even further improvement when the VSWT is de-rated and droop support is included. These results suggest that both VSWT frequency control methods can help significantly in managing large frequency disturbances.

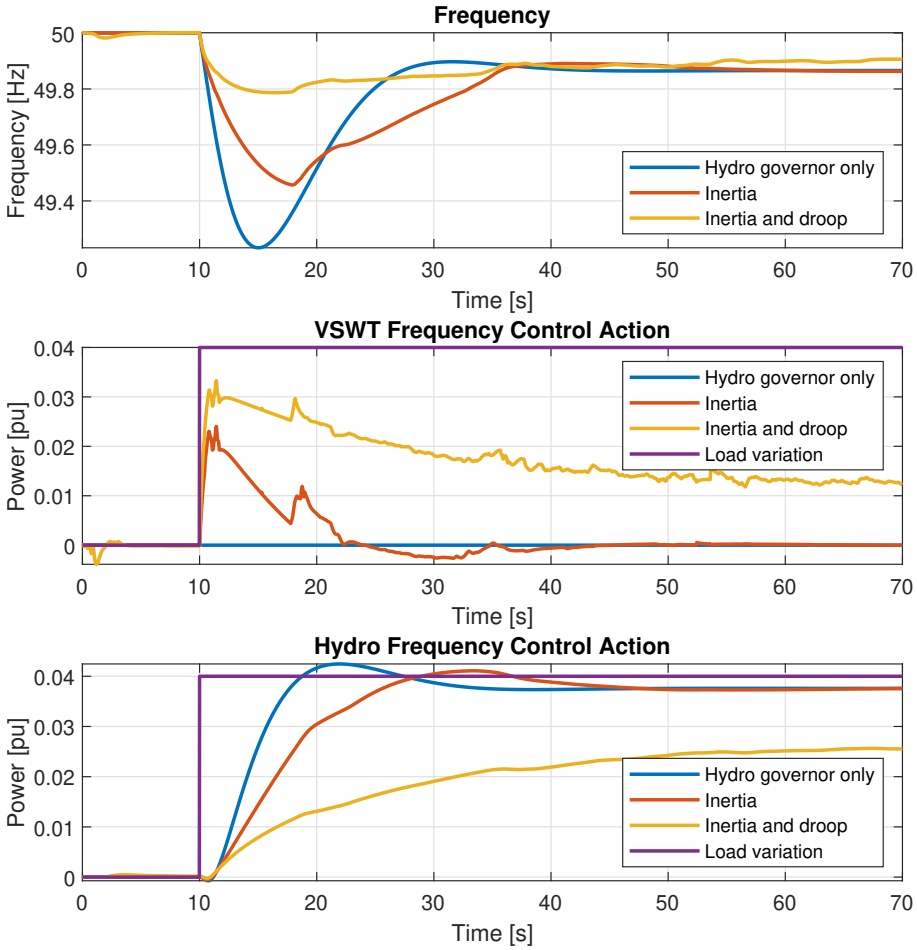

Figure 34: Frequency response and power response from hydro governor and VSWT due to a 0.04 pu power disturbance occurring at 10 s. The frequency and power responses from no VSWT frequency control, inertial emulation and inertia emulation along with droop support from VSWT when de-rated by 0.1 pu are shown.

The hydro governor is shown to have a slow power response with a small initial power decrease resulting from the water inertia, as discussed in Section 2.3. By including the VSWT inertia emulation, the initial problems of the hydro governor can be compensated. The power increase from the VSWT inertial emulation is rapid but active for a limited period of time, after which the slower hydro governor has had time to catch up and takes over to achieve a balance of power. By having a faster initial power increase, the frequency has a lower RoCoF when using inertia emulation, increasing the time until the frequency nadir occurs and making it easier for the hydro governor to respond to the falling frequency, improving the frequency stability. The spike in the inertia emulation frequency control action noticed at approximately 16 s is a result of an error in the $\omega_{wt,est}$ calculation as discussed in Section 5.1.2.

To improve the frequency response further can the VSWT be de-rated to create a power reserve, allowing for droop support. The VSWT droop causes the initial power increase to become larger as the VSWT droop can, in contrast to the hydro governor, respond rapidly to frequency variations and does not require a slow transient droop. As discussed in Section 5.2, the required power reserve, and therefore VSWT de-rating, vary depending on what

frequency variations it is designed to control and the stability improvement necessary. Figure 35 shows how the frequency nadir changes for the considered system disturbance of 0.04 pu when the power reserve is changed, and the figure shows an increased control strength as the reserve is increased. However any increase over 0.1 pu does not have any stability improvements which can be reasoned from Figure 31 as the 0.1 pu power reserve is not fully utilized. By comparing Figure 35 to Figure 33, it is shown that the necessary VSWT de-rating may increase as larger frequency disturbances are considered. However the VSWT de-rating does not need to fully cover the power increase of the worst case scenario for it to be beneficial. A balance between necessary stability improvement and acceptable VSWT power loss need to be met.

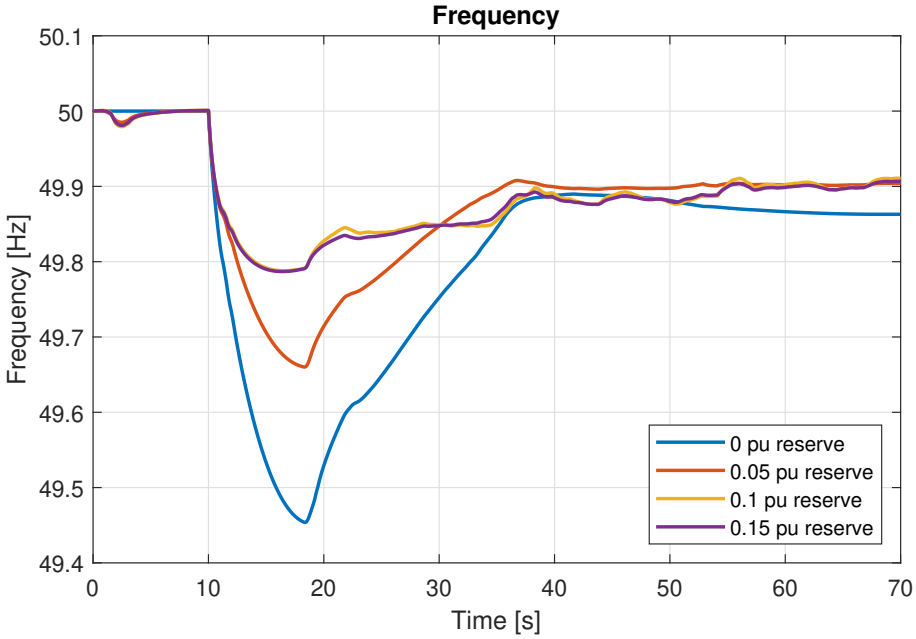

Figure 35: Frequency response due to a 0.04 pu power disturbance occurring at 10 s when the VSWT provides inertia emulation and droop support with a power reserve of 0 pu, 0.05 pu 0.1 pu and 0.15 pu.

6 System simulations in PSS/E

This section presents the result for the analysis of the island system shown in figure 24 according to the test cases presented in Table 3. Firstly will, in Section 6.1, the continuous operation of the island system while disconnected from the larger grid be analyzed as this case decides the wind power penetration used. Thereafter is the transition of the island system from being connected to the grid to being operated independently analyzed in Section 6.2. This case uses the same initial operating point of the VSWTs as in the case analyzing continuous operation, as well as the same wind speed time series and load to determine the possible power transfer to the island system.

6.1 Continues operation of island system while disconnected from the grid

For the case of operating the island system while disconnected from the grid are the frequency stability improvements analyzed for when the VSWTs within the system provide frequency support compared to when only the hydro unit is used for frequency control. The VSWT frequency support analyzed are inertia emulation and inertia emulation together with droop support while de-rating the VSWT. However, first, the operating condition for the island system is chosen in order to keep the frequency within the range of 49.5 to 50.5 Hz when no VSWT frequency control is active. This involves choosing a wind power penetration, wind speed time series and the size of load variations which gives the desired frequency range. The wind power penetration is important for the frequency variation as the variable wind speed used will cause the wind power production to vary, continuously causing power variations inside the island system. As the penetration of wind power increases, the sizes of these power variations grow, causing larger variations of the frequency. Together with the wind power induced power variations have also random variation the the load been added, causing future power variations in the island system.

6.1.1 Stability of island system during VSWT normal operation

The chosen operational condition used for the analysis of the continuous island operation is shown in Figure 36, where a 900 s simulation is used. In Figure 36a are the wind and hydro power production observed in MW. The wind power is composed of 3 arrogated 3.6 MW VSWT for a combined rated power of 10.8 MW. The same wind speed is used for every VSWT, shown in Figure 36b, giving an average power production for the wind turbines of 9.39 MW or 0.87 pu on the machine base and a power variation from 0.60 to 1 pu. The hydro unit produces on average 10.39 MW to supply the load variations shown in Figure 36c. This wind and hydro power production gives a wind power penetration of 47.5%. The resulting frequency distribution from this operation condition for the island system is shown in Figure 37 where it is observed that the resulting frequency rage is 49.56 Hz to 50.56 Hz, with is close to the 49.5 to 50.5 Hz target range.

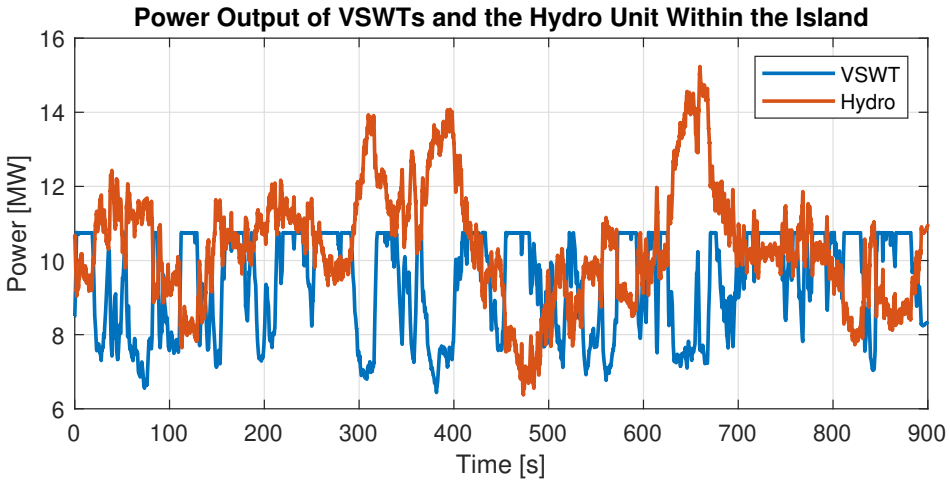

(a) Hydro and wind power production for continuous island operation with 47.5% wind power penetration and no wind power frequency control.

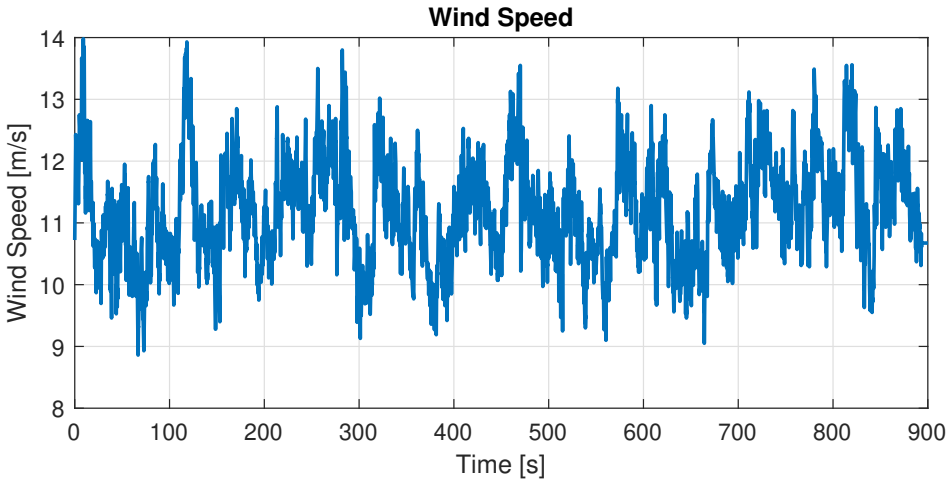

(b) Wind speed used for the wind power production in the island.

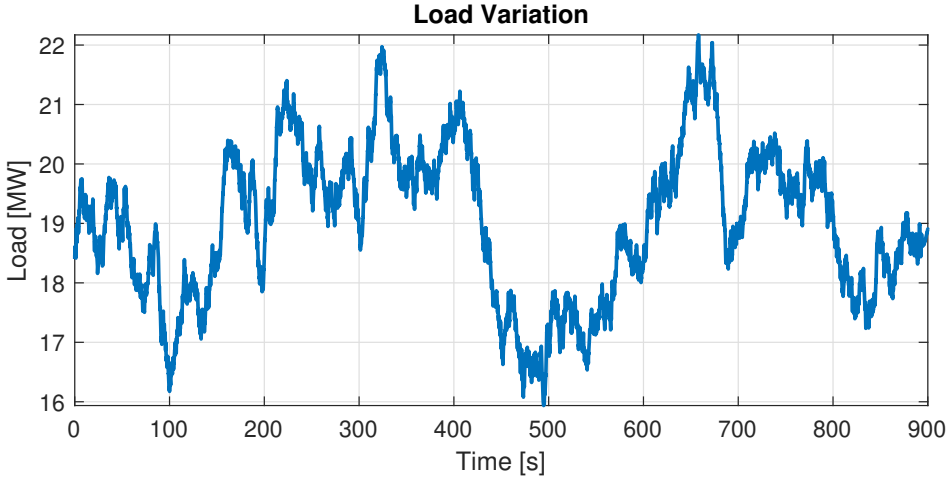

(c) Variation in the load power during the continuous island operation.

Figure 36: Power production, wind speed, and load variation for 900 s (15 minutes) of continuous island operation

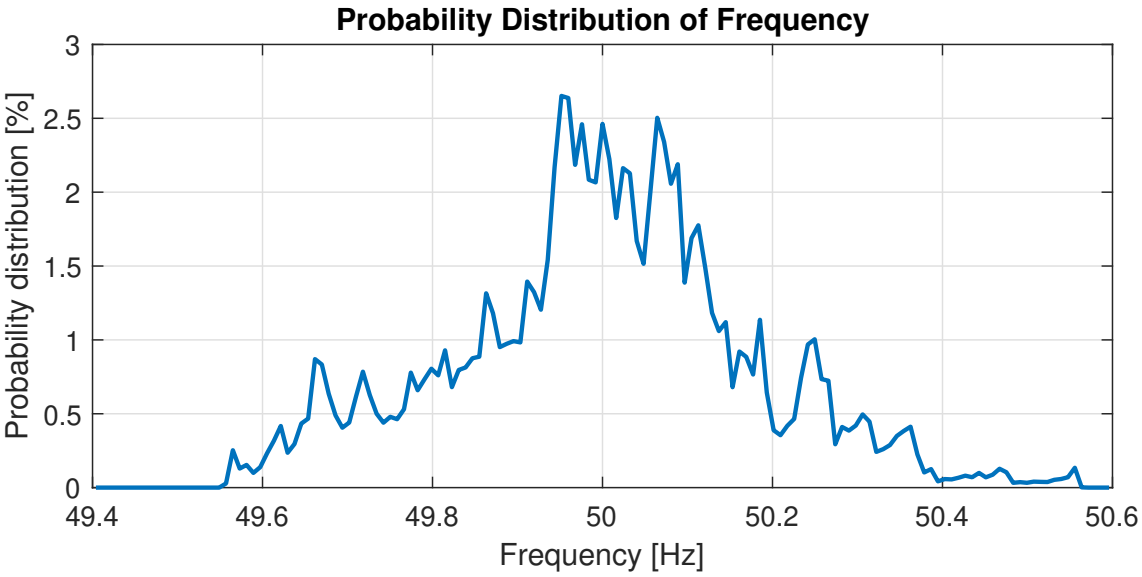

Figure 37: Frequency probability distribution for continuous island operation with 47.5% wind power penetration and no wind power frequency control.

Concerning the voltage levels in the island during this operation condition are these shown in Figure 38. From the voltages in the figure it is shown that they are all within the 0.85 to 1.1 pu range specified for the island operation in Table 1 and even within the 0.9 to 1.1 pu range specified for the grid connected operation. The buses which have a voltage deviating the most from the 1 pu nominal value are bus 4, which is the bus where the load is connected, and bus 5, where the VSWTs are connected. The voltage deviation for these buses is due to the line between bus 4 and the substation at bus 3 as well as the cable between bus 4 and bus 5 being the main distances within the island system model. Due to having a high R/X ratio on the line connecting the substation and the load, both the active and reactive power flow from the hydro unit causes a voltage drop on the load bus. However as the wind power production is increased the power flowing from the substation will decrease, raising the load bus voltage closer to the nominal value, but due to the voltage drop over the cable will the voltage on the wind power bus increase above the nominal voltage. Furthermore it is observed that the voltage varies continuously across all buses which is due to having a quite strong coupling between frequency and voltage within the system. As a power variation is the system causes a change in operational points will the change be reflected on the generator terminals. Power variation in the system will therefore result in voltage variations causing the voltage distribution to be similar to the frequency distribution.

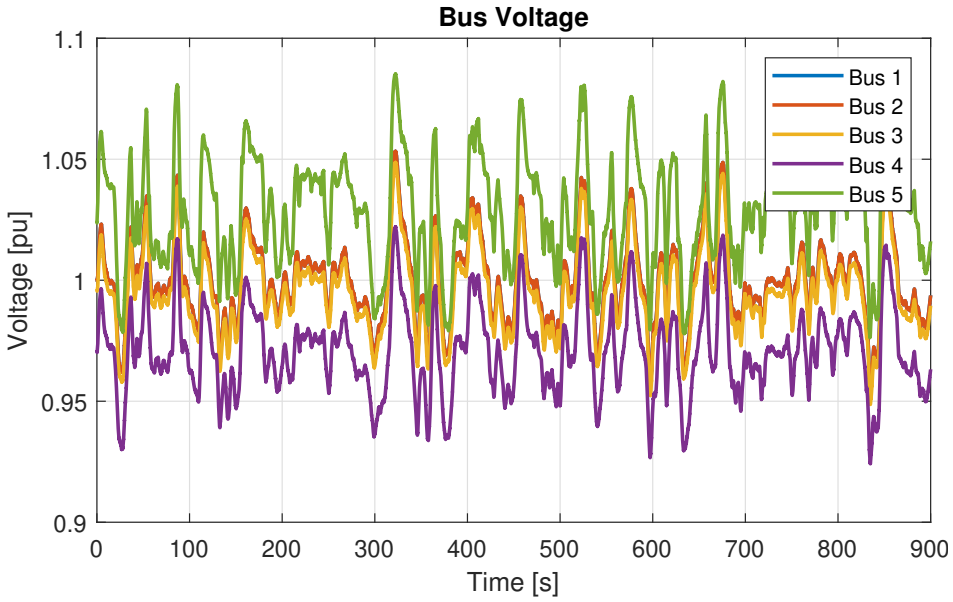

Figure 38: Voltages in the island system during continuous island operation.

6.1.2 Impact of VSWT frequency control on stability

The impact of the frequency control of the connected VSWTs on the frequency stability during the island continuous operation can be observed in Figure 39. Figure 39a shows the frequency time series during the analyzed time and Figure 39b shows the corresponding frequency probability distribution. The normal operation case without any frequency control is shown along with the cases where the VSWTs uses inertia emulation and when the VSWTs uses both inertia emulation and droop support while de-rated. By comparing the normal case to the inertia emulation case is a small improvement shown on both the up-regulation and down-regulation sides. It is shown from Figure 39b that the absolute minimum frequency are slightly higher in the inertia emulation cases where the minimum frequency increases from 49.56 Hz to 49.59 Hz and a similar effect is noticed for the maximum frequency where it is reduced from 50.56 to 50.53 when using inertia emulation. This constitutes an overall frequency range improvement of 6%

When analyzing the frequency stability improvement due to the inertia emulation and droop support with de-rated operation shown in Figure 39, a greater improvement can be observed compared to the purely inertia emulation case. This improvement is as expected due to the power reserve along with the droop resulting in a greater control strength. The improved frequency range becomes 49.68 Hz to 50.22 Hz, which is a 44% range improvement compared to the normal case, reducing the range by almost half. The down-regulation side shows a greater reduction of the range, caused by the greater VSWT droop strength for down-regulation.

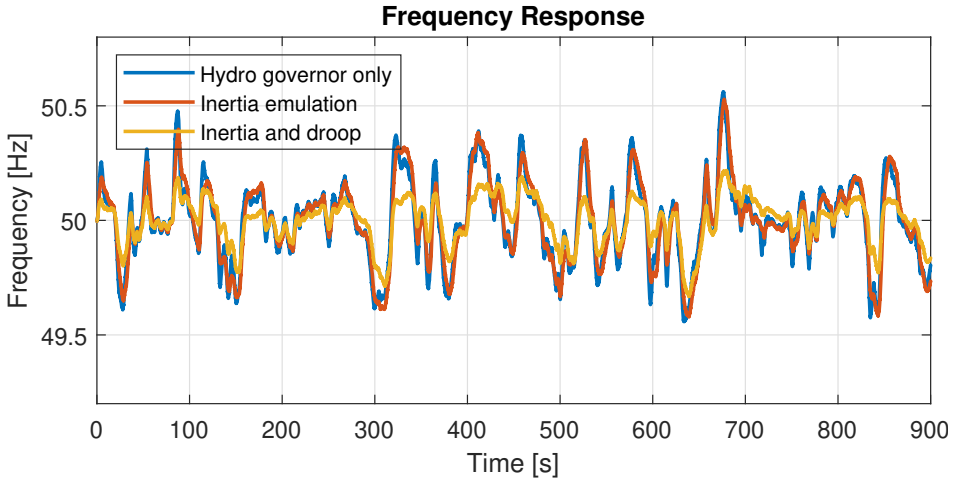

(a) Frequency response.

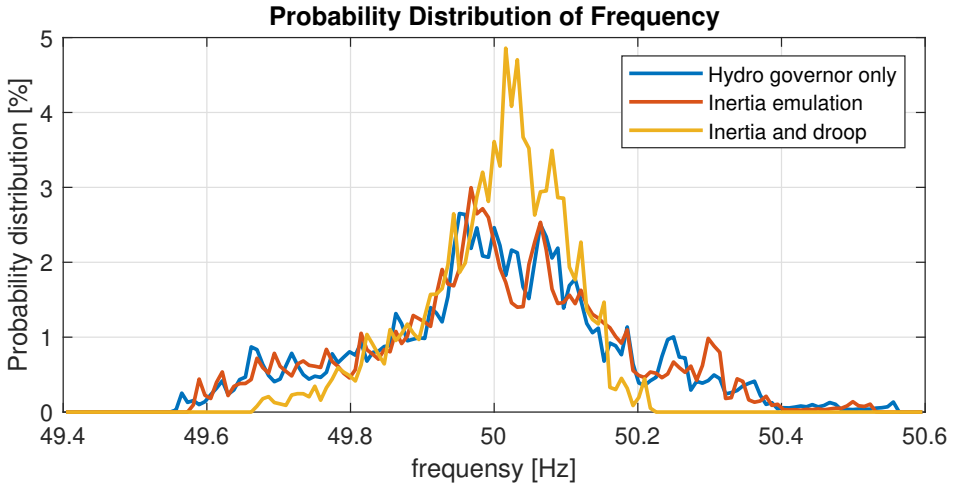

(b) Frequency probability distribution.

Figure 39: Analysis of continuous island operation frequency, comparing only using the hydro governor frequency control, using wind power inertia emulation and using wind power inertia emulation together with droop support while de-rating the wind power.

Through studying Figure 40a can it be noted that the achieved inertia emulation frequency support power is fairly accurate to its reference. The achieved frequency support is determined by calculating the VSWTs power difference between its normal control and when providing inertia emulation, while the frequency support reference is the signal $P_{aux,ie}$ shown in Figure 20. Further, Figure 40b shows the power production within the island system where the wind power and hydro power is observed to behave reasonably and the wind power penetration during the studies time is 47.4%. This is a 0.1% reduction in wind power penetration compared to the normal operation case and corresponds to a 0.003 pu power reduction. This small, although not negligible, power reduction where not noted for the MATLAB/Simulink simulation and is believed to be a product of the frequency probability distribution showing a slight predominance for over-frequencies. Therefore is there a greater need for down-regulating the frequency resulting in reduced power compared to the normal case.

The inertia emulation from the PSS/E shows less frequency improvement than expected by comparing the frequency probability distribution from the PSS/E simulation with the MATLAB/Simulink simulation from Figure 33. Figure 40a suggests that the reduced improvement for the PSS/E case is not due to inaccuracies in the inertia emulation control system. The reason instead has to do with the nature of the power variation. In the MATLAB/Simulink case the power changes instantaneously, which is in contrast to the PSS/E case. In PSS/E, the power variation caused by the wind speed and load change takes some time to realize, approximately 2 to 3 s for the faster wind speed changes up to tens of s for the load variations. The slower changes of power in the PSS/E results in a slower RoCoF and therefore causes the VSWTs inertia emulation to be less effective.

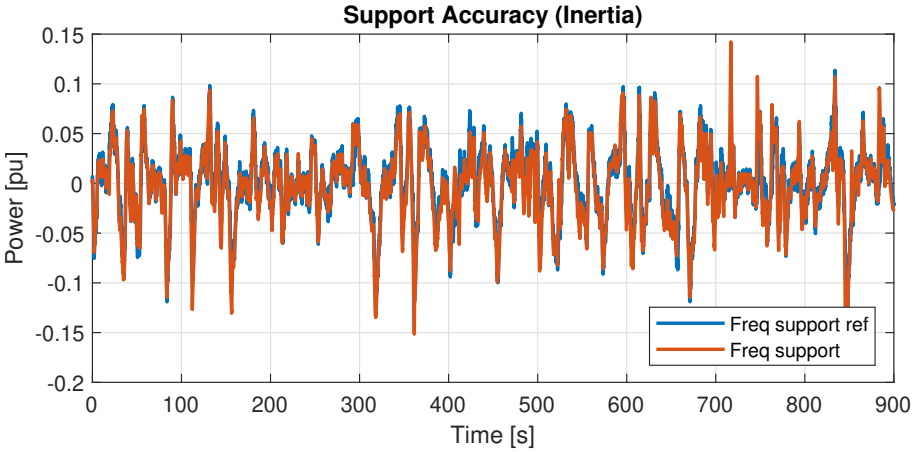

(a) Inertia emulation frequency support accuracy during continuous island operation by comparing the achieved frequency support against a reference $P_{aux,ie}$.

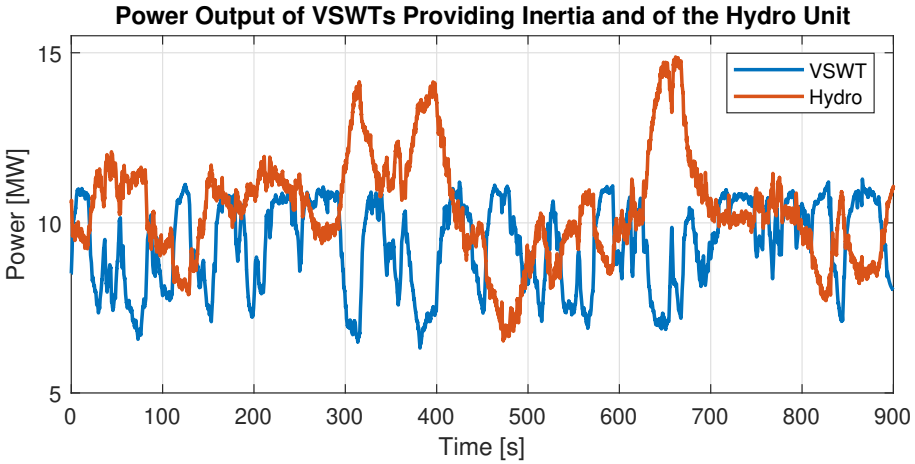

(b) Hydro and wind power production for continuous island operation with 47.5% wind power penetration and inertia emulation frequency support.

Figure 40: Wind power inertia emulation effect on power production during continuous island operation.

Figure 41a shows that an accurate achieved frequency support is observed when comparing it to the reference consisting of the sum of $P_{aux,ie}$ and $P_{aux,dr}$. However due to de-rating the

VSWTs, in this case by 0.1 pu, the VSWT output is reduced while the hydro power output is increased compared to the normal case as shown in Figure 41b. This causes a reduction of the wind power penetration from 47.5% down to 41.1%, corresponding to a power loss of 0.12 pu compared to the normal operation case. The reason for having losses greater than the power reserve are due to having a stronger down-regulation droop setting compared to the setting for the up-regulation. The loss in this case is somewhat larger then the 0.108 pu power loss observed from the MATLAB/Simulink simulations, which once again is due to the predominance for over-frequency in the PSS/E simulation, causing an increased need for down regulation the frequency. The reduction in the wind power penetration may contribute to the reduced frequency range as it causes the total inertia in the island system to increase. The reduced wind power penetration would however not cause any reduction in the VSWTs power variations as the de-rating is designed to keep a constant power reserve of 0.1 pu for the droop control to utilize. Figure 41a shows a maximum frequency power support of a level similar to the VSWT de-rating and therefore similar to the power reserve, suggesting that this de-rating setting gives the maximum frequency improvement. Reducing the de-rating will therefore result in less power loss but also less frequency improvement as discussed in Section 5.2 and in Section 5.3.

An additional factor affecting the droop support capability is the frequency restoration caused by the LCFB1 model. As either the wind power production is reduced or the load is increased for a long period of time, the power reserve for the droop control would be depleted without the frequency restoration. This depleted power reserve would cause a reduced control strength, creating difficulty in managing the frequency if any power variations would cause further frequency decrees. An example of such a time instance where the power reserve would be depleted is during a period between 620 to 670 s in Figure 36. However, when the LCFB1 controller is active it attempts to restore the VSWT power reserve, resulting in a greater ability for the droop control to manage the furthest frequency dips.

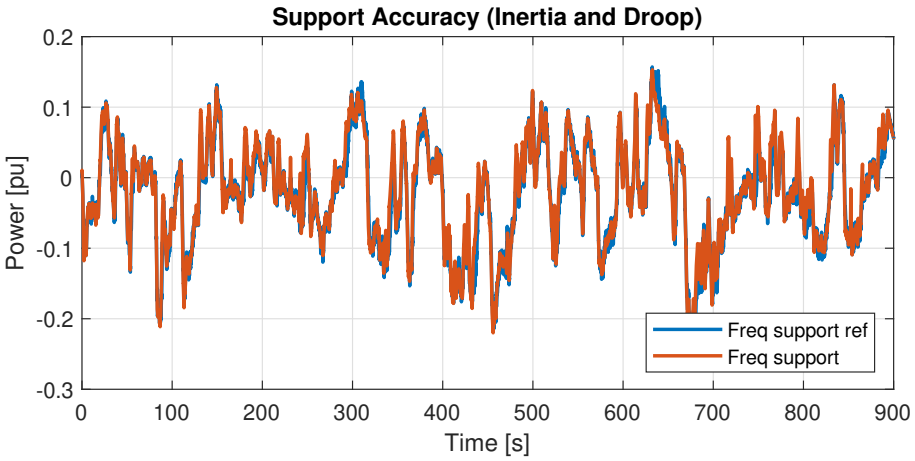

(a) Inertia emulation and droop frequency support accuracy during continuous island operation by comparing the achieved frequency support against a reference $P_{aux,ie} + P_{aux,dr}$.

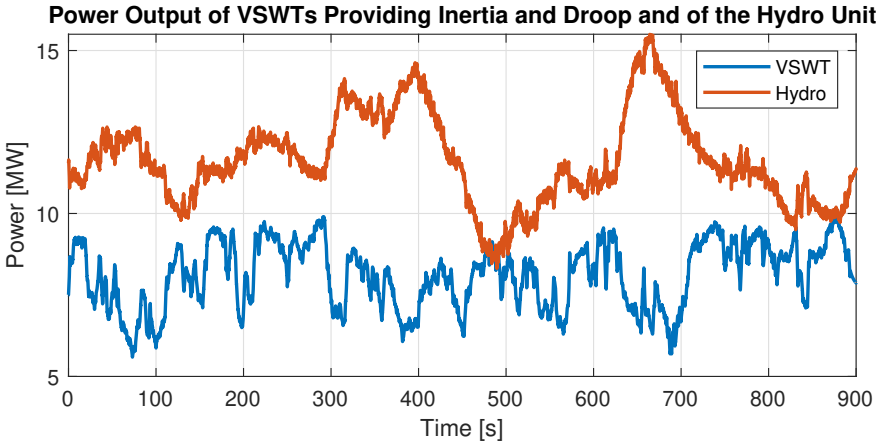

(b) Hydro and wind power production for continuous island operation with 41.1% wind power penetration and inertia emulation together with droop frequency support while de-rating the wind power.

Figure 41: Wind power inertia emulation together with droop support effect on power production during continuous island operation.

Figure 42 shows how the probability distribution of the voltage on the most vulnerable busses changes when the VSWT provides frequency control. The buses in question are bus 4, the load bus, and bus 5, the wind power bus. The figure shows an improvement of the voltage as the frequency control is applied. The extreme voltages have an increased margin to 0.9 pu in the case of bus 4 and from 1.1 pu in the case of bus 5. Furthermore the voltage range is reduced for the buses, where the addition of droop control causes a further reduction of the range compared to solely using inertia emulation. The frequency control does in general show a similar effect on voltage probability distributions as compared to the frequency probability distributions shown in 39b. The similar effect is due to the strong coupling between voltage and frequency apparent in the island system network.

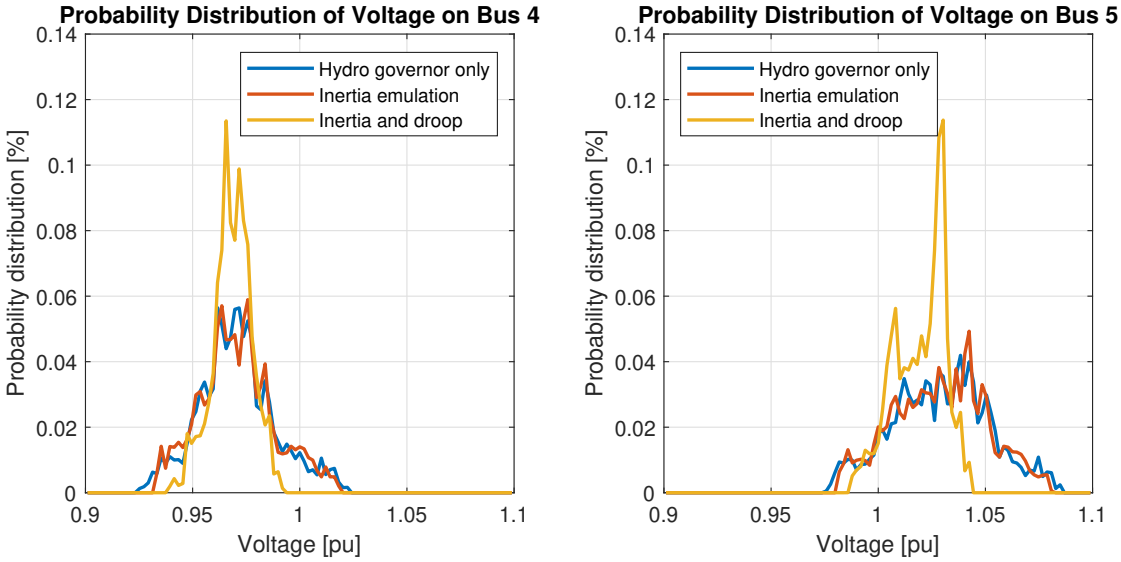

(a) Voltage probability distribution for Bus 4 (the load bus).

(b) Voltage probability distribution for Bus 5 (the wind power bus).

Figure 42: Voltage probability distribution for normal wind power operation and when the wind power is using frequency control.

Another change to the voltage caused by the frequency control is that the de-rating and droop control causes the average voltage to drop slightly for both buses. The average voltage goes from 0.971 pu to 0.968 pu for bus 4 and from 1.029 pu to 1.020 pu for bus 5. The cause for the voltage decrees is the reduction of the wind power fed into bus 4 causing a greater power transfer and therefore also greater voltage droop across the line between bus 4 and 3. There is also less power transferred across the cable between bus 4 and 5, resulting in the greater average voltage reduction of bus 5. The voltage drops are however in this case small enough to be of little significance.

6.1.3 Effects of controlling the voltage on the wind power bus by the VSWT

The reactive power production for the VSWT has normally during this work been controlled to have a constant power factor of 0.95. However Figure 43 show the voltage probability distributions if the VSWTs reactive power is instead controlled to regulate the voltage at their own bus using the REECA1 model. This local bus voltage control was implemented by changing the PFFLAG to 1, VFLAG to 1 and the QFLAG to 0 in the REECA1 model. The target value for the voltage regulation is the voltage calculated during the load flow for a power factor of 1, which is 1.008 pu for the normal as well as the inertia emulation cases and 1.002 pu for the inertia emulation together with the droop case. The target is closer to 1 pu in the later case due to de-rating the VSWTs. The voltage probability distribution at the wind power bus, bus 5, is shown in Figure 43b where the voltage range is significantly reduced compared to Figure 42b for all cases. Figure 43b also shows that the inertia together with droop still manages to have a higher proportion of the voltage at the target voltage compared to the other cases, similarly to the uncontrolled cases, also when VSWT voltage control is applied. The voltage probability distribution at bus 4 shown in Figure 43a is similar to the distribution of Figure 42a, but

shows an increased probability for the voltage to be closer to its average value, suggesting that the VSWTs voltage control also reduces the size of the voltage oscillations on bus 4. Furthermore,controlling the voltage with the VSWTs causes no noticeable effect on the ability for the VSWTs to control the frequency.

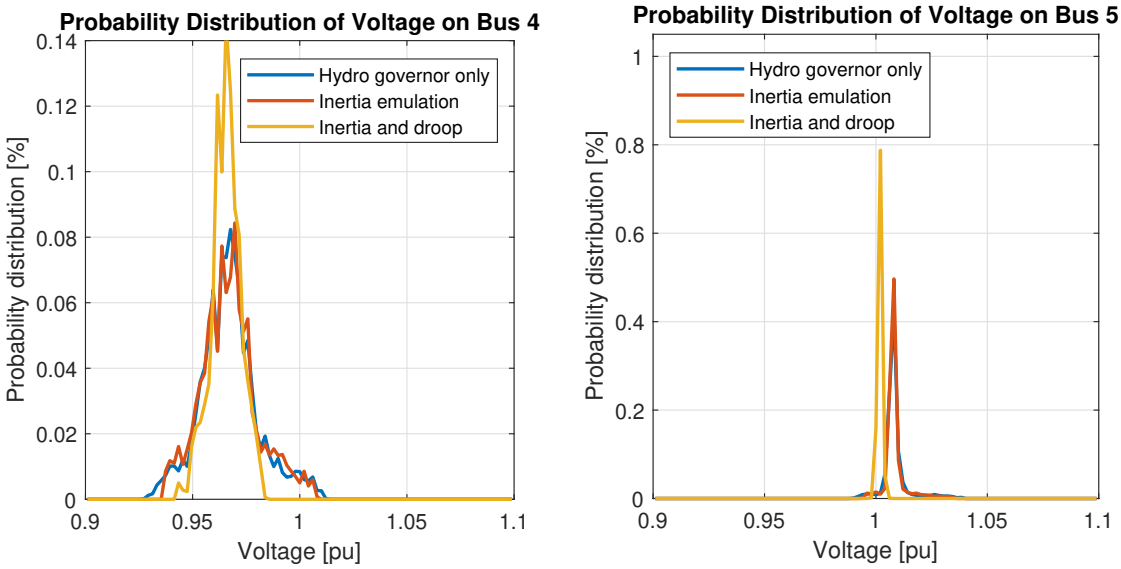

(a) Voltage probability distribution for Bus 4 (the load bus).

(b) Voltage probability distribution for Bus 5 (the wind power bus).

Figure 43: Voltage probability distribution when the wind power is controlled to maintain 1 pu voltage on bus 5 for normal wind power operation and when the wind power is using frequency control.

An investigation into using the VSWTs to control the voltage at the load bus, bus 4, was also made by changing the bus number for voltage control in the REECA1 model. However it was noted, at least for version 35.5 of PSS/E, that the REECA1 model is not able to perform remote bus voltage control and a plant model is instead necessary. Therefore, due to the extra complexity and time limitations, where therefore remote bus voltage control not simulated.

6.2 Island system stability during unplanned transition

For analyzing the island system during the transition from grid connected to island operation are the power transfer to the system of importance. This power will be cut off, resulting in a large instantaneous power difference within the island when it is disconnected. The power transfer to the island therefore has a limit, considering that the chosen frequency limit for the instantaneous frequency is 49.0 to 51.0 Hz. For the power transfer limit, the frequency nadir improvement are analyzed when the VSWTs connected to the island are controlled to help in regulating the frequency. The VSWT frequency control analysed is inertia emulation and inertia emulation together with droop control while derated. The corresponding power transfer increase from the grid that is possible when the VSWT provides frequency support is also analyzed.

6.2.1 Stability of island system during VSWT normal operation

Figure 44 shows the operation of the island system during the transition to island operation when there is no frequency support from the VSWTs. The operational point at the VSWT at the moment of transition was chosen due to this point giving an average improvement of the frequency when VSWT frequency control is activated, which is further discussed in Section 6.2.2. The wind and hydro production are shown in Figure 44a, where the wind power production is set to operate in the same manner as in Section 6.1.1, using the same wind speed, shown in Figure 44b. The hydro unit is set to operate at 5.20 MW before the transition. The wind power production is 8.62 MW and the load is 18.88 MW just before the transition, as shown in Figure 44c. When including the losses in the system does the power transfer at the moment of transition come to 5.75 MW, which is equal to 31.3% of the 18.4 MW nominal load in the island. Regarding the reactive power, approximately 1.00 MVAr were transferred to the island system at the moment of transition. The frequency response which cuts off this power transfer results in are shown in Figure 45 where the frequency nadir is 48.99 Hz, close to the target of 49.0 Hz. From the frequency figure can also the influence of the LCFB1 turbine load controller model be observed as the frequency returns to oscillating around 50 Hz after the hydro unit has responded instead of having a steady state deviation, which would be the case without the LCFB1 model.

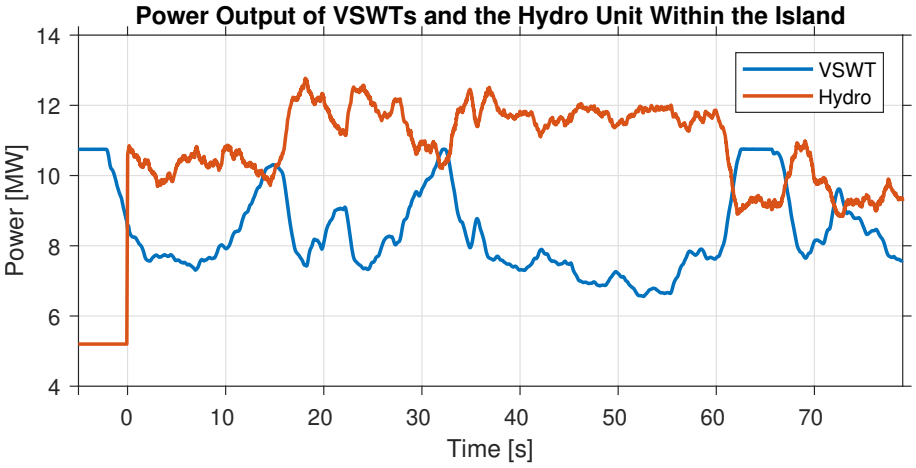

(a) Hydro and wind power production within the island for transition to island operation and no wind power frequency control.

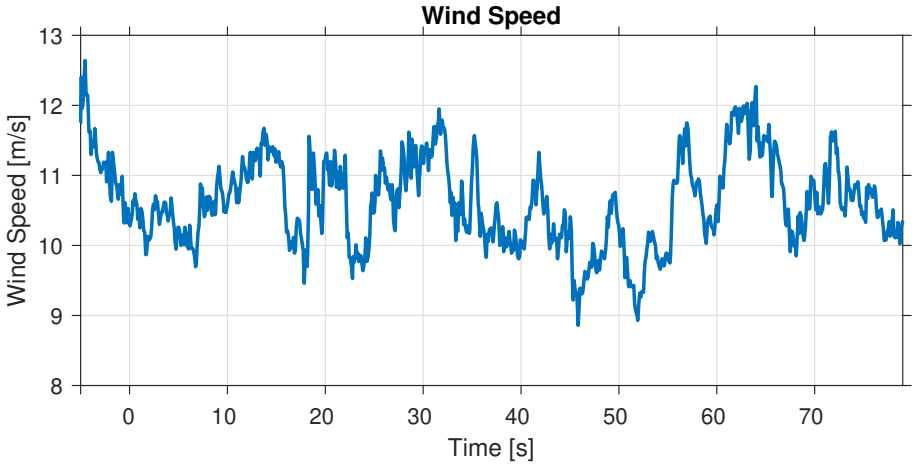

(b) Wind speed used for the wind power production on the island.

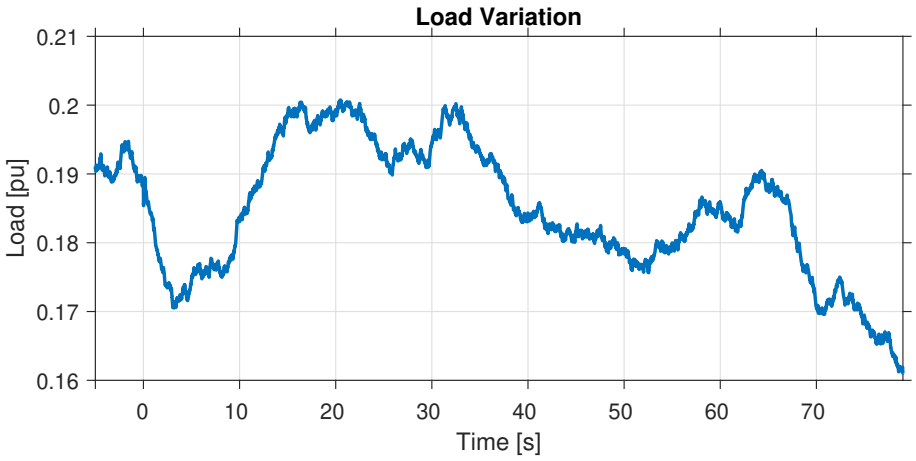

(c) Variation in the load power during the transition to island operation.

Figure 44: Power production, wind speed, and load variation for approximately 80 s when transitioning to island operation.

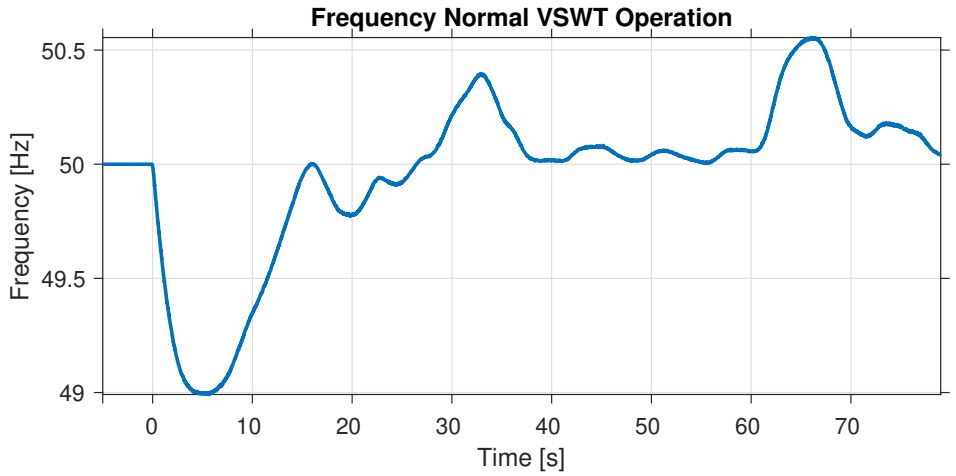

Figure 45: Frequency in the island system during transition to island operation with a power transfer of 5.75 MW.

From Figure 46 can it also be observed that the voltage drops as the transition occurs, similarly to the frequency, due to the coupling between frequency and voltage present within the island system. The bus where the voltage deviates the most from 1 pu is bus 4, the load bus, and is due to the voltage drop over the line between bus 3 and 4. The voltage briefly deviates below 0.9 pu, but stays above 0.85 pu throughout. Looking closely at Figure 46 can also a small transient in the voltage be observed just as the transition occurs. This transient is a result of the reactive power transfer from the grid being cut off, resulting in a deficit of reactive power within the island until the units in the island adjusts their reactive power production. Cutting off this reactive power flow causes in this case limited effect on the island. However if the reactive power flow is larger can this voltage transient impact the island. For example would the loading change in accordance to the load voltage sensitivity, which in this case would cause it to decrease proportionally as the load is of the constant current type.

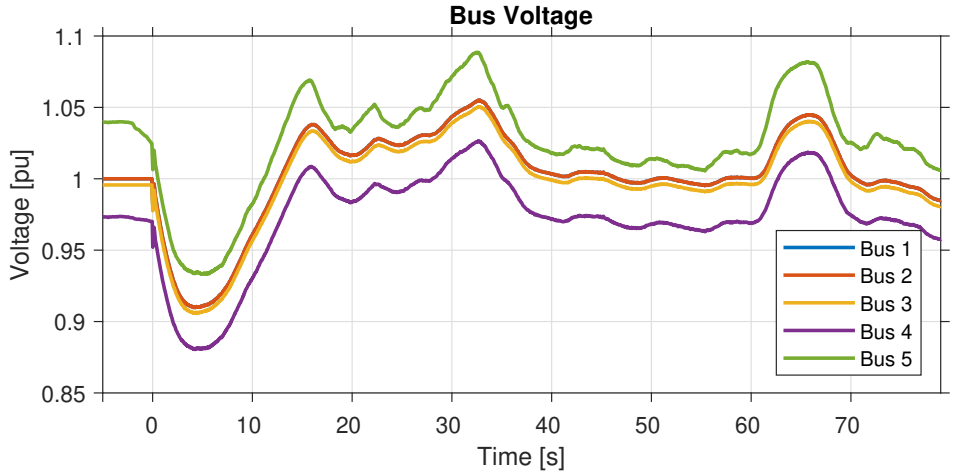

Figure 46: Voltages in the island system during transition to island operation with a power transfer of 5.75 MW.

6.2.2 Impact of VSWT frequency control on stability

Because the operational point of the VSWTs varies in time depending on the current wind speed, the effectiveness of the VSWT control strategies is observed to change depending on what time instance the island system is disconnected from the larger grid. Table 6 presents the maximum, minimum and average frequency improvement observed when analyzing the transition to island operation for 10 different time instances. The operational points for the VSWTs power when not providing frequency control during the analyzed transition instance are shown in Figure 47 where there is a 2 second gap between each case. These time instances were chosen due to that they give a wide range of operating points for the VSWTs. This range includes rated operation and medium power operation as well as including time periods when the VSWTs power is both increasing and decreasing. For a more rigorous analysis would also VSWT low power operational points be included. However the wind speed time series used did not include any operational points below 0.6 pu. For the frequency improvement studies when the VSWTs provide droop support where the de-rating set to 0.1 pu.

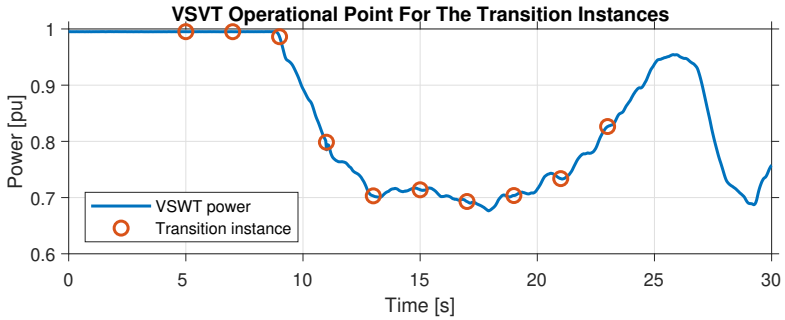

Figure 47: Operational point for the VSWTs power when not providing frequency control at the analysed transition time instances.

The transition for the different time instances result in different power transfer during the transition as the VSWTs operating point and the load changes in time. The change in power transfer causes the normal VSWT operation frequency nadir to change depending on when the transition occurs. Therefore has the instance resulting in maximum and minimum improvement in Table 6 been chosen based on the improvement percentage rather than on the absolute improvement in Hz. The improvement percentage is calculated as $max(|\Delta f_{fc}(t_i)|)/max(|\Delta f(t_i)|)$ where Δf_{fc} represents the change in frequency when VSWT frequency control is applied and the subscript i represents the transition time instance. The average improvement in Table 6 were calculated as the average nadir improvement in Hz and in percentage across all time instances. The normal VSWT operation nadir has been left blank as this is an average and does not represent a specific time instance .

Table 6: Maximum, minimum and average frequency improvement for the different frequency control strategies when transitioning to island operation at different time instances

	Minimum improvement	Maximum improvement	Average improvement
Inertia improvement	0.02 Hz / 3%	0.20 Hz / 22%	0.12 Hz / 12%
Inertia and droop improvement	0.11 Hz / 14%	0.30 / 32%	0.21 Hz / 22%
Normal VSWT operation nadir	49.18	49.06	-

From Table 6 is a frequency improvement always observed when the VSWT frequency control is applied and the average improvement for both cases is significant. A wide range in the improvement is however also observed depending on the instance of transition and when only using inertia emulation can the improvement for the worst case scenario be quite small. Figure 48 shows the frequency response from the transition time instants giving the minimum and maximum frequency improvements from VSWT frequency control, where Figure 48a and Figure 48b shows the minimum and maximum improvements respectively. Note that in Figure 48 has the time of transition time instance been represented as 0 s. With respect to Figure 47, the transition of Figure 48a and of Figure 48b occurs at 19 and 21 s respectively. From Figure 48a can it be noted that the VSWT inertia emulation has a difficulty in improving the frequency if the random power variations from the wind power and the load acts against the frequency restoration, resulting in a low frequency for a long period of time. The inertia emulation mainly helps in reducing the RoCoF and does therefore present little benefit in these situations. The opposite is the case for Figure 48b where the random power variation shortly after the transition helps in restoring the frequency, resulting in a brief frequency nadir for normal wind power operation. Therefore can the inertia emulation reduction of RoCoF significantly help the frequency response by increasing the time to the nadir. It is also of note that the frequency improvements tend to be smallest when the VSWTs are either operating at their rated power or when the power of the VSWTs are increasing. The reason for having difficulty in improving the frequency at these times is due to it being more likely to have a VSWT power change shortly thereafter which hinders the frequency recovery.

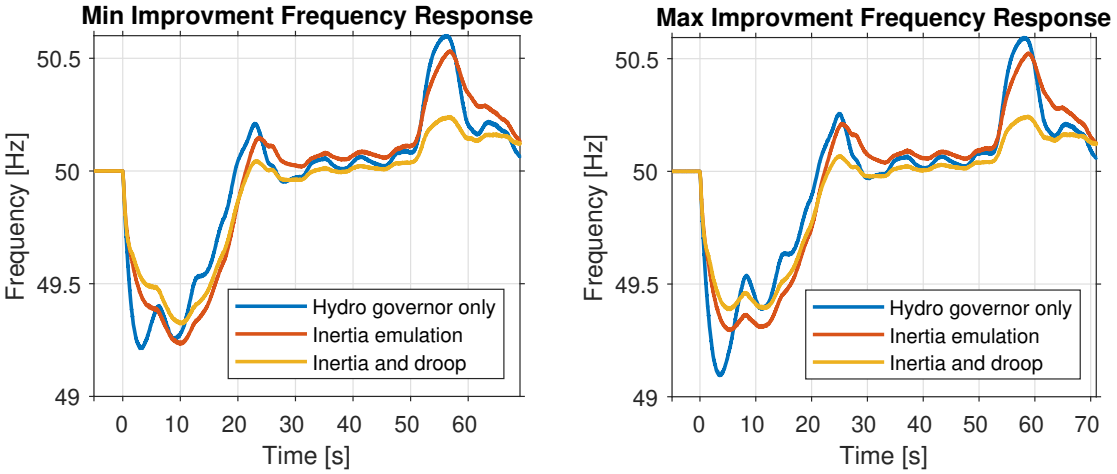

(a) Frequency response observed for minimum improvement. Transition occurs at 19 s with respect to Figure 47

(b) Frequency response observed for maximum improvement.Transition occurs at 21 s with respect to Figure 47

Figure 48: Maximum and minimum improvements observed frequency response from transitioning to island operation at different time instances. Normal VSWT operation is compared with VSWT inertia emulation and VSWT inertia emulation together with droop support while the VSWTs are de-rated

It is also important to note that for these tests have VSWTs been modeled as an aggregate wind power unit where each unit in the aggregated model operates according to the same wind speed time series and has the same operating positions. The wind power production would in reality be achieved by a number of VSWTs whose operation is determined by the wind speed at their individual location, creating an averaging effect on the aggregated wind power unit operational point. This would probably cause less power variations from the wind power and therefore a tighter range of the frequency improvement around the averages.

Figure 49 shows the frequency response of the analyzed island transition which resembles the calculated average frequency improvement from Table 6 the most. This corresponds to the transition time instance of 11 s with respect to Figure 47. The normal VSWT operation for this case was discussed in Section 6.2.1, where it was determined that a maximum power transfer of 5.75 MW was possible for the system to keep within 49.0 Hz. The nadir improvement shown in Figure 49 is a 0.10 Hz improvement for inertia emulation and 0.20 Hz improvement when droop support is also included, while the VSWTs are de-rated by 0.1 pu. From Figure 49 are also the restoration of the frequency and the continued operation within island operation shown up to approximately 80 s. This continued operation shows that the VSWT frequency control does not cause any difficulties for the frequency restoration and that the frequency is returned to 50 Hz without any problems.

Figure 45 suggest that the power transfer to the island system can be increased if the VSWTs are set to provide frequency control, considering that the set limit for the frequency is 49.0 Hz. If the average transition case of Figure 45 is considered, the inertia emulation enable a potential power transfer of 6.45 MW, equivalent to 35.1% of the island's nominal load, until the frequency nadir reaches 49.0 Hz. If droop with de-rated control is also

provided along with inertia emulation, the power transfer increases to 7.27 MW, equal to 39.5% of the island's nominal load. This is an increase in the possible power transfer of 12.2% and 26.4% respectively compared to the normal VSWT operation case. The reactive power transfer was kept the same for all cases.

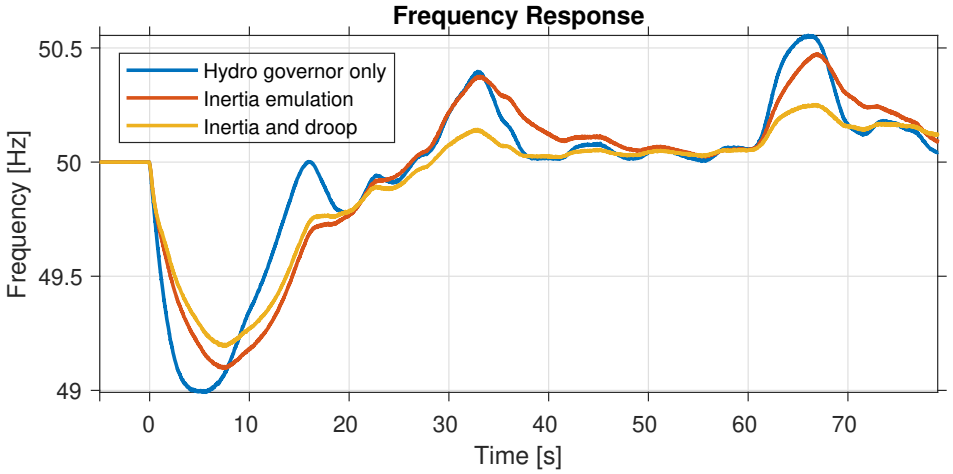

Figure 49: Frequency in the island system during transition to island operation with a power transfer of 5.75 MW, comparing only using the hydro governor frequency control against using wind power inertia emulation and against using wind power inertia emulation together with droop support while de-rating the wind power.

In Figure 50b are the power output from the VSWTs and from the island hydro unit shown for the average island transition case of Figure 45 when the VSWTs are controlled to provide inertia emulation. When the transition occurs, there is a fast increase in power noticed for both the hydro unit and the VSWTs, which is caused by the synchronous inertia response and the emulated inertia response respectively. Also noticeable are that the peak from the VSWTs emulated inertia response occurs slightly later then for the synchronous inertia response by approximately 0.75 s, which is due to the filter included on Δf in the inertia controller shown in Figure 20. Figure 50a shows that the desired emulated inertia response is achieved for the VSWT as the figure describe the accuracy of the VSWTs inertia emulation compared to a reference composed of the $P_{aux,ie}$ signal. The achieved frequency support is determined by taking the difference in the VSWTs power output between normal operation and inertia emulation operation.

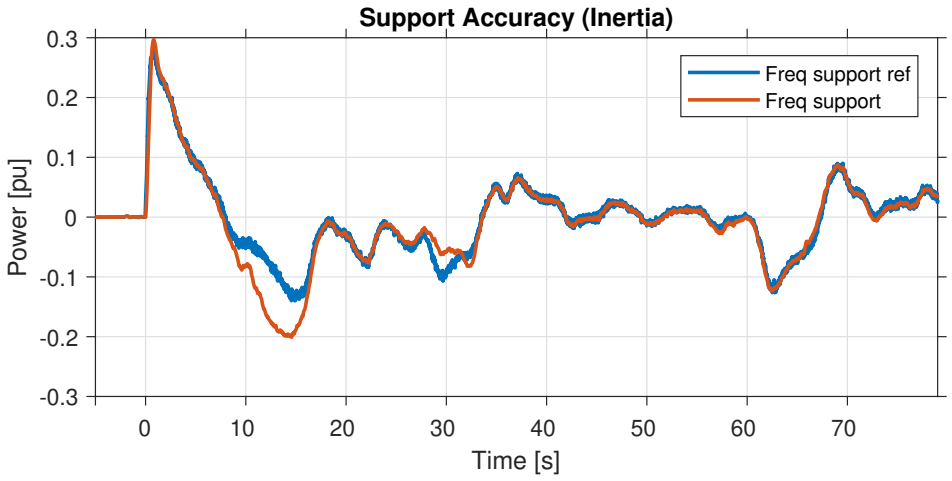

(a) Inertia emulation frequency support accuracy during transition to island operation by comparing the achieved frequency support against a reference $P_{aux,ie}$.

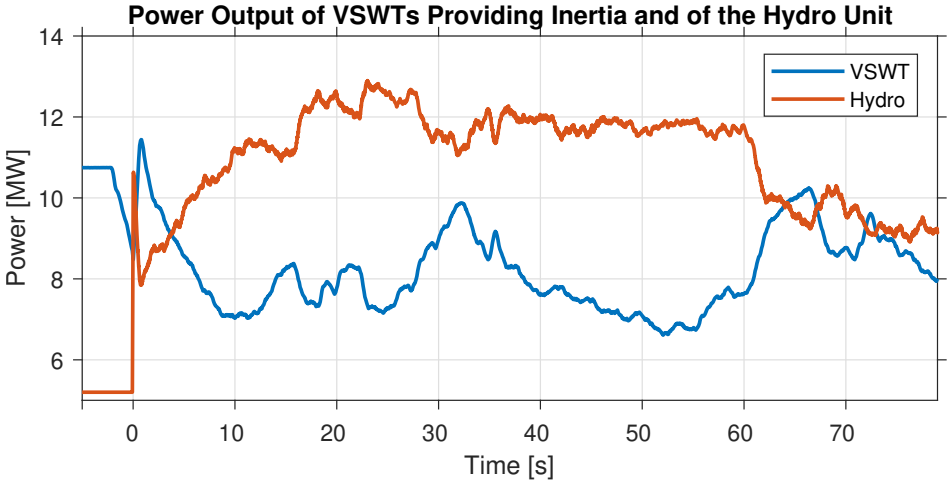

(b) Hydro and wind power production during transition to island operation with inertia emulation frequency support.

Figure 50: Wind power inertia emulation effect on power production during transition to island.

Figure 51b instead shows the VSWTs and the islands hydro unit power output for the average transition case when the VSWTs are controlled for both inertia emulation and droop support while de-rated by 0.1 pu. The hydro unit inertia response results in a similar change in power as compared to Figure 50b. The power change is of the same size when comparing the figures, although the power peak is slightly higher in Figure 51b as the hydro unit produces more power overall due to the de-rating of the VSWT. The initial power increase of the VSWT is however in this case larger compared to Figure 50b as the inertia emulation is supplemented by a quick droop response, using the power reserve for supporting the frequency.

From Figure 51a, showing the achieved frequency support against the a reference consisting of the sum of $P_{aux,ie}$ and $P_{aux,dr}$, are the achieved frequency support shown to resemble the achieved support in Figure 50a. However there is a difference between the figures in that

the inertia and droop support is increased by approximately 0.1 pu for the first 15 s after the transition, which is expected considering this is the size of the available power reserve for the droop control. After those 15 s, the frequency has recovered enough to cause the VSWTs power reserves to start being restored, reducing the VSWTs output power back down to the de-rated operating point. From Figure 51a is it also shown that the achieved frequency support do not follow its reference for the first 15 s after the transition, which is a result of the frequency nadir causing a desired droop response beyond the power reserve set for the VSWTs. Therefore are the reference frequency support unattainable unless the VSWTs are de-rated further, which these results suggest would cause a further frequency nadir improvement.

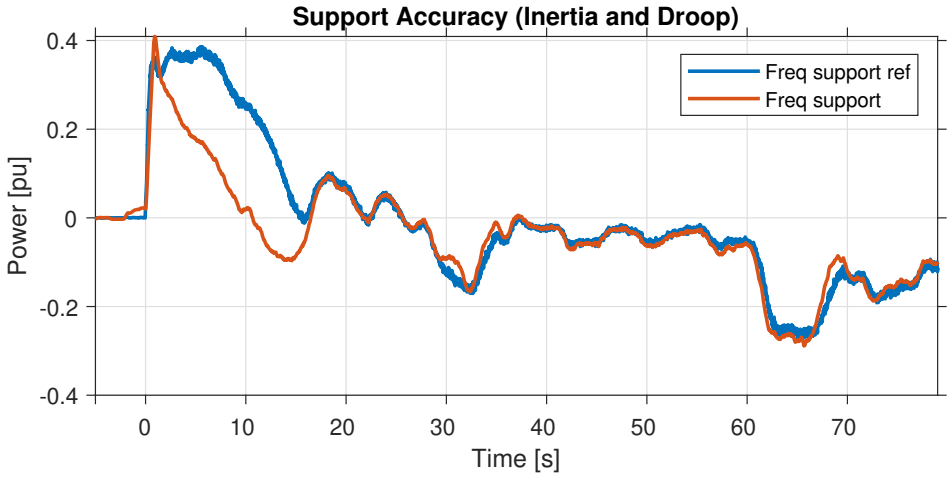

(a) Inertia emulation and droop frequency support accuracy during transition to island operation by comparing the achieved frequency support against a reference $P_{aux,ie} + P_{aux,dr}$.

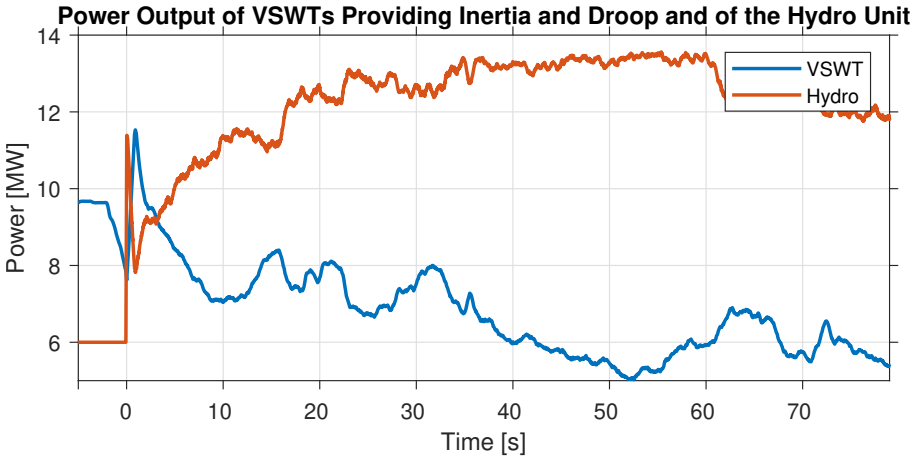

(b) Hydro and wind power production during transition to island operation inertia emulation together with droop frequency support while de-rating the wind power.

Figure 51: Wind power inertia emulation together with droop support effect on power production during transition to island operation.

Figure 52 shows the voltage of bus 4, the load bus, for the average transition case when

the VSWTs participate in the frequency control. This bus voltage is investigated as this bus deviates the most from the nominal voltage of 1 pu. Figure 52 shows that as VSWT frequency control is applied, the voltage drop caused by the transition improves. Inertia emulation causes the minimum voltage to increase from 0.880 pu to 0.893 pu, where the inclusion of the droop causes the minimum voltage to further increase to 0.901 pu. The reason for the increase in minimum voltage is the strong coupling between frequency and voltage in the island system, causing an increase in the frequency nadir due to the frequency control also resulting in less voltage drop.

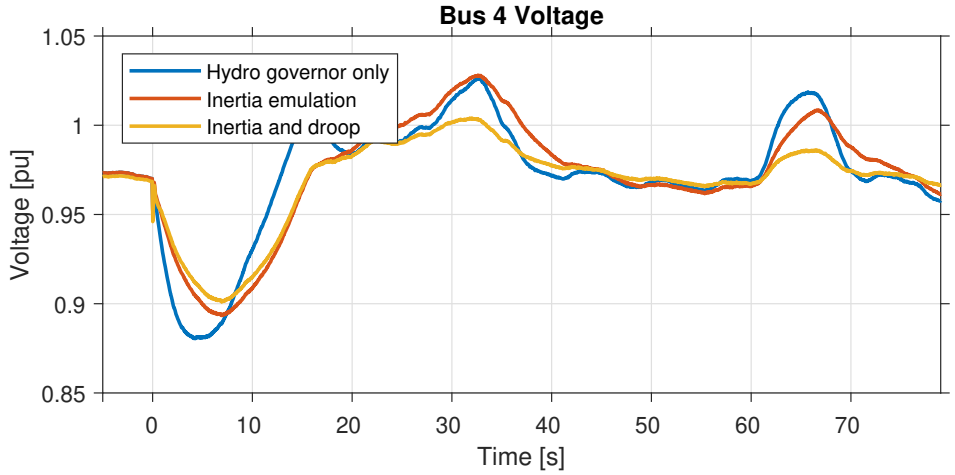

Figure 52: Voltage at bus 4 (the load bus) during transition to island operation with a power transfer of 5.75 MW, comparing only using the hydro governor frequency control against using wind power inertia emulation and against using wind power inertia emulation together with droop support while de-rating the wind power.

6.2.3 Ability for VSWT to help with Down-regulation of frequency

In Figure 53 are the frequency response to a transition case causing over-frequency shown for when the VSWTs operate normally and when they provide inertia emulation support as well as when they provide both inertia emulation and droop support while being de-rated by 0.1 pu. The transition occurs at the same VSWT operating point as in Figure 45. However there is a power flow of 8.05 MW from the island to the larger grid instead, although the reactive power flow is kept the same with 1.00 MVAr flowing from the grid to the island system. This power flow causes for the normal VSWT operation a over-frequency of 50.99 Hz as shown in Figure 53. Figure 53 also shows that the VSWT frequency control utilized are also able to be beneficial for down-regulating the frequency, reducing the over-frequency by 0.18 Hz when only inertia emulation is utilized and by 0.56 Hz when both inertia emulation and droop is used. The large frequency improvement from the droop control is a result of having a larger droop setting for down-regulating and having an increased power reserve which the droop control can use in this direction. De-rating the VSWTs for the down-regulation case is not necessary and it reduces the power which the down-regulation droop can use. However de-rating the VSWTs is necessary if both up and down-regulation droop regulation should be possible.

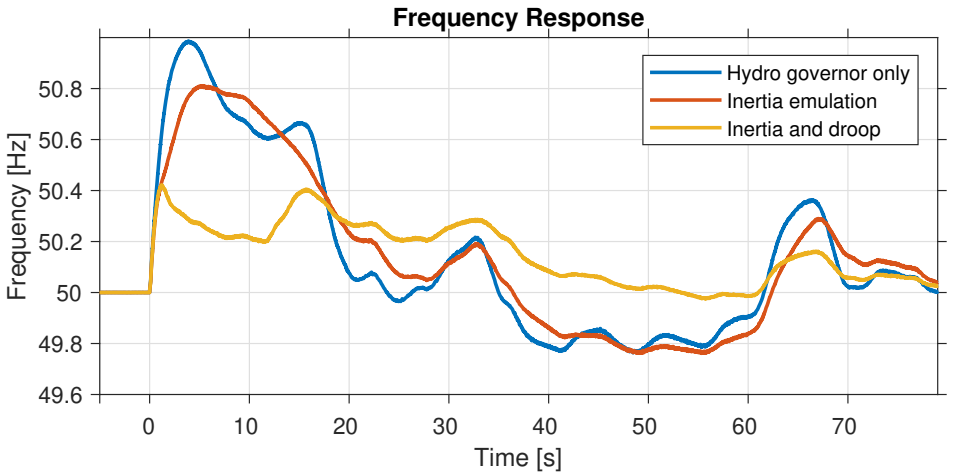

Figure 53: Frequency in the island system during transition to island operation with a power transfer of -8.05 MW causing over-frequency, comparing only using the hydro governor frequency control against using wind power inertia emulation and against using wind power inertia emulation together with droop support while de-rating the wind power.

6.3 Impact of using VSWT droop support individually while de-rated

From Figure 54 are the effects on the frequency from using VSWT droop support individually while de-rating the VSWT by 0.1 pu shown. The effect of the droop support is compared with the effect of VSWT inertia emulation and the effect of droop support while de-rated used together with inertia emulation. From Figure 54a is the effects on the frequency distribution during continuous island operations shown where the case studied is similar to the one described in Section 6.1. Figure 54a suggests that only using droop may give an improved frequency distribution even compared to inertia emulation and droop used together. However the improvement observed when using VSWT droop support individually may be a result of the wind time series used, where a different time series could show a different result, or inertia emulation may have a detrimental effect on the frequency distribution for continuous operation when paired with droop control. Further investigation, using a larger and more varied wind time series is therefore needed to conclude how using droop support individually compares with using droop together with inertia emulation.

Figure 54b instead shows the effect on the frequency from using VSWT droop support individually during the transition from grid connected to island operation. The same time instance for the transition is used as the average time instance in Section 6.2. Figure 54b shows a similar nadir for using droop support individually as for the inertia emulation case. However with a higher RoCoF. The droop nadirs do not necessarily have to be similar as the performance of the droop control can be altered by changing the size of the power reserve. However, it can be noted that in this case, using inertia emulation together with the droop causes an improved frequency response.

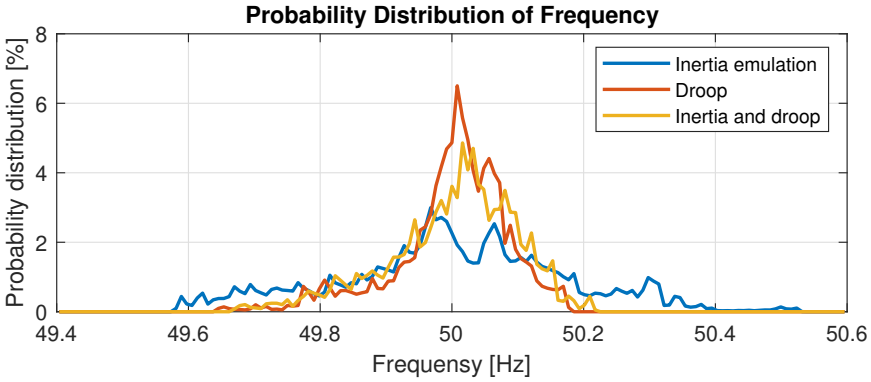

(a) Probability Distribution of Frequency for continuous island operation while using VSWT inertia emulation, droop support and inertia emulation together with droop support.

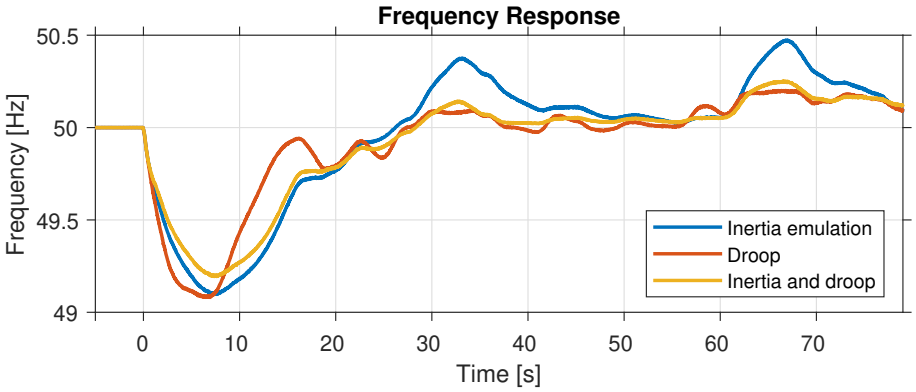

(b) Frequency Response from transition to island operation while using VSWT inertia emulation, droop support and inertia emulation together with droop support.

Figure 54: Effect on frequency stability from using VSWT droop support individually while de-rating the VSWT by 0.1 pu compared to the effect of inertia emulation and the effect of droop support together with inertia emulation.

7 Conclusions

The work evaluates the stability of an island system consisting of wind and hydro-based generation. The work analyzed what the impacts are of frequency control from the wind power units in the island. The evaluation was done during the transition from being grid connected to operating as an island as well as during the continuous operation thereafter. Furthermore, the objective of the work was also to identify some of the requirements for this wind and hydro island system to stably transition to and operate as an island. To achieve these objectives, simulations of a wind and hydro island system in MATLAB/Simulink and PSS/E were carried out. By applying the wind power frequency control strategies in the simulations, the island stability is compared to when the wind power operated normally, having no wind power frequency control active. Two methods for controlling the frequency with wind power were analyzed. The first method emulates a synchronous generator's inertia response by either using the kinetic energy stored in the rotor or changing the pitch of the turbine blades if possible. The other method, which de-rates the wind turbines in order to create a power reserve, enables the use of droop control from the wind power. No modification to the hardware is necessary for implementing these methods for controlling the frequency with wind power. It is only necessary to modify parts of the control software. The cases studied used inertia emulation alone or inertia emulation together with droop control from de-rated operation.

The wind power had during its normal operation an adverse effect on the frequency. .The wind power causes a reduction of the inertia of the system and the intermittent power production present in wind power causes continuous power variations, resulting in the frequency varying within a range. The wind power penetration was found to have a limit as the detrimental effects on the stability from wind power increases when the wind power penetration is increased. This limit will change depending on the acceptable frequency range in the island, the variations of the load in the island, the island inertia and the frequency control strength of the connected hydro power. However, in the simulated case, the penetration limit of wind power was found to be approximately 47.5%, using a continuous frequency range of 49.95 to 50.05 .and no frequency support from the wind power. Additionally, for this wind power penetration level and normal wind power control, the acceptable power imbalance for the transition was found to be approximately 31.3% of the nominal load for the island system in order to keep the transient frequency over 49 Hz.

This work has identified that the use of droop control can improve the stability, potentially by a significant amount depending on how much the wind power is de-rated, while inertia emulation can improve the stability to a lesser extent. The inertia emulation alone did cause an improvement of the frequency range for the continuous operation from 49.56 Hz - 50.56 Hz to 49.59 Hz - 50.53 Hz, which represents a 5% range improvement. The inertia together with droop reduced the range down to 49.68 Hz - 50.22 Hz,representing a 44% range improvement. Regarding the transition, the inertia emulation improves the frequency nadir on average by 12% however the worst case scenario showed an improvement of 3% . The inertia together with the droop showed an average improvement of 22% where an improvement of 14% were found to be the worst case scenario. The average improvements shown constitute an increase in the acceptable power imbalance caused by the transition of 12.2% and to 26.4% of the nominal load in the island respectively. The wind power frequency support also showed similar results for voltage stability both for the continuous operation and the transition due to having a strong correlation between

frequency and voltage in the test network. Using inertia emulation may however, when used together with the droop, have a detrimental effect for managing the power variations during continuous operation, although it was beneficial to use both together when handling a large disturbance.

.When performing inertia emulation, a higher wind speed is preferable and the wind speed needs to be high enough that there is sufficient kinetic energy in the turbine rotation to be extracted by the inertia emulation. There may also be a limit on the maximum wind speed for up-regulation from inertia emulation to avoid overloading the wind turbine converter if this overloading is not possible. The inertia emulation from kinetic energy and from the pitch behaves similarly. However as the pitch controlled inertia emulation does not cause a reduction in the rotational speed there is no need for this method to accelerate the speed back to the optimal speed, which for the kinetic energy case results in a slightly reduced inertia response. The inertia emulation for the wind power incorporates a filter on the frequency signal. Thus, the wind power inertia response is slower than for a traditional synchronous machine. In this work the time constant of the filter was set to 1 s and it resulted in the peak of the wind power inertia response occurring approximately 0.75 s after the peak of the hydro inertia response.

For the droop control where the wind turbines de-rated by 0.1 pu, meaning that the power was reduced by 0.1 pu compared to the available power, causing the stability improvement to come at the cost of the power loss this control strategy entails. .There are no technical requirements for the de-rating and the droop control other than that there is enough power in the wind for the desired de-rating to be possible. However, similar to inertia emulation, a high wind speed is preferred. The higher wind speed allows for an increased flexibility in the amount of power which can be de-rate and the possibility of greater power reserves, both for up and down-regulation. The power loss was noted for the continuous operation to be 0.12 pu which is similar, but slightly more, then the 0.1 pu expected power loss. The reason for having a greater power loss than expected is due to using a greater control strength for down-regulating the frequency and due to the test case run having slight predominance for over-frequencies. The power loss can be reduced, although this will cause a similar reduction in the stability improvement when up-regulating the frequency. A balance does therefore have to be made between needed stability improvement and acceptable power loss. However increasing the power loss only causes a stability improvement up to a point until the frequency disturbances do not fully utilize the power reserve available.

.De-rating and droop is particularly valuable during the continuous island operation where it can provide a large stability benefit when the system is more vulnerable. If necessary de-rating and droop can be applied even when grid connected to help with the transition. However, considering the ability of inertia emulation to help during the transition, one strategy may be to use inertia emulation when grid connected and preparing for a transition and not de-rate the turbine. Therefore, there are no power losses from the wind while connected to the grid. Then, the de-rating and droop control of the wind power can be applied after islanding is detected, if the hydro is able to compensate for the power loss from the wind.

7.1 Future work

Future studies could be to address the limitations of the work and to provide a more rigorous analysis of how wind power frequency control affects the stability of an island

system. Future work couls therefore include:

- **Separating the aggregated wind power unit into individual wind turbines.**
  Splitting the aggregated wind power unit utilized for the simulations into the individual wind turbines the wind unit is made out of allows for the operating point on the individual wind turbines to change independently to the operating point of the other wind turbines. Therefore, by using an individual wind speed time series for each wind turbine, a more realistic combined power output from the is achieved. The combined power output should have less power variation than the aggregated wind power unit as the individual wind speed time series causes an averaging effect on the combined power output. The individual wind speed time series could be implemented by shifting them in time, where the time shifted is calculated by the distance between the wind turbines in the wind farm and the average wind speed applied.

- **Using a detailed model of a wind farm.**
  By having the wind power unit instead be represented by a detailed model of a wind farm using individual models of wind turbines, as in the above point, as well as including the cables connecting the wind turbines together, could the wind power frequency control effect on the voltage within the wind farm can be analyzed.

- **Using a more detailed test network for the PSS/E studies.**
  To analyze how the wind power frequency control affects the rotor angle stability in the island during transition to island operation as well as during continuous island operation thereafter should the wind power frequency control be applied to a larger and more detailed island network, with multiple generation units, loads and power lines. Additional will the more detailed network provide further insight on the frequency control effect on the voltage stability.

- **Further analysis using a different wind time series.**
  The wind time series was chosen as it gives a good variation of operating points for the wind turbines, including operation at rated power down to operation at 0.6 pu. However, to further analyze the effect of wind power frequency control on the island system stability during low wind speed scenarios is it necessary to use a wind speed time series causing wind turbine operation within the power interval of 0 pu to 0.6 pu. Furthermore, is it necessary to use a wider sample size of wind speeds to investigate what effect wind power inertia emulation has on managing the power variations during continuous island operation when used together with wind power droop control.

- **Analysis of the effect caused by the reactive power flow to the grid.**
  No analysis over the effects of the reactive power flow between the grid and the island system at the moment of transition was investigated and the reactive power flow was kept constant for all cases. To therefore also evaluate the requirements on the reactive power flow should further cases be simulated for different reactive power flows.

- **Voltage control at remote bus**
  To further analyze what effects the wind power voltage control has on the island stability could it be useful to investigate voltage control from the wind power at a remote bus. In the island system presented in this work would voltage control at

the load bus be interesting to investigate. However it was not done in this work as it requires the wind power unit to be modeled with an extra dynamic plant model.

Additionally could also future work aim to improve the UDMs constructed for this work. The UDMs were constructed in order to be able to be applied on a general wind turbine or on an aggregated representation of multiple wind turbines. The UDMs have however only been tested on the 3.6 MW and there aggregate representation used in this work, as well as tested to a limited extent on a representation of Chalmers wind turbine. Therefore could the UDMs applied to a general wind turbine result in issues that need to be fixed before general application of the UDMs is possible. Additionally could it be useful to combine the UDMs created for this work into a single UDM as they need to be used together.

References

[1] L. Mehigan, J. P. Deane, B. P. Gallachóir, and V. Bertsch, "A review of the role of distributed generation (dg) in future electricity systems," *Energy*, vol. 163, pp. 822–836, 2018. [Online]. Available: https://www.sciencedirect.com/science/article/pii/S0360544218315366

[2] L. Das, S. Munikoti, B. Natarajan, and B. Srinivasan, "Measuring smart grid resilience: Methods, challenges and opportunities," *Renewable and Sustainable Energy Reviews*, vol. 130, p. 109918, 2020. [Online]. Available: https://www.sciencedirect.com/science/article/pii/S1364032120302094

[3] V. Debusschere et al., "Technical requirements for the operation of microgrids in both interconnected and islanded modes," International Conference on Electricity Distribution, Tech. Rep., 2021. [Online]. Available: http://www.cired.net/cired-working-groups/microgrids-in-interconnected-and-islanded-modes-wg-2018-3

[4] M. L. Pestana et al., "Resilience of distribution grids," International Conference on Electricity Distribution, Tech. Rep., 2018. [Online]. Available: http://cired.net/cired-working-groups/resilience-of-distribution-grids

[5] Energimyndigheten, "Vindkraftsstatistik," 2023, available: https://www.energimyndigheten.se/statistik/den-officiella-statistiken/statistikprodukter/vindkraftsstatistik/?currentTab=2 (accessed on: 2024-01-19).

[6] Y. Xu, C.-C. Liu, K. P. Schneider, F. K. Tuffner, and D. T. Ton, "Microgrids for service restoration to critical load in a resilient distribution system," *IEEE Transactions on Smart Grid*, vol. 9, no. 1, pp. 426–437, 2018. [Online]. Available: https://ieeexplore.ieee.org/document/7513408

[7] P. Kundur, et al., "Definition and classification of power system stability ieee/cigre joint task force on stability terms and definitions," *IEEE Transactions on Power Systems*, vol. 19, no. 3, pp. 1387–1401, 2004. [Online]. Available: https://ieeexplore.ieee.org/document/1318675

[8] N. Hatziargyriou, et al., "Definition and classification of power system stability revisited and extended," *IEEE Transactions on Power Systems*, vol. 36, no. 4, pp. 3271–3281, 2021. [Online]. Available: https://ieeexplore.ieee.org/document/9286772

[9] P. Denholm, T. Mai, R. W. Kenyon, B. Kroposki, and M. O. Malley, "Inertia and the power grid : A guide without the spin," National Renewable Energy Laboratory, Denver, CO, Tech. Rep. TP-6A20-73856, 2020. [Online]. Available: https://www.nrel.gov/docs/fy20osti/73856.pdf

[10] M. Rezkalla, M. Pertl, and M. Marinelli, "Electric power system inertia: requirements, challenges and solutions," *Electrical Engineering*, vol. 100, 2018. [Online]. Available: https://link.springer.com/article/10.1007/s00202-018-0739-z

[11] Erik, "Future system inertia," ENTSO-E, Belgum, Tech. Rep., 2018. [Online]. Available: https://eepublicdownloads.entsoe.eu/clean-documents/Publications/SOC/Nordic/Nordic_report_Future_System_Inertia.pdf

[12] D. Zografos, "Power system inertia estimation and frequency response assessment," Ph.D. dissertation, Kungliga Tekniska Högskolan, Stockholm, Sweden, 2018. [Online]. Available: https://kth.diva-portal.org/smash/get/diva2:1369967/FULLTEXT01.pdf

[13] M. S. Hossan, H. M. Mesbah Maruf, and B. Chowdhury, "Comparison of the zip load model and the exponential load model for cvr factor evaluation," in *2017 IEEE Power and Energy Society General Meeting*, 2017, pp. 1–5. [Online]. Available: https://ieeexplore.ieee.org/document/8274490

[14] P. Kundur, *Power System Stability and Control*. New York: McGraw-Hill, 1994.

[15] A. Fernández-Guillamón, E. Gómez-Lázaro, E. Muljadi, and Ángel Molina-García, "Power systems with high renewable energy sources: A review of inertia and frequency control strategies over time," *Renewable and Sustainable Energy Reviews*, vol. 115, p. 109369, 2019. [Online]. Available: https://www.sciencedirect.com/science/article/pii/S1364032119305775

[16] N. Modig et al., "Overview of frequency control in the nordic power system," ENTSO-E, Belgum, Tech. Rep., 2022. [Online]. Available: https://www.epressi.com/media/userfiles/107305/1648196866/overview-of-frequency-control-in-the-nordic-power-system-1.pdf

[17] ——, "FFR design of requirements external document," ENTSO-E, Belgum, Tech. Rep., 2020. [Online]. Available: https://energinet.dk/media/rwbbyspn/1c-ffr-design-requirements-external-document.pdf

[18] ENTSO-E, "Nordic balancing philosophy," ENTSO-E, Belgum, Tech. Rep., 2021. [Online]. Available: https://eepublicdownloads.azureedge.net/clean-documents/Publications/SOC/Nordic/2022/Nordic%20Balancing%20Philosophy%20updated%202021%20for%20publication.pdf

[19] E. Bompard, A. Mazza, and L. Toma, "Chapter 3 - classical grid control: Frequency and voltage stability," in *Converter-Based Dynamics and Control of Modern Power Systems*, A. Monti, F. Milano, E. Bompard, and X. Guillaud, Eds. Academic Press, 2021, pp. 31–65. [Online]. Available: https://www.sciencedirect.com/science/article/pii/B9780128184912000031

[20] H. Bevrani, H. Golpîra, A. R. Messina, N. Hatziargyriou, F. Milano, and T. Ise, "Power system frequency control: An updated review of current solutions and new challenges," *Electric Power Systems Research*, vol. 194, p. 107114, 2021. [Online]. Available: https://www.sciencedirect.com/science/article/pii/S037877962100095X

[21] ENTSO-E, "Technical requirements for frequency containment reserve provision in the nordic synchronous area," ENTSO-E, Belgum, Tech. Rep., 2023. [Online]. Available: https://www.svk.se/siteassets/aktorsportalen/bidra-med-reserver/om-olika-reserver/fcr/fcr-technical-requirements-may-23.pdf

[22] E. Agneholm et al., "FCR-D design of requirements phase 2," ENTSO-E, Belgum, Tech. Rep., 2019. [Online]. Available: https://www.svk.se/contentassets/8c9449a914f848a0b258cf8c1d189c84/fcr-d-design-of-requirements--phase-2.pdf

[23] M. Farrokhabadi et al., "Microgrid stability definitions, analysis, and examples," *IEEE Transactions on Power Systems*, vol. 35, no. 1, pp. 13–29, 2020. [Online]. Available: https://ieeexplore.ieee.org/document/8750828

[24] "IEEE guide for design, operation, and integration of distributed resource island systems with electric power systems," *IEEE Std 1547.4-2011*, pp. 1–54, 2011. [Online]. Available: https://ieeexplore.ieee.org/document/5960751

[25] J. Björnstedt, "Island operation with induction generators - frequency and voltage control," Ph.D. dissertation, Lund University, 2009. [Online]. Available: https://www.iea.lth.se/publications/Theses/LTH-IEA-1058.pdf

[26] "COMMISSION REGULATION (EU) 2016/631," 14th Apr. 2016, available: https://eur-lex.europa.eu/legal-content/EN/TXT/PDF/?uri=CELEX:32016R0631&from=RO.

[27] E. C. Resende, M. G. Simoes, and L. C. G. Freitas, "Anti-islanding techniques for integration of inverter-based distributed energy resources to the electric power system," *IEEE Access*, vol. 12, pp. 17 195–17 230, 2024. [Online]. Available: https://ieeexplore.ieee.org/abstract/document/10412050

[28] S. S. Mohapatra, M. kumar Maharana, A. Pradhan, P. K. Panigrahi, and R. C. Prusty, "Anti-islanding detection in grid-connected inverter system using active frequency drift technique with random forest," *Electrical Engineering*, 2023. [Online]. Available: https://link.springer.com/article/10.1007/s00202-023-02137-2

[29] S. Dutta, P. K. Sadhu, M. Jaya Bharata Reddy, and D. K. Mohanta, "Shifting of research trends in islanding detection method - a comprehensive survey," *Protection and Control of Modern Power Systems*, vol. 3, p. 1, 2018. [Online]. Available: https://pcmp.springeropen.com/articles/10.1186/s41601-017-0075-8

[30] Working Group Prime Mover and Energy Supply, "Hydraulic turbine and turbine control models for system dynamic studies," *IEEE Transactions on Power Systems*, vol. 7, no. 1, pp. 167–179, 1992. [Online]. Available: https://ieeexplore.ieee.org/abstract/document/141700

[31] S. Mathew, *Basics of wind energy conversion*. Berlin, Heidelberg: Springer Berlin Heidelberg, 2006, pp. 11–43. [Online]. Available: https://doi.org/10.1007/3-540-30906-3_2

[32] C. Carrillo, A. Obando Montaño, J. Cidrás, and E. Díaz-Dorado, "Review of power curve modelling for wind turbines," *Renewable and Sustainable Energy Reviews*, vol. 21, pp. 572–581, 2013. [Online]. Available: https://www.sciencedirect.com/science/article/pii/S1364032113000439

[33] N. R. Ullah, T. Thiringer, and D. Karlsson, "Temporary primary frequency control support by variable speed wind turbines potential and applications," *IEEE Transactions on Power Systems*, vol. 23, no. 2, pp. 601–612, 2008. [Online]. Available: https://ieeexplore.ieee.org/document/4480153

[34] J. H. Chow and J. J. Sanchez-Gasca, "Wind power generation and modeling," *Power System Modeling, Computation, and Control*, New York, NY, USA:Wiley-IEEE Press, 2020, ch. 15, pp. 487-530. [Online]. Available: https://ieeexplore.ieee.org/document/8958871

[35] M. Singh, E. Muljadi, J. Jonkman, and V. Gevorgian, "Simulation for Wind Turbine Generators With FAST and MATLAB-Simulink Modules," National

Renewable Energy Labotory, Denver, CO, Tech. Rep. TM-2009-215587, 2014. [Online]. Available: https://www.nrel.gov/docs/fy14osti/59195.pdf

[36] E. Muljadi, V. Gevorgian, M. Singh, and S. Santoso, "Understanding inertial and frequency response of wind power plants," in *2012 IEEE Power Electronics and Machines in Wind Applications*, 2012, pp. 1–8. [Online]. Available: https://ieeexplore.ieee.org/document/6316361

[37] N. Miller, J. Sanchez-Gasca, W. Price, and R. Delmerico, "Dynamic modeling of ge 1.5 and 3.6 mw wind turbine-generators for stability simulations," in *2003 IEEE Power Engineering Society General Meeting (IEEE Cat. No.03CH37491)*, vol. 3, 2003, pp. 1977–1983. [Online]. Available: https://ieeexplore.ieee.org/stamp/stamp.jsp?tp=&arnumber=1267470

[38] J. Jonkman, S. Butterfield, W. Musial, and G. Scott, "Definition of a 5-mw reference wind turbine for offshore system development," National Renewable Energy Laboratory, Denver, CO, Tech. Rep. TP-500-38060, 2009. [Online]. Available: https://www.nrel.gov/docs/fy20osti/73856.pdf

[39] J. Boyle, T. Littler, and A. M. Foley, "Frequency regulation and operating reserve techniques for variable speed wind turbines," in *2021 IEEE Madrid PowerTech*, 2021, pp. 1–5. [Online]. Available: https://ieeexplore.ieee.org/document/9495072

[40] E. Ela, et al., "Active Power Controls from Wind Power: Bridging the Gaps ," National Renewable Energy Labotory, Denver, CO, Tech. Rep. TP-5D00-60574, 2014. [Online]. Available: https://www.nrel.gov/docs/fy14osti/60574.pdf

[41] K. Clark, N. Miller, and J. Sanchez-Gasca, "Modeling of ge wind turbine-generators for grid studies, version 4.5," General Electric International, Inc., Schenectady, NY, Tech. Rep., 2010. [Online]. Available: https://www.researchgate.net/publication/267218696_Modeling_of_GE_Wind_Turbine-Generators_for_Grid_Studies_Prepared_by

[42] L. Suja-Thauvin, "Chalmers report, hönö and v90 turbines in ashes for ffr analysis," Simis AS, Trondheim, Norge, Tech. Rep. 2021-1001, 2021.

[43] M. Persson, "Frequency response by wind farms in power systems with high wind power penetration," Ph.D. dissertation, Division of Electric Power Engineering, Chalmers University of Technology, Gothenburg, Sweden, 2017. [Online]. Available: https://publications.lib.chalmers.se/records/fulltext/250313/250313.pdf

[44] A. Sunjaq, P. Chen, M. Bongiorno, R. Majumder, and J. Svensson, "Frequency control by bess for smooth island transition of a hydropowered microgrid," *IET Smart Grid*, vol. 7, pp. 63 – 77, 11 2023. [Online]. Available: https://ietresearch.onlinelibrary.wiley.com/doi/10.1049/stg2.12140

[45] S. H. Dolatabadi, M. Ghorbanian, P. Siano, and N. D. Hatziargyriou, "An enhanced ieee 33 bus benchmark test system for distribution system studies," *IEEE Transactions on Power Systems*, vol. 36, no. 3, pp. 2565–2572, 2021. [Online]. Available: https://ieeexplore.ieee.org/abstract/document/9258930

[46] *AXLJ TT 36 kV*, Paris, France, Nexans. [Online]. Available: https://www.nexans.se/.rest/catalog/v1/product/pdf/21062898-901-00

[47] B. Lund, "Estimation of inter-area oscillationsin the nordic power systemusing dynamic mode decomposition," MSc thesis, Department of Electrical Engineering, Chalmers University of Technology, Gothenburg, Sweden, 2023. [Online]. Available: https://odr.chalmers.se/server/api/core/bitstreams/76babd8a-45e6-4bdc-9df2-0e63315edf13/content

Appendix

A Parameters used for the MATLAB/Simulink models

Table 7: Parameters used for the power system

Value	Name	Description
0.9	D	Frequency dependent load (pu)
0.3	WPP	Wind power penetration (-)

Table 8: Parameters used for the hydro generator and governor

Value	Name	Description
0.05	Rp_h	Droop (-)
0.55	Rt_h	Transiant droop (-)
4.08	T_r	Reset time (s)
0.2	T_y	Actuator time constant (s)
0.5	T_w	Water time constant (s)
0.55	T_t	Filter time constant (s)
4.9	H_h	Hydro inertia (s)

Table 9: Parameters used for the wind turbine aerodynamics and drivetrain

Value	Name	Description
8	R	Radius (m)
1.225	ρ	Air density (kg/m^3)
7.85	$\omega(_0)$	Turbine rated speed (rad/s)
0.445	$C_{p,\max}$	Maximum Cp (-)
0.0049	b	Dampening constant (pu)
3.2	H_{wt}	WT inertia (s)

Table 10: Parameters used for the VSWT torque controller

Value	Name	Description
6	Kp_{sc}	Speed/torque controller proportional gain
1.2	Ki_{sc}	Speed/torque controller integral gain
0.0049	b	Compensation for WT dampening constant (pu)
1	P_{max}	Maximum power (pu)
-1	P_{min}	Minimum power (pu)
2.2	$P_{\text{rat,max}}$	Maximum torque rate of change (pu)
0.97	*RefSpd*	Reference speed max (pu)
0.4	*CutSpt*	Cut in speed (pu)
8.75	λ_{opt}	Optimal lambda (-)
8	R	WT radius (m)
7.85	ω_0	Rated Speed (rad/s)
25000	P_0	Rated Power (W)
1.225	ρ	Air density (kg/m^3)
0.445	$C_{p,\text{max}}$	Cp maximum (-)
1	T_s	Speed reference filter time constant (s)
0.2	$k_{aw,tc}$	Anti wind up gain (-)

Table 11: Parameters used for the VSWT pitch control

Value	Name	Description
460	$K_{p,\text{pc}}$	Proportional gain
290	$K_{i,\text{pc}}$	Integral gain
90	β_{max}	Maximum pitch (deg)
11	*Pith rate max*	Maximum pitch rate of change (deg/s)
-11	*Pith rate min*	Maximum pitch rate of change (deg/s)
1	$\omega_{(0,\text{pu})}$	Rated speed (pu)
0.2	$k_{aw,pc}$	Anti wind up gain (-)

Table 12: Parameters used for the wind speed estimation

Value	Name	Description
8	R	WT Radius (m)
7.85	ω_0	Turbine rated speed (rad/s)
1.225	ρ	Air density (kg/m^3)
25000	P_0	Rated Power (W)
0.445	$C_{p,\text{max}}$	C_p max (-)

Table 13: Parameters used for the available power estimation

Value	Name	Description
8	R	WT Radius (m)
7.85	ω_0	Turbine rated speed (rad/s)
1.225	ρ	Air density (kg/m^3)
25000	P_0	Rated Power (W)
8.75	λ_{opt}	Lambda optimal (-)
1	$\omega_{\text{wt,max}}$	Max speed (pu)
0	$\omega_{\text{wt,min}}$	Min speed (pu)
1	P_{max}	Max power (pu)
-1	P_{min}	Min power (pu)

Table 14: Parameters used for the droop and de-rated control

Value	Name	Description
0.00	$D_{b,\text{dr}}$	Frequency deadband for de-rating control (pu)
0.05	$R_{p,\text{u,wt}}$	Droop for up regulation (-)
0.02	$R_{p,\text{d,wt}}$	Droop for down regulation
0.1	P_{reserve}	Power reserve (pu)
0.445	$C_{p,\text{max}}$	C_p max (-)
1	DeRatedON	Turn on or off de-rated and droop

Table 15: Parameters used for the inertia control

Value	Name	Description
0.00	$D_{b,\text{ie}}$	Frequency deadband for inertia control (pu)
1	T_f	Inertia filter time constant (s)
3.2	H_{wt}	Wind turbine inertia (s)
5	k_i	Wind turbine inertia gain (-)
0.02	k_{sc}	Feedback for returning to optimal speed (-)
0.5	$\omega_{(\text{ie,min})}$	Lower speed limit for inertia emulation (pu)
1	InertaON	Turn on or off inertia emulation

Look-up tables

Table 16: $C_p(\beta, \lambda)$

β / λ	0	2	4	6	8	10	12	14	16	18	20	22	24	26	28	30	32	34	36	38	40
1,000	0,013	0,013	0,014	0,014	0,014	0,014	0,014	0,015	0,015	0,015	0,015	0,016	0,016	0,017	0,017	0,018	0,019	0,020	0,021	0,022	0,023
1,250	0,017	0,017	0,017	0,017	0,018	0,018	0,018	0,019	0,019	0,020	0,021	0,021	0,022	0,024	0,025	0,027	0,028	0,029	0,030	0,030	0,029
1,500	0,020	0,020	0,021	0,021	0,022	0,022	0,023	0,024	0,025	0,026	0,028	0,030	0,032	0,034	0,036	0,038	0,038	0,038	0,036	0,033	0,028
1,750	0,023	0,023	0,024	0,025	0,026	0,028	0,029	0,031	0,033	0,036	0,039	0,041	0,044	0,047	0,047	0,046	0,043	0,039	0,034	0,028	0,021
2,000	0,025	0,027	0,028	0,030	0,031	0,034	0,037	0,041	0,045	0,049	0,053	0,056	0,058	0,057	0,054	0,048	0,042	0,034	0,026	0,017	0,010
2,250	0,028	0,03	0,032	0,035	0,039	0,044	0,049	0,055	0,060	0,066	0,070	0,070	0,066	0,060	0,053	0,044	0,034	0,024	0,014	0,004	0,000
2,500	0,031	0,034	0,038	0,044	0,051	0,058	0,065	0,073	0,081	0,084	0,081	0,076	0,068	0,058	0,047	0,035	0,022	0,010	0,000	0,000	0,000
2,750	0,034	0,040	0,048	0,058	0,067	0,075	0,086	0,096	0,098	0,095	0,088	0,077	0,065	0,051	0,037	0,022	0,007	0,000	0,000	0,000	0,000
3,000	0,040	0,050	0,063	0,075	0,085	0,099	0,110	0,113	0,109	0,101	0,088	0,074	0,058	0,041	0,023	0,005	0,000	0,000	0,000	0,000	0,000
3,250	0,049	0,065	0,080	0,093	0,110	0,125	0,130	0,126	0,117	0,103	0,086	0,067	0,048	0,027	0,006	0,000	0,000	0,000	0,000	0,000	0,000
3,500	0,063	0,082	0,098	0,118	0,139	0,147	0,145	0,134	0,120	0,101	0,080	0,057	0,033	0,009	0,000	0,000	0,000	0,000	0,000	0,000	0,000
3,750	0,081	0,102	0,123	0,151	0,164	0,164	0,155	0,140	0,120	0,096	0,071	0,044	0,016	0,000	0,000	0,000	0,000	0,000	0,000	0,000	0,000
4,000	0,101	0,124	0,157	0,180	0,185	0,177	0,162	0,142	0,117	0,089	0,060	0,028	0,000	0,000	0,000	0,000	0,000	0,000	0,000	0,000	0,000
4,250	0,121	0,156	0,190	0,205	0,201	0,187	0,167	0,142	0,112	0,079	0,044	0,009	0,000	0,000	0,000	0,000	0,000	0,000	0,000	0,000	0,000
4,500	0,147	0,192	0,220	0,226	0,214	0,195	0,169	0,139	0,104	0,066	0,026	0,000	0,000	0,000	0,000	0,000	0,000	0,000	0,000	0,000	0,000
4,750	0,185	0,225	0,246	0,242	0,224	0,200	0,169	0,134	0,094	0,050	0,006	0,000	0,000	0,000	0,000	0,000	0,000	0,000	0,000	0,000	0,000
5,000	0,222	0,257	0,268	0,256	0,232	0,203	0,168	0,126	0,081	0,033	0,000	0,000	0,000	0,000	0,000	0,000	0,000	0,000	0,000	0,000	0,000
5,250	0,254	0,284	0,286	0,268	0,239	0,204	0,164	0,118	0,067	0,013	0,000	0,000	0,000	0,000	0,000	0,000	0,000	0,000	0,000	0,000	0,000
5,500	0,284	0,307	0,302	0,277	0,244	0,205	0,158	0,107	0,049	0,000	0,000	0,000	0,000	0,000	0,000	0,000	0,000	0,000	0,000	0,000	0,000
5,750	0,313	0,329	0,315	0,285	0,246	0,202	0,152	0,093	0,030	0,000	0,000	0,000	0,000	0,000	0,000	0,000	0,000	0,000	0,000	0,000	0,000
6,000	0,338	0,347	0,326	0,292	0,249	0,199	0,143	0,078	0,009	0,000	0,000	0,000	0,000	0,000	0,000	0,000	0,000	0,000	0,000	0,000	0,000
6,250	0,361	0,362	0,336	0,297	0,249	0,195	0,132	0,061	0,000	0,000	0,000	0,000	0,000	0,000	0,000	0,000	0,000	0,000	0,000	0,000	0,000
6,500	0,381	0,375	0,344	0,300	0,248	0,189	0,120	0,042	0,000	0,000	0,000	0,000	0,000	0,000	0,000	0,000	0,000	0,000	0,000	0,000	0,000
6,750	0,399	0,385	0,350	0,303	0,246	0,182	0,107	0,022	0,000	0,000	0,000	0,000	0,000	0,000	0,000	0,000	0,000	0,000	0,000	0,000	0,000
7,000	0,413	0,394	0,355	0,304	0,243	0,174	0,092	0,000	0,000	0,000	0,000	0,000	0,000	0,000	0,000	0,000	0,000	0,000	0,000	0,000	0,000
7,250	0,423	0,401	0,359	0,305	0,239	0,164	0,075	0,000	0,000	0,000	0,000	0,000	0,000	0,000	0,000	0,000	0,000	0,000	0,000	0,000	0,000
7,500	0,431	0,406	0,362	0,304	0,234	0,155	0,056	0,000	0,000	0,000	0,000	0,000	0,000	0,000	0,000	0,000	0,000	0,000	0,000	0,000	0,000
7,750	0,436	0,411	0,365	0,303	0,229	0,142	0,036	0,000	0,000	0,000	0,000	0,000	0,000	0,000	0,000	0,000	0,000	0,000	0,000	0,000	0,000
8,000	0,440	0,414	0,367	0,302	0,222	0,128	0,015	0,000	0,000	0,000	0,000	0,000	0,000	0,000	0,000	0,000	0,000	0,000	0,000	0,000	0,000
8,250	0,443	0,416	0,368	0,299	0,215	0,114	0,000	0,000	0,000	0,000	0,000	0,000	0,000	0,000	0,000	0,000	0,000	0,000	0,000	0,000	0,000
8,500	0,444	0,418	0,368	0,296	0,206	0,097	0,000	0,000	0,000	0,000	0,000	0,000	0,000	0,000	0,000	0,000	0,000	0,000	0,000	0,000	0,000
8,750	0,445	0,418	0,367	0,292	0,198	0,080	0,000	0,000	0,000	0,000	0,000	0,000	0,000	0,000	0,000	0,000	0,000	0,000	0,000	0,000	0,000
9,000	0,445	0,418	0,366	0,287	0,188	0,063	0,000	0,000	0,000	0,000	0,000	0,000	0,000	0,000	0,000	0,000	0,000	0,000	0,000	0,000	0,000
9,250	0,443	0,418	0,365	0,282	0,178	0,043	0,000	0,000	0,000	0,000	0,000	0,000	0,000	0,000	0,000	0,000	0,000	0,000	0,000	0,000	0,000
9,500	0,441	0,417	0,363	0,276	0,166	0,024	0,000	0,000	0,000	0,000	0,000	0,000	0,000	0,000	0,000	0,000	0,000	0,000	0,000	0,000	0,000
9,750	0,438	0,415	0,360	0,269	0,153	0,001	0,000	0,000	0,000	0,000	0,000	0,000	0,000	0,000	0,000	0,000	0,000	0,000	0,000	0,000	0,000
10,000	0,435	0,412	0,356	0,262	0,140	0,000	0,000	0,000	0,000	0,000	0,000	0,000	0,000	0,000	0,000	0,000	0,000	0,000	0,000	0,000	0,000
10,250	0,430	0,409	0,352	0,254	0,125	0,000	0,000	0,000	0,000	0,000	0,000	0,000	0,000	0,000	0,000	0,000	0,000	0,000	0,000	0,000	0,000
10,500	0,425	0,406	0,348	0,246	0,113	0,000	0,000	0,000	0,000	0,000	0,000	0,000	0,000	0,000	0,000	0,000	0,000	0,000	0,000	0,000	0,000
10,750	0,419	0,402	0,342	0,238	0,095	0,000	0,000	0,000	0,000	0,000	0,000	0,000	0,000	0,000	0,000	0,000	0,000	0,000	0,000	0,000	0,000
11,250	0,405	0,392	0,330	0,218	0,060	0,000	0,000	0,000	0,000	0,000	0,000	0,000	0,000	0,000	0,000	0,000	0,000	0,000	0,000	0,000	0,000
11,500	0,397	0,386	0,324	0,210	0,038	0,000	0,000	0,000	0,000	0,000	0,000	0,000	0,000	0,000	0,000	0,000	0,000	0,000	0,000	0,000	0,000
11,750	0,388	0,379	0,316	0,197	0,016	0,000	0,000	0,000	0,000	0,000	0,000	0,000	0,000	0,000	0,000	0,000	0,000	0,000	0,000	0,000	0,000
12,000	0,378	0,373	0,308	0,184	0,000	0,000	0,000	0,000	0,000	0,000	0,000	0,000	0,000	0,000	0,000	0,000	0,000	0,000	0,000	0,000	0,000

Table 17: $C_p(\lambda)\Big|_{\beta=0}$

λ	C_p
1,000	0,013
1,250	0,017
1,500	0,020
1,750	0,023
2,000	0,025
2,250	0,028
2,500	0,031
2,750	0,034
3,000	0,040
3,250	0,049
3,500	0,063
3,750	0,081
4,000	0,101
4,250	0,121
4,500	0,147
4,750	0,185
5,000	0,222
5,250	0,254
5,500	0,284
5,750	0,313
6,000	0,338
6,250	0,361
6,500	0,381
6,750	0,399
7,000	0,413
7,250	0,423
7,500	0,431
7,750	0,436
8,000	0,440
8,250	0,443
8,500	0,444
8,750	0,445
9,000	0,445
9,250	0,443
9,500	0,441
9,750	0,438
10,000	0,435
10,250	0,430
10,500	0,425
10,750	0,419
11,250	0,405
11,500	0,397
11,750	0,388
12,000	0,378

Table 18: $\beta_{min}(k_{dr})$

C_p	β
0,000	12,0
0,080	10,0
0,198	8,0
0,292	6,0
0,367	4,0
0,418	2,0
0,445	0,0

B Parameters used for the PSS/E dynamic models

Wind models

Table 19: Parameters used for the aerodynamic user defined model, UAERO

Value	Name	Description
52	R	Radius (m)
1.225	ρ	Air density (kg/m^3)
1.8	ω_0	Turbine rated speed (rad/s)
0.445	$C_{p,max}$	Maximum C_p (-)
0.0049	b	Damping constant b (pu)
0.1888	a_{00}	$C_p(pitch, \lambda)$ fourth order polynomial approximation
-0.2278	a_{01}	
0.08289	a_{02}	
-0.00852	a_{03}	
0.0002763	a_{04}	
-0.01901	a_{10}	
0.01862	a_{11}	
-0.003496	a_{12}	
0.0001721	a_{13}	
0	a_{14}	
0.0002697	a_{20}	
-0.0001652	a_{21}	
-2.347e-05	a_{22}	
0	a_{23}	
0	a_{24}	
1.158e-06	a_{30}	
6.187e-07	a_{31}	
0	a_{32}	
0	a_{33}	
0	a_{34}	
-4.824e-08	a_{40}	
0	a_{41}	
0	a_{42}	
0	a_{43}	
0	a_{44}	

Table 20: Parameters used for the drivtrain user defined model, UDRIV

Value	Name	Description
5.74	H_{wt}	WT inertia (s)
0.0049	b	WT damping (pu)
8.75	λ_{opt}	Lambda optimal (-) (for initializing)
52	R	WT Radius (m) (for initializing)
1.8	ω_0	Rated Speed (rad/s) (for initializing)
3.6	P_0	Rated Power (MW) (for initializing)
1.225	ρ	Air density (kg/m^3) (for initializing)
0.445	$C_{p,max}$	Cp max (-) (for initializing)
0.97	$RefSpd$	Reference speed (pu) (for initializing)
0.4	$CutSpd$	Cut in speed (pu) (for initializing)

Table 21: Parameters used for the torque user defined model, UTORQ

Value	Name	Description
10	Kp_{sc}	Speed/torque controller proportional gain
2	Ki_{sc}	Speed/torque controller integral gain
0.0049	b	Compensation for WT damping constant (pu)
1	P_{max}	Maximum power (pu)
0	P_{min}	Minimum power (pu)
0.97	$RefSpd$	Reference speed max (pu)
0.4	$CutSpt$	Cut in speed (pu)
8.75	λ_{opt}	Optimal lambda (-)
52	R	WT radius (m)
1.8	ω_0	Rated Speed (rad/s)
3.6	P_0	Rated Power (MW)
1.225	ρ	Air density (kg/m^3)
0.445	$C_{p,max}$	Cp maximum (-)
1	T_s	Speed reference filter time constant (s)

Table 22: Parameters used for the pitch user defined model, UPIT

Value	Name	Description
460	Kp_{pc}	Proportional gain
290	Ki_{pc}	Integral gain
90	β_{max}	Maximum pitch (deg)
11	*Pitch rate max*	Minimum pitch rate of change (deg/s)
-11	*Pitch rate min*	Maximum pitch rate of change (deg/s)
1	$\omega_{0,pu}$	Rated speed (pu)

Table 23: Parameters used for the frequency control user defined model, UPLANT

Value	Name	Description
52	R	WT Radius (m)
1.8	ω_0	Turbine rated speed (rad/s)
1.225	ρ	Air density (kg/m^3)
3.6	P_0	Rated Power (MW)
8.75	λ_{opt}	Lambda optimal (-)
1	$\omega_{\mathrm{wt,max}}$	Max speed (pu)
0	$\omega_{\mathrm{wt,min}}$	Min speed (pu)
1	$P_{\mathrm{e,wt,max}}$	Max power (pu)
0	$P_{\mathrm{e,wt,min}}$	Min power (pu)
0.00	Db_{dr}	Frequency deadband for de-rating control (pu)
0.05	$Rp_{\mathrm{u,wt}}$	Droop for up regulation
0.02	$Rp_{\mathrm{d,wt}}$	Droop for down regulation
0.1	P_{reserve}	Power reserve (pu)
0.445	$C_{p,\mathrm{max}}$	Cp max (-)
0.00	Db_{ie}	Frequency deadband for inertia control (pu)
0.5	T_f	Inertia filter time constant (s)
5.74	H_{wt}	Wind turbine inertia (pu)
5	k_i	Wind turbine inertia gain (-)
0.02	k_{sc}	Feedback for returning to optimal speed (-)
0.5	$\omega_{\mathrm{ie,min}}$	Lower speed limit for inertia emulation (pu)
0.1888	a_{00}	$C_p(\beta, \lambda)$ fourth order polynomial approximation
-0.2278	a_{01}	
0.08289	a_{02}	
-0.00852	a_{03}	
0.0002763	a_{04}	
-0.01901	a_{10}	
0.01862	a_{11}	
-0.003496	a_{12}	
0.0001721	a_{13}	
0	a_{14}	
0.0002697	a_{20}	
-0.0001652	a_{21}	
-2.347e-05	a_{22}	
0	a_{23}	
0	a_{24}	
1.158e-06	a_{30}	
6.187e-07	a_{31}	
0	a_{32}	
0	a_{33}	
0	a_{34}	
-4.824e-08	a_{40}	
0	a_{41}	
0	a_{42}	
0	a_{43}	
0	a_{44}	

Continued on next page

Continued from last page		
Value	**Name**	**Description**
0.07917	b_0	$C_p(\beta = 0, \lambda)$ fourth order polynomial approximation
-0.0868	b_1	
0.04574	b_2	
-0.00491	b_3	
0.0001562	b_4	
11.98	c_0	$\beta_{min}(k_{\mathrm{dr}})$ fourth order polynomial approximation
-25.16	c_1	
8.12	c_2	
144.6	c_3	
-382.3	c_4	

Table 24: Parameters used for the generic renewable generator model REGCA1. Description is from the PSS/E model library

Value	**Description**
0	Lvplsw (Low Voltage Power Logic) switch (0: LVPL not present, 1:LVPL present)
0.20000E-01	Tg, Converter time constant (s)
10.000	Rrpwr, Low Voltage Power Logic (LVPL) ramp rate limit (pu/s)
0.90000	Brkpt, LVPL characteristic voltage 2 (pu)
0.40000	Zerox, LVPL characteristic voltage 1 (pu)
1.2000	Lvpl1, LVPL gain (pu)
1.2000	Volim, Voltage limit (pu) for high voltage reactive current management
0.80000	Lvpnt1, High voltage point for low voltage active current management (pu)
0.40000	vpnt0, Low voltage point for low voltage active current management (pu)
-1.2500	Iolim, Current limit (pu) for high voltage reactive current management
0.15000E-01	(specified as a negative value)
0.70000	Tfltr, Voltage filter time constant for low voltage active current management (s)
999.00	Khv, Overvoltage compensation gain used in the high voltage reactive current management
-999.00	Iqrmax, Upper limit on rate of change for reactive current (pu)
1.0000	Iqrmin, Lower limit on rate of change for reactive current (pu)

Table 25: Parameters used for the generic renewable electrical model REECA1. Description is from the PSS/E model library

Value	Description
0	Bus number for voltage control; local control if 0 (Remote contol not posibal)
1	PFFLAG: 1 if power factor control 0 if Q control (which can be controlled by an external signal)
1	VFLAG: 1 if Q control 0 if voltage control
0	QFLAG: 1 if voltage or Q control 0 if constant pf or Q control
0	PFLAG: 1 if active current command has speed dependence, 0 for no dependency
0	PQFLAG, P/Q priority flag for current limit: 0 for Q priority, 1 for P priority
0.90000	Vdip (pu), low voltage threshold to activate reactive current injection logic
1.2000	Vup (pu), Voltage above which reactive current injection logic is activated
0.20000E-01	Trv (s), Voltage filter time constant
-0.50000E-01	dbd1 (pu), Voltage error dead band lower threshold (0)
0.50000E-01	dbd2 (pu), Voltage error dead band upper threshold (0)
5.0000	Kqv (pu), Reactive current injection gain during over and undervoltage conditions
1.0500	Iqh1 (pu), Upper limit on reactive current injection Iqinj
-1.0500	Iql1 (pu), Lower limit on reactive current injection Iqinj
0.0000	Vref0 (pu), User defined reference (if 0, model initializes it to initial terminal voltage)
0.15000	Iqfrz (pu), Value at which Iqinj is held for Thld seconds following a voltage dip if Thld > 0
0.0000	Thld (s), Time for which Iqinj is held at Iqfrz after voltage dip returns to zero (see Note 3)
0.0000	Thld2 (s) (0), Time for which the active current limit (IPMAX) is held at the faulted value after voltage dip returns to zero
0.15000E-01	Tp (s), Filter time constant for electrical power
0.40000	QMax (pu), limit for reactive power regulator
-0.40000	QMin (pu) limit for reactive power regulator
1.1500	VMAX (pu), Max. limit for voltage control
0.90000	VMIN (pu), Min. limit for voltage control
0.0000	Kqp (pu), Reactive power regulator proportional gain
0.10000	Kqi (pu), Reactive power regulator integral gain
1.0000	Kvp (pu), Voltage regulator proportional gain
50.000	Kvi (pu), Voltage regulator integral gain
0.0000	Vbias (pu), User-defined bias (normally 0)
0.20000E-01	Tiq (s), Time constant on delay s4
0.45000	dPmax (pu/s) (>0) Power reference max. ramp rate
-0.45000	dPmin (pu/s) (<0) Power reference min. ramp rate
1.2000	PMAX (pu), Max. power limit
0.0000	PMIN (pu), Min. power limit

Continued on next page

Continued from last page	
Value	**Description**
1.3000	Imax (pu), Maximum limit on total converter current
0.40000E-01	Tpord (s), Power filter time constant
0.29000	Vq1 (pu), Reactive Power V-I pair, voltage
1.2500	Iq1 (pu), Reactive Power V-I pair, current
1.3300	Vq2 (pu) (Vq2>Vq1), Reactive Power V-I pair, voltage
0.0000	Iq2 (pu) (Iq2>Iq1), Reactive Power V-I pair, current
0.0000	Vq3 (pu) (Vq3>Vq2), Reactive Power V-I pair, voltage
0.0000	Iq3 (pu) (Iq3>Iq2), Reactive Power V-I pair, current
0.0000	Vq4 (pu) (Vq4>Vq3), Reactive Power V-I pair, voltage
0.0000	Iq4 (pu) (Iq4>Iq3), Reactive Power V-I pair, current
0.0000	Vp1 (pu), Real Power V-I pair, voltage
1.1500	Ip1 (pu), Real Power V-I pair, current
1.1000	Vp2 (pu) (Vp2>Vp1), Real Power V-I pair, voltage
1.2400	Ip2 (pu) (Ip2>Ip1), Real Power V-I pair, current
2.0000	Vp3 (pu) (Vp3>Vp2), Real Power V-I pair, voltage
1.2400	Ip3 (pu) (Ip3>Ip2), Real Power V-I pair, current
0.0000	Vp4 (pu) (Vp4>Vp3), Real Power V-I pair, voltage
0.0000	Ip4 (pu) (Ip4>Ip3), Real Power V-I pair, current

Hydro

Table 26: Parameters used for the generic generator model GENROU. Description is from the PSS/E model library

Value	**Description**
5.89	T$\acute{}$do (>0) (sec)
0.05	Tdo (>0) (sec)
0.60	T$\acute{}$qo (>0) (sec)
0.05	Tqo (>0) (sec)
4.9	H, Inertia
0.9	D, Speed damping
1.68	Xd
1.61	Xq
0.23206	X$\acute{}$d
0.32	X$\acute{}$q
0.21	Xd = Xq
0.1536	Xl
1.01	S(1.0)
1.02	S(1.2)

Table 27: Parameters used for the excitation system model SEXS. Description is from the PSS/E model library

Value	Description
0	TA/TB
0.02	TB (>0) (s)
150	K
0	TE (s)
-4	EMIN (pu on EFD base)
4	EMAX (pu on EFD base)

Table 28: Parameters used for the stabilizer model STAB1. Description is from the PSS/E model library

Value	Description
8	K/T (1/sec)
10	T (sec) (>0)
2.5	T1/T3
0.02	T3 (sec) (>0)
0.555	T2/T4
5.4	T4 (sec) (>0)
0.5	HLIM

Table 29: Parameters used for the hydro turbine-governor model HYGOV. Description is from the PSS/E model library

Value	Description
0,0500	R, permanent droop
0,5500	r, temporary droop
4,0816	Tr (>0) governor time constant
0,0550	Tf (>0) filter time constant
0,2000	Tg (>0) servo time constant
0,1000	ś VELM, gate velocity limit
1,0000	GMAX, maximum gate limit
0,0000	GMIN, minimum gate limit
0,5000	TW (>0) water time constant
1,0577	At, turbine gain
0,5000	Dturb, turbine damping
0,1000	qNL, no power flow

Table 30: Parameters used for the Turbine load controller model LCFB1. Description is from the PSS/E model library

Value	Description
1	fbf, Frequency bias flag
0	pbf, Power Controller flag
1.0	Fb, Frequency bias gain(pu/pu)
0.0	Tpelec, Electrical power transducer time constant(sec)
0.0	db, Controller dead band(pu)
0.1	emax, Maximum control error(pu)
0.0	Kp, Proportional gain
0.04	Ki, Integral gain
0.05	lrmax, Maximum turbine speed/load reference bias(pu)

Grid

Table 31: Parameters used for the generator model GENCLS. Description is from the PSS/E model library

Value	Description
0	H, Inertia
0	D, Damping constant

Load

Table 32: Parameters used for the user defined load model BL_FIL from [47]

Value	Description
0	Force dual timestep? (1=Yes)
4	Data file identifier number
0.9	K, Frequency Sensitivity factor
0.0002	sigma, Stoch. process standard dev./ file input gain
0.9950	cosPhi, Load deviation power factor
0.0000	Time of activation (s)

C MATLAB/Simulink frequency response

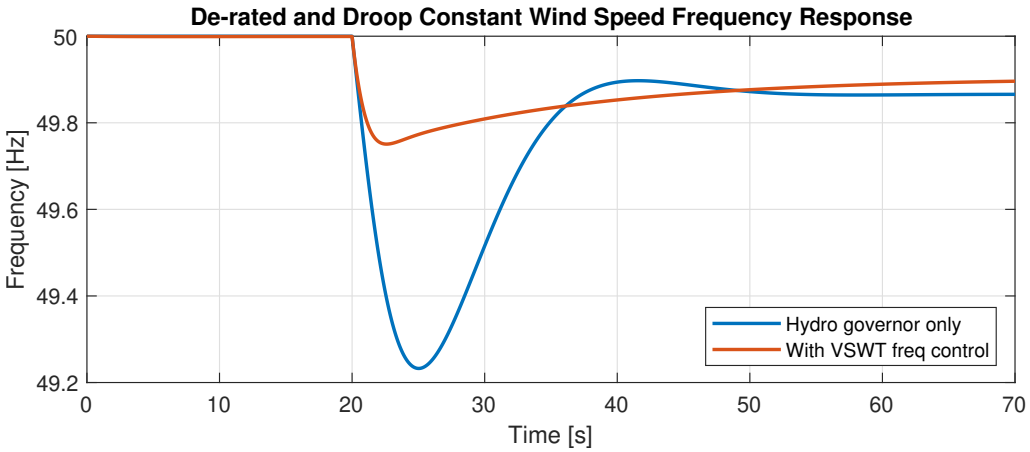

Figure 55: Frequency response while VSWT is de-rated by 0.1 pu and providing droop frequency support for up-regulation of frequency after a power disturbance of 0.04 pu on the system base at 20 s during a constant wind speed of 7 m/s. Frequency response with VSWT support compared to the response without

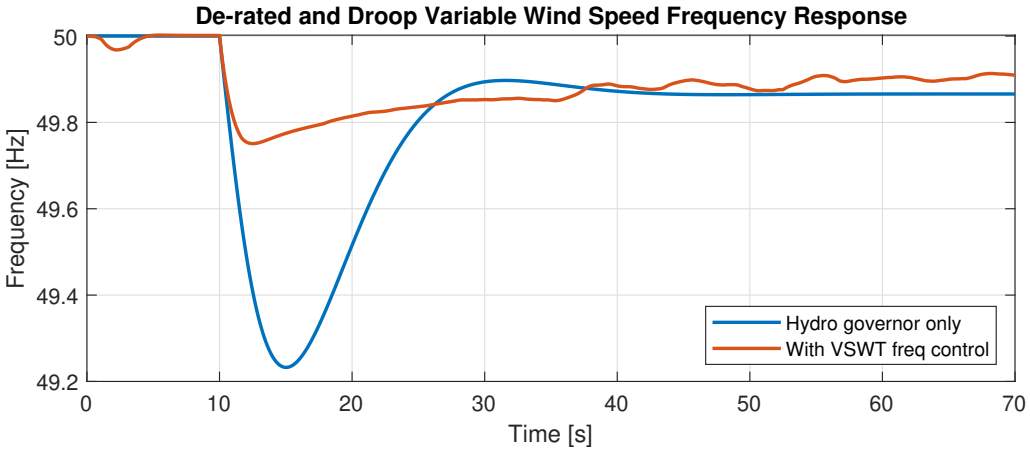

Figure 56: Frequency response while VSWT is de-rated by 0.1 pu and providing droop frequency support for up-regulation of frequency after a power disturbance of 0.04 pu on the system base at 10 s during a variable wind speed. Frequency response with VSWT support compared to the response without

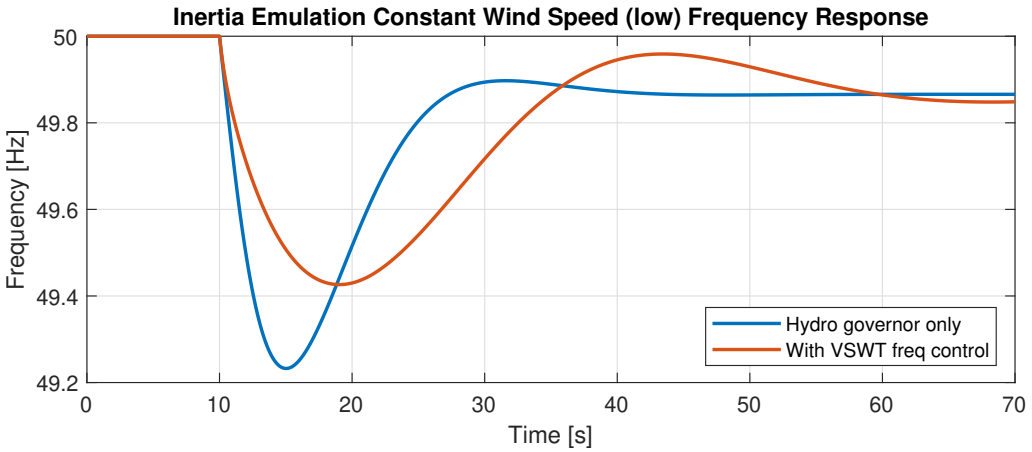

Figure 57: Frequency response while VSWT is providing inertia emulation support for up-regulation of frequency after a power disturbance of 0.04 pu on the system base at 10 s during a constant wind speed of 7 m/s (below rated speed). Frequency response with VSWT support compared to the response without

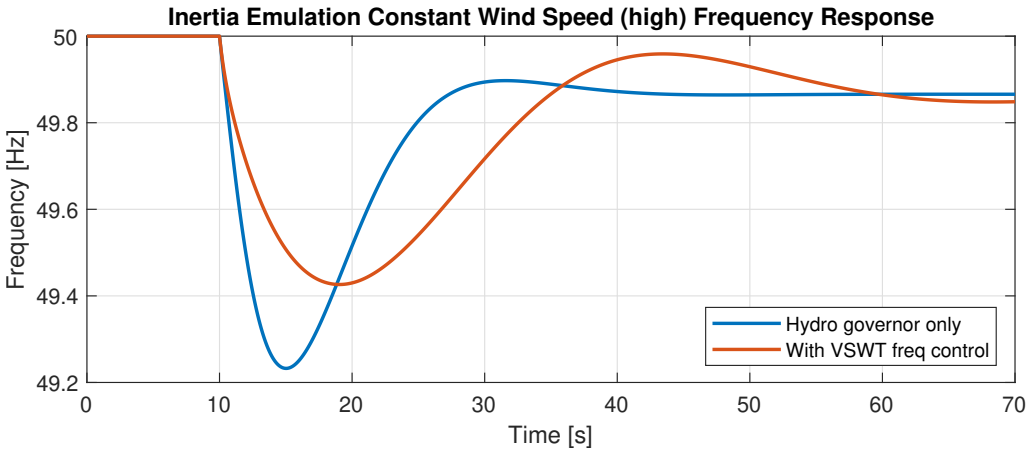

Figure 58: Frequency response while VSWT is providing inertia emulation support for up-regulation of frequency after a power disturbance of 0.04 pu on the system base at 10 s during a constant wind speed of 9 m/s (above rated speed). Frequency response with VSWT support compared to the response without

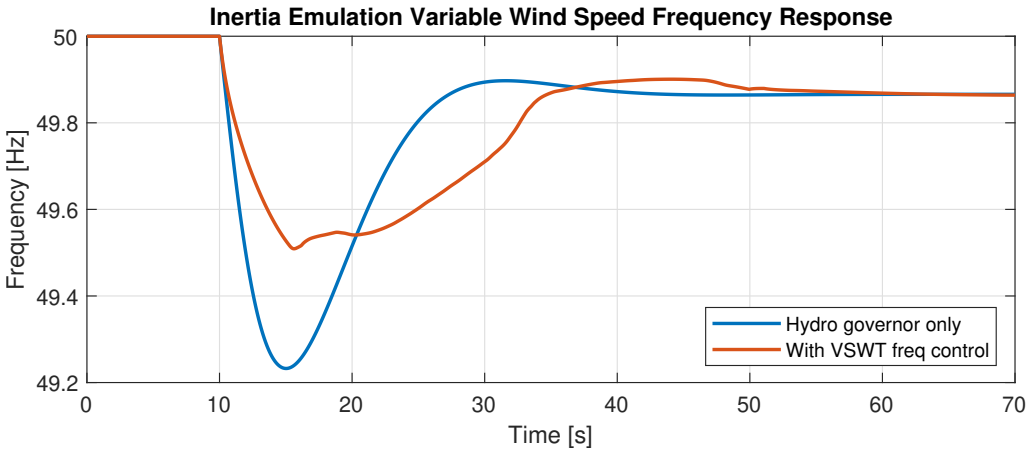

Figure 59: Frequency response while VSWT is providing inertia emulation support for up-regulation of frequency after a power disturbance of 0.04 pu on the system base at 10 s during a variable wind speed. Frequency response with VSWT support compared to the response without

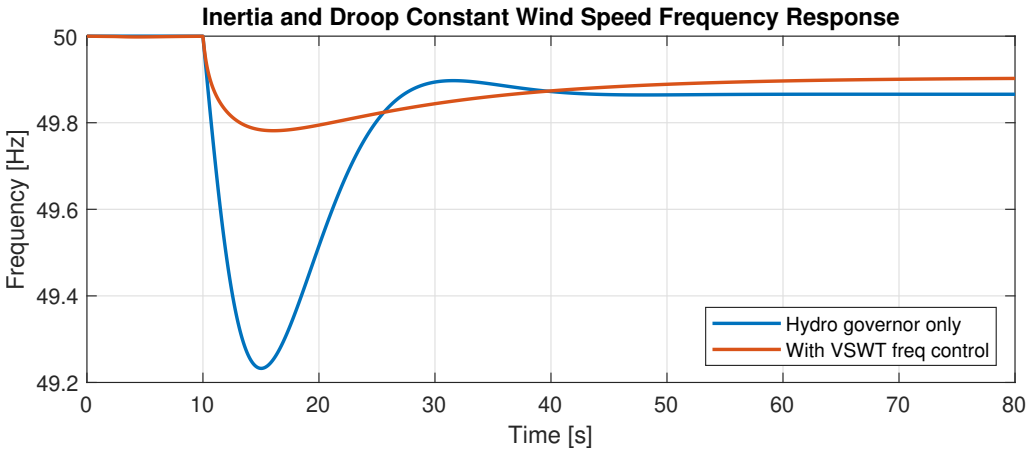

Figure 60: Frequency response while VSWT is de-rated by 0.1 pu and providing droop and inertia emulation frequency support for up-regulation of frequency after a power disturbance of 0.04 pu on the system base at 10 s during a constant wind speed of 7 m/s. Frequency response with VSWT support compared to the response without

D User defined models

UAERO

```
1     SUBROUTINE UAERO(MC,SLOT)
2         INCLUDE 'COMON4.INS'
3         IMPLICIT NONE
4         INTEGER J           ! starting CON index
5         INTEGER K           ! starting STATE index
6         INTEGER L           ! starting VAR index
```

```
7         INTEGER M           ! starting ICON index
8         INTEGER MC          ! machine index
9         INTEGER SLOT        ! index into STRT array allocation
10        INTEGER ioflag
11        INTEGER already_open_fileunit
12
13        CHARACTER(LEN = 4) filenumchar
14        CHARACTER(LEN = 12) filename
15
16        REAL DEL2, lambda, Cp, x, y, WIND, Cptemp, PMtemp
17        EXTERNAL  NOTMID
18
19        J=WSTRTIN(1,SLOT)                              ! STARTING
    'CON'
20        K=WSTRTIN(2,SLOT)                              ! STARTING
    'STATE'
21        L=WSTRTIN(3,SLOT)                              ! STARTING
    'VAR'
22        M=WSTRTIN(4,SLOT)                              ! STARTING
    'ICON'
23
24        DEL2 = 2.0 * DELT
25
26        !MODE 8 - GET DATA DESCRIPTIONS
27        IF (MODE.EQ.8) THEN
28
29            !Add CON_DSCRPT here
30            CON_DSCRPT(1) = 'Radius (m)'
31            CON_DSCRPT(2) = 'Air density (kg/m^3)'
32            CON_DSCRPT(3) = 'Turbine rated speed (rad/s)'
33            CON_DSCRPT(4) = 'Maximum Cp '
34            CON_DSCRPT(5) = 'Dampening constant b (p.u)'
35
36            !CP(pitch,lambda) forth order polynomial approximation
37            CON_DSCRPT(6) = 'a00'
38            CON_DSCRPT(7) = 'a01'
39            CON_DSCRPT(8) = 'a02'
40            CON_DSCRPT(9) = 'a03'
41            CON_DSCRPT(10) = 'a04'
42            CON_DSCRPT(11) = 'a10'
43            CON_DSCRPT(12) = 'a11'
44            CON_DSCRPT(13) = 'a12'
45            CON_DSCRPT(14) = 'a13'
46            CON_DSCRPT(15) = 'a14'
47            CON_DSCRPT(16) = 'a20'
48            CON_DSCRPT(17) = 'a21'
49            CON_DSCRPT(18) = 'a22'
50            CON_DSCRPT(19) = 'a23'
51            CON_DSCRPT(20) = 'a24'
52            CON_DSCRPT(21) = 'a30'
53            CON_DSCRPT(22) = 'a31'
54            CON_DSCRPT(23) = 'a32'
55            CON_DSCRPT(24) = 'a33'
56            CON_DSCRPT(25) = 'a34'
57            CON_DSCRPT(26) = 'a40'
58            CON_DSCRPT(27) = 'a41'
```

```
59            CON_DSCRPT(28) = 'a42'
60            CON_DSCRPT(29) = 'a43'
61            CON_DSCRPT(30) = 'a44'
62
63            !Add ICON_DSCRPT here
64            ICON_DSCRPT(1) = 'Wind file number'
65            ICON_DSCRPT(2) = 'Number of aggregated units'
66
67           RETURN
68         ENDIF
69
70         !MODE 1 - INITIALIZATION
71         IF (MODE.EQ.1) THEN
72
73            DO WIND=0,14,0.00001      ! Sweep wind speed ie.
   lambda, since speed is fixed from drivetrain
74               x = WNDSP3(WNDNUM(MC))
75               y = CON(J)*CON(J+2)/WIND*(WTRBSP(WNDNUM(MC))+1)
76
77               Cptemp = CON(J+5) + CON(J+6)*y + CON(J+7)*y**2 +
   CON(J+8)*y**3 + CON(J+9)*y**4 + CON(J+10)*x + CON(J+11)*x*y +
   CON(J+12)*x*y**2  & ! Cp from forth order polynomial
   aproximation
78               + CON(J+13)*x*y**3 + CON(J+14)*x*y**4 +
   CON(J+15)*x**2 + CON(J+16)*x**2*y + CON(J+17)*x**2*y**2 +
   CON(J+18)*x**2*y**3           &
79               + CON(J+19)*x**2*y**4 + CON(J+20)*x**3 +
   CON(J+21)*x**3*y + CON(J+22)*x**3*y**2 + CON(J+23)*x**3*y**3 +
   CON(J+24)*x**3*y**4     &
80               + CON(J+25)*x**4 + CON(J+26)*x**4*y +
   CON(J+27)*x**4*y**2 + CON(J+28)*x**4*y**3 + CON(J+29)*x**4*y**4
81
82               IF (Cptemp .GT. CON(J+3)) THEN      ! Limit Cp to
   reasnoabel values for high/low lambda
83                  Cptemp =  CON(J+3)
84               ELSE IF (Cptemp .LT. 0) THEN
85                  Cptemp = 0
86               END IF
87
88               PMtemp =
   ((0.5*CON(J+1)*3.14*(CON(J)**2)*CPtemp*(WIND**3))
   /(MBASE(MC)*10**6))*ICON(M+1) ! Aggregated PMECH in p.u.
   machine base
89               VAR(L+5) = y ! lambda_0
90
   IF(ABS(PMtemp-PELEC(MC)*SBASE/MBASE(MC)-CON(J+4)*(WTRBSP(WNDNUM(MC))+1))
   .LE. 0.00001) THEN !If mecanical power equeal to load power
   including possibal dampening term, then the wind speed is corect
91                  ! Save the corect wind speed and other
   initalisation paramiters
92                  VAR(L) = WIND ! Wind_speed
93                  VAR(L+1) = y ! lambda_0
94                  VAR(L+2) = x ! beta_0
95                  VAR(L+3) = CPtemp  ! C_p0, initial C_p
96                  VAR(L+4) = PMtemp  ! Pmech calculation that
   mached.
```

```
97
98                  ENDIF
99              END DO
100
101             !File opening
102             VAR(L+7) = ICON(M) + 10000
103             IF (ICON(M) > 9999) THEN
104                 ICON(M) = -1
105                 RETURN
106             ELSE
107                 WRITE(filenumchar, '(i4.4)') ICON(M)
108                 filename = 'WIND'//filenumchar//'.DAT'
109             ENDIF
110
111             INQUIRE(file = filename,number =
    already_open_fileunit, opened = ioflag)
112             IF(ioflag > 0) CLOSE(already_open_fileunit)
113
114             OPEN(unit = VAR(L+7), file = filename, status = 'old',
    action = 'read', iostat = ioflag)
115
116             IF(ioflag > 0) VAR(L+7) = -1
117
118             READ(VAR(L+7), *, iostat = ioflag) x  ! x contains the
    read wind speed data
119             IF(ioflag == 0) VAR(L+8) = VAR(L) - x % ! Callculate
    wind speed data offset to initelized wind speed
120
121             RETURN
122         ENDIF
123
124         !MODE 2 - CALCULATE DERIVATIVES
125         IF (MODE.EQ.2) THEN
126
127            RETURN
128         ENDIF
129
130
131         !MODE 3 - SET Model output
132         IF (MODE.EQ.3) THEN
133
134             ! wind data read
135             READ(VAR(L+7), *, iostat = ioflag) x ! x contains the
    read wind speed data
136             IF(ioflag == 0) VAR(L) = x + VAR(L+8) ! Shift wind
    speed by offset to satesfy init
137             WVLCTY(WNDNUM(MC)) = VAR(L)
138
139             lambda = CON(J)*CON(J+2)/VAR(L)*(WTRBSP(WNDNUM(MC))+1)
    ! Calculate lambda
140             VAR(L+5) = lambda
141
142             x = WPITCH(WNDNUM(MC))  ! x = pitch, y = lambda
143             y = VAR(L+5)
144
145             Cp = CON(J+5) + CON(J+6)*y + CON(J+7)*y**2 +
```

```
    CON(J+8)*y**3 + CON(J+9)*y**4 + CON(J+10)*x + CON(J+11)*x*y +
    CON(J+12)*x*y**2  & ! Cp from forth order polynomial
    aproximation
146                 + CON(J+13)*x*y**3 + CON(J+14)*x*y**4 +
    CON(J+15)*x**2 + CON(J+16)*x**2*y + CON(J+17)*x**2*y**2 +
    CON(J+18)*x**2*y**3           &
147                 + CON(J+19)*x**2*y**4 + CON(J+20)*x**3 +
    CON(J+21)*x**3*y + CON(J+22)*x**3*y**2 + CON(J+23)*x**3*y**3 +
    CON(J+24)*x**3*y**4     &
148                 + CON(J+25)*x**4 + CON(J+26)*x**4*y +
    CON(J+27)*x**4*y**2 + CON(J+28)*x**4*y**3 + CON(J+29)*x**4*y**4
149              IF (Cp .GT. CON(J+3)) THEN      ! Limit Cp to
    reasnoabel values for high/low lambda
150                     Cp =  CON(J+3)
151              ELSE IF (Cp .LT. 0) THEN
152                     Cp = 0
153              END IF
154              VAR(L+6) = Cp
155
    WAEROT(WNDNUM(MC))=(VAR(L)**3*Cp*CON(J)**2*3.14*CON(J+1)
    /(MBASE(MC)*10**6*2)/(WTRBSP(WNDNUM(MC))+1))*ICON(M+1)        !
    Aggregated Mecanical torque in p.u. machine base
156             RETURN
157          ENDIF
158
159
160          !MODE 4 - set NINTEG
161
162          IF (MODE.EQ.4) THEN
163             IF (MIDTRM) THEN
164                CALL NOTMID
165             ELSE
166
167          !Set NINTEG
168             IF(NINTEG < K+1) NINTEG = K+1
169             ENDIF
170
171             RETURN
172          ENDIF
173
174          RETURN
175
176
177          END SUBROUTINE UAERO
```

UDRIV

```
1     SUBROUTINE UDRIV(MC,SLOT)
2         INCLUDE 'COMON4.INS'
3         IMPLICIT NONE
4         INTEGER J           ! starting CON index
5         INTEGER K           ! starting STATE index
6         INTEGER L           ! starting VAR index
7         INTEGER M           ! starting ICON index
8         INTEGER MC          ! machine index
9         INTEGER SLOT        ! index into STRT array allocation
10        REAL DEL2, Pe, Tm, Te, PowToSpd
11        EXTERNAL  NOTMID
12        J=WSTRTIN(1,SLOT)                              ! STARTING
    'CON'
13        K=WSTRTIN(2,SLOT)                              ! STARTING
    'STATE'
14        L=WSTRTIN(3,SLOT)                              ! STARTING
    'VAR'
15        M=WSTRTIN(4,SLOT)                              ! STARTING
    'ICON'
16
17
18        DEL2 = 2.0 * DELT
19        PowToSpd = CON(J+2)/(CON(J+3)*CON(J+4)) *
    (2*CON(J+5)*1000000/(CON(J+6)*CON(J+3)**2*3.14*CON(J+7)))**(1./3.)
20
21        !MODE 8 - GET DATA DESCRIPTIONS
22        IF (MODE.EQ.8) THEN
23
24        !Add CON_DSCRPT here
25        CON_DSCRPT(1) = 'H_wt, WT inertia (s)'
26        CON_DSCRPT(2) = 'b, WT dampening (pu)'
27        CON_DSCRPT(3) = 'Lambda optimal'
28        CON_DSCRPT(4) = 'WT Radius (m)'
29        CON_DSCRPT(5) = 'Rated Speed (rad/s)'
30        CON_DSCRPT(6) = 'Rated Power (MW)'
31        CON_DSCRPT(7) = 'Air density'
32        CON_DSCRPT(8) = 'Cp max'
33        CON_DSCRPT(9) = 'Reference speed (pu)'
34        CON_DSCRPT(10) = 'Cut in speed (pu)'
35
36
37        !Add ICON_DSCRPT here
38
39           RETURN
40        ENDIF
41
42        !MODE 1 - INITIALIZATION
43        IF (MODE.EQ.1) THEN
44
45            Pe = PELEC(MC)*SBASE/MBASE(MC)      ! electric power
    pu. machine base
46            VAR(L+2) = PowToSpd
47
48            STATE(K) =  (Pe/WAUXSG(WNDNUM(MC)))**(1./3.) *
```

```
   PowToSpd - 1      ! Initalize WT rot speed delta from power
   output
49           VAR(L) = STATE(K)
50           IF (STATE(K) + 1 .GT. CON(J+8)) THEN
             ! Rot speed within speed refrence
51               STATE(K) = CON(J+8) - 1
52           ELSE IF (STATE(K) + 1 .LT. CON(J+9)) THEN
53               STATE(K) = CON(J+9) - 1
54           ENDIF
55           WTRBSP(WNDNUM(MC)) = STATE(K)
             ! Set speed for use in aerodynamics and torqe model
56
57           RETURN
58        ENDIF
59
60        !MODE 2 - CALCULATE DERIVATIVES
61        IF (MODE.EQ.2) THEN
62
63        Pe = PELEC(MC)*SBASE/MBASE(MC)                ! electric
   power pu. machine base
64        Tm = WAEROT(WNDNUM(MC))                       ! mec torque
   pu. machine base
65        Te = Pe/(WTRBSP(WNDNUM(MC))+1)                ! elec torque
   pu. machine base
66        VAR(L+1) = Te
67
68        DSTATE(K) = (Tm-Te-((STATE(K)+1)*CON(J+1)))/(2*CON(J))
    ! Speed delta DSTATE
69
70           RETURN
71        ENDIF
72
73
74        !MODE 3 - SET Model output
75        IF (MODE.EQ.3) THEN
76           WTRBSP(WNDNUM(MC)) = STATE(K)         ! Set Speed delta
   output chanel
77
78           RETURN
79        ENDIF
80
81
82        !MODE 4 - set NINTEG
83        IF (MODE.EQ.4) THEN
84           IF (MIDTRM) THEN
85              CALL NOTMID
86           ELSE
87
88        !Set NINTEG
89           IF(NINTEG < K+1) NINTEG = K+1
90
91           ENDIF
92
93           RETURN
94        ENDIF
95
```

```
96          RETURN
97          END SUBROUTINE UDRIV
```

UPIT

```
1     SUBROUTINE UPIT(MC,SLOT)
2
3
4         INCLUDE 'COMON4.INS'
5
6         IMPLICIT NONE
7
8         INTEGER J           ! starting CON index
9         INTEGER K           ! starting STATE index
10        INTEGER L           ! starting VAR index
11        INTEGER M           ! starting ICON index
12        INTEGER MC          ! machine index
13        INTEGER SLOT        ! index into STRT array allocation
14        REAL DEL2
15        INTEGER IERR
16        REAL VINP
17        REAL VOUT
18        EXTERNAL  NOTMID
19        J=WSTRTIN(1,SLOT)                              ! STARTING
    'CON'
20        K=WSTRTIN(2,SLOT)                              ! STARTING
    'STATE'
21        L=WSTRTIN(3,SLOT)                              ! STARTING
    'VAR'
22        M=WSTRTIN(4,SLOT)                              ! STARTING
    'ICON'
23
24        DEL2 = 2.0 * DELT
25
26
27        !MODE 8 - GET DATA DESCRIPTIONS
28        IF (MODE.EQ.8) THEN
29
30            !Add CON_DSCRPT here
31            CON_DSCRPT(1) = 'KP_pc'
32            CON_DSCRPT(2) = 'KI_pc'
33            CON_DSCRPT(3) = 'Max pitch (deg)'
34            CON_DSCRPT(4) = 'Min pitch (deg) (not used)'
35            CON_DSCRPT(5) = 'Max pitch rate of change (deg/s))'
36            CON_DSCRPT(6) = 'Rated speed (pu)'
37            !Add ICON_DSCRPT here
38
39           RETURN
40        ENDIF
41
42        !MODE 1 - INITIALIZATION
43        IF (MODE.EQ.1) THEN
44
45            VOUT = WNDSP3(WNDNUM(MC))
46            VINP
    =NWPI_MODE1(CON(J),CON(J+1),CON(J+2),WNDSP3(WNDNUM(MC)),VOUT,K,IERR)
    ! Initialyze pitch NON-WINDUP pi
47            WPITCH(WNDNUM(MC)) = VOUT
48            VAR(L) = VOUT
```

```
49            VAR(L+1) = WPITCH(WNDNUM(MC))     !Pitch
50           RETURN
51        ENDIF
52
53        !MODE 2 - CALCULATE DERIVATIVES
54        IF (MODE.EQ.2) THEN
55
56            VINP = (WTRBSP(WNDNUM(MC)) + 1) - CON(J+5)        !
    Speed error
57            VOUT =
    NWPI_MODE2(CON(J),CON(J+1),CON(J+2),WNDSP3(WNDNUM(MC)),VINP,K)
    ! Pitch PI DSTATE
58
59            IF (VOUT .GT. CON(J+2)) THEN       ! Make sure that
    pitch is less then max pitch
60                VOUT = CON(J+2)
61            END IF
62
63
64            IF (VAR(L+1)-VOUT .GT. DELT*CON(J+4)) THEN ! Pitch
    rate limit
65                VOUT = VAR(L+1) - DELT*CON(J+4)
66            ELSE IF (VAR(L+1)-VOUT .LT. -DELT*CON(J+4)) THEN
67                VOUT = VAR(L+1) + DELT*CON(J+4)
68            END IF
69
70            VAR(L+1) = VOUT
71
72           RETURN
73        ENDIF
74
75
76        !MODE 3 - SET Model output
77        IF (MODE.EQ.3) THEN
78
79           WPITCH(WNDNUM(MC)) =  VAR(L+1)       ! Set pitch output
    chanel
80
81           RETURN
82        ENDIF
83
84
85        !MODE 4 - set NINTEG
86        IF (MODE.EQ.4) THEN
87           IF (MIDTRM) THEN
88              CALL NOTMID
89           ELSE
90        !Set NINTEG
91           IF(NINTEG < K) NINTEG = K
92           ENDIF
93           RETURN
94        ENDIF
95
96        RETURN
97
98        END SUBROUTINE UPIT
```

UTORQ

```
1     SUBROUTINE UTORQ(MC,SLOT)
2         INCLUDE 'COMON4.INS'
3         IMPLICIT NONE
4         INTEGER J           ! starting CON index
5         INTEGER K           ! starting STATE index
6         INTEGER L           ! starting VAR index
7         INTEGER M           ! starting ICON index
8         INTEGER MC          ! machine index
9         INTEGER SLOT        ! index into STRT array allocation
10
11        REAL DEL2, PowToSpd, Pel, U
12        REAL VINP
13        REAL VOUT
14        EXTERNAL  NOTMID
15
16        J=WSTRTIN(1,SLOT)                              ! STARTING
    'CON'
17        K=WSTRTIN(2,SLOT)                              ! STARTING
    'STATE'
18        L=WSTRTIN(3,SLOT)                              ! STARTING
    'VAR'
19        M=WSTRTIN(4,SLOT)                              ! STARTING
    'ICON'
20
21        ! Calculate the power to speed relationship for optimal WT
    operation
22        PowToSpd = CON(J+8)/(CON(J+9)*CON(J+10)) *
    (2*CON(J+11)*1000000/(CON(J+12)*CON(J+9)**2*3.14*CON(J+13)))**(1./3.)
23
24        DEL2 = 2.0 * DELT
25
26        !MODE 8 - GET DATA DESCRIPTIONS
27        IF (MODE.EQ.8) THEN
28
29            !Add CON_DSCRPT here
30            CON_DSCRPT(1) = 'Speed/torque controller proportional
    gain'
31            CON_DSCRPT(2) = 'Speed/torque controller integral gain'
32            CON_DSCRPT(3) = 'Compensation for WT dampening
    constant (pu)'
33            CON_DSCRPT(4) = 'Maximum power (pu)'
34            CON_DSCRPT(5) = 'Minimum power (pu)'
35            CON_DSCRPT(6) = 'Maximum power rate of change (not
    used)'
36            CON_DSCRPT(7) = 'Reference speed max (pu)'
37            CON_DSCRPT(8) = 'Cut in speed (pu)'
38            CON_DSCRPT(9) = 'Optimal lambda (-)'
39            CON_DSCRPT(10) = 'WT radius (m)'
40            CON_DSCRPT(11) = 'Rated Speed (rad/s)'
41            CON_DSCRPT(12) = 'Rated Power (MW)'
42            CON_DSCRPT(13) = 'Air density (kg/m3 )'
43            CON_DSCRPT(14) = 'Cp maximum (-)'
44            CON_DSCRPT(15) = 'Speed reference filter time constant
    (s)'
```

```
45
46            !Add ICON_DSCRPT here
47
48           RETURN
49         ENDIF
50
51
52         !MODE 1 - INITIALIZATION
53         IF (MODE.EQ.1) THEN
54            STATE(K) = WTRBSP(WNDNUM(MC)) + 1   ! Initial Speed
   referece equal to speed form drivesystem
55
56            STATE(K+1) =
   PELEC(MC)*SBASE/MBASE(MC)/WAUXSG(WNDNUM(MC))/(WTRBSP(WNDNUM(MC))+1)
   + CON(J+2)*(WTRBSP(WNDNUM(MC))+1) ! Initial torqe integrator
   back calculated from output power, speed and de-rating factor
57            IF (STATE(K+1) .GT. CON(J+3)/(WTRBSP(WNDNUM(MC))+1))
   THEN       ! Make sure initial torque are within power limit
58               STATE(K+1) = CON(J+3)/(WTRBSP(WNDNUM(MC))+1)
59            ELSE IF (STATE(K+1) .LT. CON(J+4)) THEN
60               STATE(K+1) = CON(J+4)
61            ENDIF
62
63
64            Pel = (STATE(K+1)-CON(J+2)*(WTRBSP(WNDNUM(MC))+1)) *
   (WTRBSP(WNDNUM(MC)) + 1)       ! Aggregated P electric pu.
   machine base (befor frequency control)
65            VAR(L) = Pel
66            WPCMND(WNDNUM(MC)) = (VAR(L)*WAUXSG(WNDNUM(MC)) +
   WNDSP1(WNDNUM(MC)))             ! Aggregated P electric pu.
   machine base (after frequency control)
67            VAR(L+1) = WPCMND(WNDNUM(MC))
68
69            RETURN
70         ENDIF
71
72         !MODE 2 - CALCULATE DERIVATIVES
73         IF (MODE.EQ.2) THEN
74
75            ! PI controle non-windup DSTATE calculation for torque
   PI controler
76
77            VINP = WTRBSP(WNDNUM(MC)) + 1 - STATE(K) -
   WNDSP2(WNDNUM(MC))
78            VOUT = NWPI_MODE2(CON(J), CON(J+1),
   CON(J+3)/(WTRBSP(WNDNUM(MC))+1),
   CON(J+4)/(WTRBSP(WNDNUM(MC))+1), VINP, K+1)
79
80            Pel = (VOUT-CON(J+2)*(WTRBSP(WNDNUM(MC))+1)) *
   (WTRBSP(WNDNUM(MC)) + 1) ! P electric pu. machine base (before
   frequency control)
81            VAR(L+2) = Pel
82
83            U = Pel**(1./3.) * PowToSpd     ! Speed refrence
   filter input signal limited to speed ref max
84            IF (U .GT. CON(J+6)) THEN
```

```
85                U = CON(J+6)
86             ELSE IF (U .LT. CON(J+7)) THEN
87                U = CON(J+7)
88             ENDIF
89
90             ! LP-filter for speed refrence DSTATE clacualtion
91             VINP = U
92             VOUT = LAG_MODE2( 1.0,CON(J+14),VINP,K )
93
94          RETURN
95       ENDIF
96
97
98       !MODE 3 - SET Model output
99       IF (MODE.EQ.3) THEN
100           WPCMND(WNDNUM(MC))=(VAR(L+2)*WAUXSG(WNDNUM(MC)) +
    WNDSP1(WNDNUM(MC)))       ! Set power refrence output chanel to
    P electric pu. machine base (after frequency control)
101           WNDSP4(WNDNUM(MC)) = VAR(L+2)
102           VAR(L+3) = WPCMND(WNDNUM(MC))
103          RETURN
104       ENDIF
105
106       !MODE 4 - set NINTEG
107       IF (MODE.EQ.4) THEN
108          IF (MIDTRM) THEN
109             CALL NOTMID
110          ELSE
111
112       !Set NINTEG
113          IF(NINTEG < K+1) NINTEG = K+1
114          ENDIF
115
116          RETURN
117       ENDIF
118
119
120       RETURN
121
122       END SUBROUTINE UTORQ
```

UPLANT

```
1     SUBROUTINE UPLANT(MC,SLOT)
2         INCLUDE 'COMON4.INS'
3         IMPLICIT NONE
4         INTEGER J           ! starting CON index
5         INTEGER K           ! starting STATE index
6         INTEGER L           ! starting VAR index
7         INTEGER M           ! starting ICON index
8         INTEGER MC          ! machine index
9         INTEGER SLOT        ! index into STRT array allocation
10        INTEGER IBUS
11        REAL DEL2, omega , b, Pe, lambda, CpE, CpA, WindspeedEst,
    A, omegaOpt
12        REAL lambdaOptPos, PAvail, x, y, freq, db, Paux, omegaEst
13        REAL Pdiff, D_factor, CpDmax, PitchMin, PauxI, DeltaW
14        EXTERNAL  NOTMID
15
16        J=WSTRTIN(1,SLOT)                              ! STARTING
    'CON'
17        K=WSTRTIN(2,SLOT)                              ! STARTING
    'STATE'
18        L=WSTRTIN(3,SLOT)                              ! STARTING
    'VAR'
19        M=WSTRTIN(4,SLOT)                              ! STARTING
    'ICON'
20        IBUS = ABS(NUMTRM(MC))                    ! BUS INTERNAL
    INDEX NUMBER
21        freq = -BSFREQ(IBUS)
22
23
24        DEL2 = 2.0 * DELT
25
26        !MODE 8 - GET DATA DESCRIPTIONS
27        IF (MODE.EQ.8) THEN
28            !CON description
29            CON_DSCRPT(1) = 'Wind turbine radius (m)'
30            CON_DSCRPT(2) = 'Rated speed (rad/s)'
31            CON_DSCRPT(3) = 'Air density (kg/m^3)'
32            CON_DSCRPT(4) = 'Wind turbine rated power (MW)'
33            CON_DSCRPT(5) = 'Optimal lambda (-)'
34            CON_DSCRPT(6) = 'Max speed (pu)'
35            CON_DSCRPT(7) = 'Min speed (pu)'
36            CON_DSCRPT(8) = 'Max power (pu)'
37            CON_DSCRPT(9) = 'Min power (pu)'
38            CON_DSCRPT(10) = 'Frequency deadband for de-rating
    control (pu)'
39            CON_DSCRPT(11) = 'Droop for up regulation'
40            CON_DSCRPT(12) = 'Droop for down regulation'
41            CON_DSCRPT(13) = 'Power reserve (pu)'
42            CON_DSCRPT(14) = 'Maximum Cp (-)'
43            CON_DSCRPT(15) = 'Frequency deadband for inertia
    control (pu)'
44            CON_DSCRPT(16) = 'Inertia filter time constant (s)'
45            CON_DSCRPT(17) = 'Wind turbine inertia'
46            CON_DSCRPT(18) = 'Wind turbine inertia gain'
```

```
47            CON_DSCRPT(19) = 'Feedback for returning to optimal
    speed'
48            CON_DSCRPT(20) = 'Lower speed limit for inertia
    emulation'
49            CON_DSCRPT(21) = 'Anti wind-up feedback'
50
51            !CP(pitch,lambda) forth order polynomial aproximation
52            CON_DSCRPT(22) = 'a00'
53            CON_DSCRPT(23) = 'a01'
54            CON_DSCRPT(24) = 'a02'
55            CON_DSCRPT(25) = 'a03'
56            CON_DSCRPT(26) = 'a04'
57            CON_DSCRPT(27) = 'a10'
58            CON_DSCRPT(28) = 'a11'
59            CON_DSCRPT(29) = 'a12'
60            CON_DSCRPT(30) = 'a13'
61            CON_DSCRPT(31) = 'a14'
62            CON_DSCRPT(32) = 'a20'
63            CON_DSCRPT(33) = 'a21'
64            CON_DSCRPT(34) = 'a22'
65            CON_DSCRPT(35) = 'a23'
66            CON_DSCRPT(36) = 'a24'
67            CON_DSCRPT(37) = 'a30'
68            CON_DSCRPT(38) = 'a31'
69            CON_DSCRPT(39) = 'a32'
70            CON_DSCRPT(40) = 'a33'
71            CON_DSCRPT(41) = 'a34'
72            CON_DSCRPT(42) = 'a40'
73            CON_DSCRPT(43) = 'a41'
74            CON_DSCRPT(44) = 'a42'
75            CON_DSCRPT(45) = 'a43'
76            CON_DSCRPT(46) = 'a44'
77
78            !CP(pitch=0,lambda) forth order polynomial aproximation
79            CON_DSCRPT(47) = 'b0'
80            CON_DSCRPT(48) = 'b1'
81            CON_DSCRPT(49) = 'b2'
82            CON_DSCRPT(50) = 'b3'
83            CON_DSCRPT(51) = 'b4'
84
85            !Pitch_min(k_dr) forth order polynomial aproximation
86            CON_DSCRPT(52) = 'c0'
87            CON_DSCRPT(53) = 'c1'
88            CON_DSCRPT(54) = 'c2'
89            CON_DSCRPT(55) = 'c3'
90            CON_DSCRPT(56) = 'c4'
91
92            !ICON description
93            ICON_DSCRPT(1) = 'De-rated on'
94            ICON_DSCRPT(2) = 'Inertia on'
95
96          RETURN
97        ENDIF
98
99        !MODE 1 - INITIALIZATION
100       IF (MODE.EQ.1) THEN
```

```
101           Pe = PELEC(MC)*SBASE/MBASE(MC)                          !
    Convert electrical power to machine base
102           D_factor = Pe/(Pe+CON(J+12))                            !
    Initialyze de-rated factor for use in torque model
103
104           CpDmax = CON(J+13) * D_factor
105           PitchMin = CON(J+51) + CON(J+52)*CpDmax +
    CON(J+53)*CpDmax**2 + CON(J+54)*CpDmax**3 + CON(J+55)*CpDmax**4
          ! Initialyze min pitch for use in pitch model
106            IF (PitchMin .LT. 0) THEN
107               PitchMin = 0
108            END IF
109
110           IF (ICON(M) == 0) THEN          ! Set de-rated factor
    and min pitch if de-ratet operation is not used
111               PitchMin = 0
112               D_factor = 1
113           END IF
114           VAR(L+6) = D_factor
115
116           WNDSP3(WNDNUM(MC)) =  PitchMin
117           WAUXSG(WNDNUM(MC)) =  D_factor
118
119           WindspeedEst = 3                ! Set wind speed
    estimate to random to avoid div with 0
120           VAR(L) = WindspeedEst
121
122           db = freq
123           IF (db .GT. CON(J+9)) THEN
124               db = CON(J+9)
125           ELSE IF (db .LT. -CON(J+9)) THEN
126               db = -CON(J+9)
127           ENDIF
128           freq = freq - db                ! frequency error with
    de-rating deadband
129
130           STATE(K) = freq/CON(J+15)       ! Set derivitave state
131           STATE(K+1) = 0                  ! Set speed change
    estimation intergral state
132
133           RETURN
134       ENDIF
135
136       !MODE 2 - CALCULATE DERIVATIVES
137       IF (MODE.EQ.2) THEN
138           db = freq
139           IF (db .GT. CON(J+9)) THEN
140               db = CON(J+9)
141           ELSE IF (db .LT. -CON(J+9)) THEN
142               db = -CON(J+9)
143           ENDIF
144           freq = freq - db        ! frequency error with
    de-rating deadband
145
146           DSTATE(K) = (freq/CON(J+15)-STATE(K))/CON(J+15)     !
    Calculate DSTATE
```

```
147
148           IF (-freq .GT. 0 .AND. (WTRBSP(WNDNUM(MC)) + 1) .GE.
    CON(J+5)-0.005 ) THEN
149               DSTATE(K+1) = 0-STATE(K+1)*CON(J+18)
150           ELSE
151               DSTATE(K+1) = VAR(L+7)-STATE(K+1)*CON(J+18)
152           END IF
153
154           RETURN
155       ENDIF
156
157       !MODE 3 - SET Model output
158       IF (MODE.EQ.3) THEN
159
160
161           omega = WTRBSP(WNDNUM(MC)) + 1                        !
    WT speed ref
162           b = WPITCH(WNDNUM(MC))                               ! WT
    pitch
163           Pe = PELEC(MC)*SBASE/MBASE(MC)                       ! WT
    power on machine base
164           A = CON(J)**2.*3.14                                  ! WT
    area
165
166           lambda = omega *CON(J)*CON(J+1)/VAR(L)                !
    Calcualte lambda
167
168           x = b                                                ! set
    x = pitch and y = lambda
169           y = lambda
170
171           CpE = CON(J+21) + CON(J+22)*y + CON(J+23)*y**2
                &       ! Calcualte Cp from forth oder polynomial
    aproximation
172            + CON(J+24)*y**3 + CON(J+25)*y**4 + CON(J+26)*x
                 &
173            + CON(J+27)*x*y + CON(J+28)*x*y**2 + CON(J+29)*x*y**3
                 &
174            + CON(J+30)*x*y**4 + CON(J+31)*x**2 +
    CON(J+32)*x**2*y               &
175            + CON(J+33)*x**2*y**2 + CON(J+34)*x**2*y**3 +
    CON(J+35)*x**2*y**4    &
176            + CON(J+36)*x**3 + CON(J+37)*x**3*y +
    CON(J+38)*x**3*y**2            &
177            + CON(J+39)*x**3*y**3 + CON(J+40)*x**3*y**4 +
    CON(J+41)*x**4         &
178            + CON(J+42)*x**4*y + CON(J+43)*x**4*y**2 +
    CON(J+44)*x**4*y**3       &
179            + CON(J+45)*x**4*y**4
180
181           IF (CpE .LT. 0.01) THEN         ! Make sure the
    aproximation do not create unresonabel Cp values for high/low
    lambda
182               CpE = 0.01
183           ELSE IF (CpE .GT. CON(J+13)) THEN
184                CpE = CON(J+13)
```

```
185             ENDIF
186             VAR(L+1) = CpE
187
188
    WindspeedEst=(Pe*CON(J+3)*10**6.*2./(CpE*A*CON(J+2)))**(1./3.)
    ! Calcualte wind speed estimate
189             VAR(L) = WindspeedEst
190
191             omegaOpt = WindspeedEst*CON(J+4)/(CON(J)*CON(J+1))
                ! Calcualte optimal speed
192             omegaOpt = omegaOpt + WNDSP2(WNDNUM(MC))
                ! Compenstare for inertia emulation speed change
193             IF (omegaOpt .GT. CON(J+5)) THEN
                ! Limit speed to get optimal possibel speed
194                 omegaOpt = CON(J+5)
195             ELSE IF (omegaOpt .LT. CON(J+6)) THEN
196                 omegaOpt = CON(J+6)
197             ENDIF
198             lambdaOptPos = omegaOpt*CON(J)*CON(J+1)/WindspeedEst
                ! Calcualte optimal possibel lambda
199
200             CpA =  CON(J+46) + CON(J+47)*lambdaOptPos +
    CON(J+48)*lambdaOptPos**2 + CON(J+49)*lambdaOptPos**3 +
    CON(J+50)*lambdaOptPos**4       ! Calculate the avalibe Cp at
    normal operation (diragarding the pitch)
201             IF (CpA .LT. 0) THEN
202               CpA = 0
203             ENDIF
204             VAR(L+2) = CpA
205
206             PAvail =
    CpA*A*CON(J+2)*WindspeedEst**3./(2.*CON(J+3)*10**6)        !
    Calcualte the avalibel power from avalibel Cp
207             IF (PAvail .GT. CON(J+7)+WNDSP1(WNDNUM(MC))) THEN
                    ! Limit avalibel power to simulate pitch control
    and compensate for Inertia emulation
208                 PAvail = CON(J+7)+WNDSP1(WNDNUM(MC))
209             ELSE IF (PAvail .LT. CON(J+8)) THEN
210                 PAvail = CON(J+8)
211             ENDIF
212             VAR(L+3) = PAvail
213
214             db = freq
215             IF (db .GT. CON(J+9)) THEN
216                 db = CON(J+9)
217             ELSE IF (db .LT. -CON(J+9)) THEN
218                 db = -CON(J+9)
219             ENDIF
220             freq = freq - db                    ! Frequency error
    signal with inertia emulation deadband
221
222             IF (freq .GE. 0.) THEN
223                 Paux = freq/CON(J+10)           ! droop up
    regulation
224             ELSE IF (freq .LT. 0.) THEN
225                 Paux = freq/CON(J+11)           ! droop down
```

```
    regulation
226             END IF
227             Pdiff = Paux - CON(J+12)            ! droop auxilery
    power
228             IF (ICON(M) == 0) THEN              ! If no de-rating
    set droop auxilery power to 0
229                 Pdiff = 0
230                 Paux = 0
231             END IF
232             VAR(L+4) = Paux
233
234             D_factor = (Pdiff+PAvail)/PAvail    ! Calculate
    de-rating factor
235
236             IF (D_factor .LT. 0.1) THEN         ! Make sure
    de-rating factor is not zero or wind estimation will not work
237                 D_factor = 0.2
238             ELSE IF (D_factor .GT. 1) THEN      ! Limit de-rating
    factor to 1
239                 D_factor = 1
240             END IF
241
242              IF (VAR(L+6)-D_factor .GT. DELT*0.5) THEN ! Rate limit
243                 D_factor = VAR(L+6) - DELT*0.5
244             ELSE IF (VAR(L+6)-D_factor .LT. -DELT*0.5) THEN
245                 D_factor = VAR(L+6) + DELT*0.5
246             END IF
247
248             CpDmax = CON(J+13) * D_factor
249             PitchMin = CON(J+51) + CON(J+52)*CpDmax +
    CON(J+53)*CpDmax**2 + CON(J+54)*CpDmax**3 + CON(J+55)*CpDmax**4
      ! Calculate min pitch for de-rated operation
250             IF (PitchMin .LT. 0) THEN
251                 PitchMin = 0
252             END IF
253
254             IF (ICON(M) == 0) THEN              ! If no de-rating
    set de-rating factor to 1 and pitch min to 0
255                 PitchMin = 0
256                 D_factor = 1
257             END IF
258             VAR(L+5) = PitchMin
259             VAR(L+6) = D_factor
260
261
    PauxI=(freq/CON(J+15)-STATE(K))*(freq+1)*CON(J+16)*CON(J+17)*2.
    ! Calcualte inertia emulation auxilary power
262             IF (omega .LT. CON(J+19)) THEN
263                 PauxI = 0
264             ENDIF
265
266             omegaEst = (omega**2-STATE(K+1)/CON(J+16))**(1./2.)
267             DeltaW = omegaEst-omega         ! Calculate the chage
    in speed due to inertia emulation
268             IF (ICON(M+1) == 0) THEN        ! If no inertia
    emulation set speed change and inertia emulation auxilary power
```

```
   to 0
269                PauxI = 0
270                DeltaW = 0
271             END IF
272             VAR(L+7) = PauxI
273             VAR(L+8) = DeltaW
274
275             ! Change output chanels
276             WAUXSG(WNDNUM(MC)) =  D_factor
277             WNDSP1(WNDNUM(MC)) =  PauxI
278             WNDSP2(WNDNUM(MC)) =  DeltaW
279             WNDSP3(WNDNUM(MC)) =  PitchMin
280
281             RETURN
282          ENDIF
283
284          !MODE 4 - set NINTEG
285          IF (MODE.EQ.4) THEN
286             IF (MIDTRM) THEN
287                CALL NOTMID
288             ELSE
289
290          !Set NINTEG
291             IF(NINTEG < K+1) NINTEG = K+1
292
293             ENDIF
294
295             RETURN
296          ENDIF
297
298          RETURN
299
300          !FORMAT STATEMENTS
301
302          END SUBROUTINE UPLANT
```